Delft University of Technology

Master of Science Thesis

Analysis of 2D homogeneous space solutions of the seismoelectric P-SV-TM mode for interferometric purposes

Author:
Iris Hartstra

Supervisors:
N. Grobbe M.Sc. and Prof. dr. ir. E. C. Slob

August 26, 2012

Title: Analysis of 2D homogeneous space solutions of the seismoelectric P-SV-TM mode for interferometric purposes

Author: Iris Hartstra

Master program: IDEA League Joint Master's in Applied Geophysics, class of 2010

Supervisors: N. Grobbe M.Sc. and Prof. dr. ir. E. C. Slob

Readers: dr. F. Bosch, N. Grobbe M.Sc. and Prof. dr. ir. E. C. Slob

TU Delft
Delft
University of
Technology

Abstract

Seismic and electromagnetic imaging methods both provide the geophysicist with different types of medium parameters. Seismic methods are sensitive to the elastic properties of the medium, while electromagnetic methods are sensitive to the electric properties. In porous-saturated media, these two wave fields occur as a coupled system, which is known as 'seismoelectrics'. This coupling is caused by physical interactions at the grain surface boundary and is a function of several medium parameters, such as dynamic permeability. This medium parameter is valuable to the oil and gas industry, as well to the field of hydrology. By conducting a seismoelectric survey it would theoretically be possible to provide an extra control on this medium parameter. However, both practice and theory have shown that this coupling mechanism also results in a low signal-to-noise ratio. A possible solution to this problem would be to apply interferometric Green's retrieval, which is a technique based on stacking of cross-correlated data. This approach has been proved successful for the SH-TE mode in 1D. The SH-TE mode forms together with the P-SV-TM mode, the total seismoelectric system. In this thesis the first steps are taken towards the proof that this technique could also work for the P-SV-TM mode of the system. This is supported by a modelling experiment of 2D homogeneous space solutions of the seismoelectric P-SV-TM mode for different configurations and an evaluation of the effects of cross-correlation on these responses. This evaluation turned out that the unwanted artefacts observed in the interferometric retrieval are generated by cross-correlations between P-waves and SV-waves.

Contents

Acknowledgements

I want to thank my supervisors, Niels Grobbe and Evert Slob, for being an inspiration to me and supporting me always during the entire length of this project.
It has been an honour working with you.

Chapter 1

Introduction

Electromagnetic and mechanical wave fields are two very powerful physical phenomenons, which both aid the geophysicist in imaging the Earth's structure. The electromagnetic waves provide us with information on the electric properties of the investigated medium, such as electric permittivity and conductivity, whereas mechanical wave fields can provide us with valuable mechanical properties, such as bulk density and other elastic medium parameters. One way to obtain both mechanical as electric properties, is by conducting independent electromagnetic and seismic surveys of the medium. Another way to obtain both, is by considering the coupling possibility of these two different wave fields within the investigated medium. The field describing this coupling of both wave fields, is known as 'electrokinetics', which has been developed since the first experiment was conducted by Reuss in 1809 which reported such a coupling. Afterwards, a long history of attempts followed in order to develop a theory to explain this electrokinetic phenomenon (for a review of this history, the reader is referred to [9]). A key moment occurred in 1994, when Pride [7] came up with a full set of equations which coupled Maxwell's equations to the full elastodynamic wave theory in 1994. This theory was experimentally validated by Schoemaker et al. in 2012 [9]. Seismoelectrics does not only provide a great potential due to the ability to obtain both relevant wave field responses by conducting a single survey. In addition to that, the seismoelectric SP coupling coëfficient could be derived from such a measurement. This coupling coëfficient depends on several valuable medium parameters, such as the dynamic permeability. The dynamic permeability is a valuable medium parameter to the oil and gas industry, as well as to the field of hydrology. However, it is exactly this valuable coupling factor which causes the complications in seismoelectric applications. Due to the fact that the coupling factor is of a relatively low value, the conversion of one wave-type into another via this mechanism decreases the amplitude, resulting in a low signal-to-noise ratio. In order to make it possible to retrieve this coupling coëfficient from seismoelectric surveys in practice, it is required to apply a technique to this phenomenon in order to improve this signal-to-noise ratio. An interesting technique, presented in 2004 by Wapenaar [12], is the principle of interferometry, based on the reciprocity theorem of the correlation type [4]. It prescribes an elegant way of cross-correlating traces of shot gathers of the acquired data and a subsequent stacking of those cross-correlated gathers, in order to obtain a desired signal from that data. The basis of this technique was founded by Claerbout [3], who pioneered in this field by obtaining the reflection response from the auto-correlation of a transmission response for a 1D medium. Wapenaar [12] extended this for 3D inhomogeneous media, as well as for any class of wave phenomena, including the seismoelectric wave field system as formulated by Pride [7]. The improvement of the signal-to-noise ratio by use of this technique depends primarily on the amount of sources used. One way to increase this amount is by conducting a passive measurement of uncorrelated noise of a sufficient length of time. In Appendix F of the paper by Wapenaar and Fokkema [15], an interferometry scheme is provided for Pride's [7] seismoelectric system of equations. In 2009, de Ridder [5] used this scheme to numerically validate that signal retrieval of a seismoelectric response is theoretically possible for the SH-TE mode in a 1D layered medium. The objective of this thesis is to validate the same for the seismoelectric P-SV-TM mode in a 2D homogeneous medium. For that, it is required to exactly formulate the interferometry relation with homogeneous Green's functions derived from Pride's [7] system of equations. Subsequently, a detailed analysis of these Green's functions of the 2D P-SV-TM system was undertaken with the objective to improve the understanding of this seismoelectric mode and possibly discover where the errors observed in the modelled interferometric retrieval are caused by.

Chapter 2

Seismoelectric wave theory

In this Chapter the details of the seismoelectric coupling mechanism at a micro-scale are explained, as well as the effects of this coupling in the case of the presence of an interface. Subsequently, the consequences of simplifying a 3D medium to a 2D medium are explained with the purpose of introducing the seismoelectric wave equation system of the P-SV-TM mode in 2D.

2.1 Seismoelectric coupling at the electric double-layer

In this section the relevance of the electrokinetic coupling mechanism is explained with help of the microscopic electric double-layer model [8]. In a fluid saturated porous medium, ions are adsorbed on the grain surface, resulting in an immobile layer of surface charge Q on the grain surface, referred to as the Stern layer. This surface charge is counteracted by charge of opposite valence provided by the fluid electrolyte surrounding the grain surface, referred to as the diffuse layer. This mobile fluid phase layer can be moved relative to the immobile Stern layer of the solid grain surface due to a pressure gradient. This pressure gradient can be established by either a longitudinal P-wave or a transversal S-wave travelling through the medium. The result of this, is a relative movement of charge, referred to as a streaming current. This streaming current, in turn, results in a charge build-up which is consequently counteracted by a conduction current, due to the formed electric field acting in the opposite direction of the streaming current. This results in the oscillatory storage and release of electric energy in the form of free charge, which effectively decreases the conductivity. In equation 2.5, which describes the modified Ampere's law for electrokinetic systems, can indeed be seen that the coupling term $\hat{L}\hat{\xi}$ effectively reduces the conductivity of the original Ampere's law. This dependent electromagnetic field propagates at the same speed and frequency as this mechanical wave and is referred to as the 'coseismic' field [8]. However, this electromagnetic field is not a real electromagnetic wave, because in the continuous storage and release of electric energy is not a function of electric permittivity, but purely of the oscillatory pressure gradient. As stated by Pride [7] the coupling mechanism is assumed linear, for which reason reciprocity applies. This means it is as well able to convert electromagnetic waves into seismic waves. In this case the oscillating electric field strength due to the electromagnetic wave polarization induces movement of the mobile diffusive layer relative to the immobile grain surface. This relative movement of particles induces a pressure gradient which moves inherently along within the electromagnetic wave. This pressure gradient will propagate at the same speed and frequency of the electromagnetic wave through the medium. This dependent form of a mechanical wave is referred to as the 'coelectric' field [9].

2.2 What happens at an interface

In the previous subsection the generation of dependent fields was discussed. In seismoelectric wave propagation it is also possible for an independent wave to be generated from a wave field of a different type. However, this can only occur at an interface across which either the mechanical or electrical properties of the medium change. For the generation of an independent electromagnetic diffusive field from a mechanical wave, the mechanism at an interface is as follows: The free charge separation induced by the mechanical pressure wave experiences asymmetry due to the change in properties at the interface and a part of the conduction current is not completely counteracted by the pressure wave oscillation. This gives rise to a resultant oscillatory conductive current. This oscillating current acts as an electric dipole source, which has the ability to generate an independent electromagnetic diffusive field. However, due to the relative low frequency of the initial mechanical wave, this electromagnetic wave is more of a diffusive nature. This is because in general even at ultrasonic frequencies, order of a few MHz, the electromagnetic field is dominated by the electric conductivity and hence behaves as a diffusive field. The other way round it is also possible, an incident electromagnetic wave can generate an independent mechanical wave at the interface. The oscillating pressure gradient induced by the electromagnetic wave experiences asymmetry at the medium interface. Due to that, there is a resultant force acting at the interface, which acts as a dipole source for a mechanical wave. This mechanical wave will inherit the electromagnetic frequency of its original generator, but its speed is now equal to the mechanical wave speed of the medium. This wave speed is considerably lower than the electromagnetic wave speed. If the initial electromagnetic wave is of a frequency, which exceeds the order of MHz, the resulting seismic wave would have a wavelength of the order of the grain size, or even smaller. Therefore, the electroseismic theory is not valid for frequencies above a few MHz, because the wave length should always be much bigger than the grain size. Therefore, seismoelectric theory is only valid for a frequency range up to the order of 10^6 Hz [8].

2.3 Electrokinetic wave fields from 3D to 2D

In this thesis the electroseismic system will be investigated in 2D, which has significant consequences for the mechanics of the seismoelectric system, as well as for the geometry of the propagating wave field as is given by the 2D Green's function.

2.3.1 Seismoelectrics in 2D

In the 3D world the grain boundary surface can have any spatial orientation. This gives a great diversity of coupling possibilities, because in the seismic as well as the electromagnetic world different wave field types are defined by their polarization. This is of course not the case for dilatational wave fields, P-waves, because then the particle displacement is simply in the same direction as the direction of propagation in an isotropic medium. Shear waves on the other hand are transversal in nature. In this case, for a certain direction of propagation the polarization is in any direction in the plane perpendicular to the wave vector. In the case of an anisotropic medium this fact is non-trivial, because the wave velocity now depends on the polarization direction and possibly also on the propagation direction. This is why the shear wave field is divided in two modes, which form two end members of shear wave polarization. One is the wave polarized in the plane of propagation, referred to as the vertically polarized shear wave. The other end member is referred to as the horizontally polarized shear wave, which is purely polarized in the plane perpendicular to the plane of propagation. In an anisotropic medium the fields polarized in a direction in between these two perpendicular planes of course can also have a different wave speed, but in this theory it is assumed that this wave can be expressed as a superposition of the two [11]. Electromagnetic waves are geometrically similar to shear waves, in that the changes in the electric field strength are also perpendicular to the direction of propagation [6]. However, an important difference is that the electromagnetic wave is also characterized by an oscillating magnetic field strength, which is always perpendicular to the electric field polarization. In the same way as for shear waves two main modes are defined for the electromagnetic wave field as well. The transverse magnetic field is the mode in which the electric field oscillates in the plane of propagation, naturally the magnetic field oscillates in the plane perpendicular to it. The other mode is the transverse electric field, in this case the electric field oscillates in the plane perpendicular to the plane of propagation. The magnetic field vector lies within the plane of incidence in the latter case. In the case of a 3D isotropic medium, P-waves, SH-waves and SV-waves all have the possibility to induce a pressure gradient perpendicular to the grain surface and induce a relative movement of the charged diffusive layer, generating a coseismic electromagnetic field. And vice versa, both TE and TM wave fields can generate all of the possible mechanical waves. However, in this thesis the 2D isotropic case is addressed. In this case, the grain surface is a 2D function of position in the 2D plane and a constant in the dimension perpendicular to that plane. The diversity of coupling possibilities is restrained accordingly, which results in an effective decoupling of the two modes of the seismoelectric system, SH-TE and P-SV-TM. If a P-wave would be generated in this 2D medium, it can only induce a pressure gradient in the direction along the 2D model plane, which is the plane of propagation. The pressure gradient can generate an electric field oscillation in the plane of the medium, which is the coseismic TM mode. At an interface, the pressure gradient could generate an S-wave with a polarization directed along the plane of the medium, which is therefore a vertically polarized S-wave. In turn, it is also possible for the SV-wave to generate a coseismic electric field of the TM mode, but this happens via induction. Because of this, the coseismic electric field of an S-wave is in general weaker than the coseismic of a P-wave [8]. The SH-TE mode can only be generated completely independently of the P-SV-TM mode. The SH-TE mode establishes a horizontally polarized shear wave, which accelerates the charged mobile layer of the EDL in the x_2-direction. This effectively results in an electric streaming current in this direction. According to Ampere's law (2.5), this electric current induces a magnetic flux, which rotates spatially around the electric current direction. In turn, as dictated by Faraday's law (2.6) this magnetic field flux generates an electric field variation perpendicular to the medium plane. This varying electric field vector represents the TE-mode of the electric field [6]. In this thesis only the P-SV-TM mode will be analysed in 2D.

2.4 Wave fields in 2D

In the 2D world wave fields require a different formulation than wave fields in 3D. In the 3D world a wave field can be visualized as a spherical wave front which expands with increasing time and thereby decreases its amplitude due to the geometrical spreading of the wave energy. However, in a 2D medium it is required that all wave field vectors are a constant function of the x_2 - direction, which is the direction perpendicular to the medium under consideration. In order to meet this requirement, the original 3D spherical field is integrated over this constant spatial direction. The result of this, is a wave field which can be visualized as a field which is induced by an infinite line source directed in the constant x_2 - direction. The wave front of this wave field is of a cylindrical shape, of which the long axis coincides with the imaginary line source. Such a cylindrical function can only be represented in integral form as a modified Bessel function of order zero. Refer to Appendix A for this Bessel function expression, including its spatial derivatives [1], which will be required later for the derivation of the seismoelectric Green's functions in 2D.

2.5 Derivation of the wave equations for the coupled P-SV-TM mode in 2D

Macroscopic equations describing the P-SV-TM mode in a 2D homogeneous and isotropic domain are derived in order to clarify the complex coupling mechanisms and the generated wave fields associated with this system. In a 2D model, any spatial variation in the x_2-direction is zero. In order to obtain the P-SV-TM mode all field components belonging to its complementary mode, the SH-TE system, are set to zero, which are:

- Transverse Electric components E_2, H_1 and H_3
- Transverse Electric source components $J_2^{(e)}$, J_1^m and J_3^m
- Horizontally polarized elastodynamic components v_2^s, τ_{12}, τ_{32}, τ_{22} and w_2
- Horizontally active elastodynamic source components f_2, h_{12}, h_{32} and h_{22}.

The medium for which the equations hold is porous-saturated, homogeneous, isotropic and dissipative. The derivation is based on volume averaged Maxwell's electrodynamic equations [6] and Biot's elastodynamic equations [2], as formulated by Pride [7]. Biot's equations [2] for a porous medium are represented by two sets of equations: elastodynamic propagation in the fluid phase and in the solid phase, which are coupled to each other due to the existence of boundary conditions for the particle motion fields at the grain boundaries [2]. In Pride's system of equations, Biot's equations for the fluid and solid phase equations are averaged over a volume, which size exceeds the grain size scale, but is smaller than the minimum wavelength [7]. Biot's equations are also coupled to Ampere's law of Maxwell's equations. The underlying principle of this theory lies in the theory of the EDL, as explained in section 2.1. These coupling mechanisms described here will be explained further with the help of the governing equations.

2.5.1 Basic equations

The equations presented in this section form together the coupled set of first order macroscopic seismoelectric equations for the P-SV-TM mode in 2D. All derivations are done in the Laplace domain for the special case when the real part of the Laplace parameter is zero, which is also known as the Fourier domain. In the subsequent paragraphs these equations will be combined together into higher order equations, in order to clarify the wave behaviour of this system. The symmetry properties of the stress, strain and stiffness parameter tensors, which are valid in an isotropic domain, are applied at all times [11]. Note that in case of a vector equation, only the non-zero components are displayed, which are in most cases the first and third component. However, if a vector equation occurs which is of an alternative structure, it will be explicitly noted which non-zero components are displayed in those cases, or whether an equation is of scalar nature. The source terms will exclusively be written on the right hand-side. The following substitutions are made,

$$s = i\omega \tag{2.1}$$
$$\hat{w} = \phi(\hat{v}^f - \hat{v}^s) \tag{2.2}$$
$$\zeta = \hat{\sigma}^m + s\mu \tag{2.3}$$
$$\hat{\xi} = \eta\hat{L}/\hat{k} \tag{2.4}$$

Here, the velocity of the particles in the fluid phase and in the solid phase are defined as $\hat{v}^f$ and $\hat{v}^s$, respectively. The filtration velocity is given by $\hat{w}$. The fluid viscosity is given by η, the porosity by ϕ and the dynamic permeability by $\hat{k}$. The electric and magnetic bulk conductivities are given by $\hat{\sigma}^e$ and $\hat{\sigma}^m$. The bulk magnetic permeability is given by μ. The Laplace parameter is given by s, which is equal to the imaginairy unit multiplied with the angular frequency, ω.

Generalized Ampere's law [6],

$$\partial_3\hat{H}_2 + \left(\hat{\sigma}^e + s\varepsilon - \hat{L}\hat{\xi}\right)\hat{E}_1 + \hat{\xi}\hat{w}_1 = -\hat{J}^e_1, \tag{2.5a}$$
$$-\partial_1\hat{H}_2 + \left(\hat{\sigma}^e + s\varepsilon - \hat{L}\hat{\xi}\right)\hat{E}_3 + \hat{\xi}\hat{w}_3 = -\hat{J}^e_3, \tag{2.5b}$$

In equation 2.5 $\hat{H}$ represents the magnetic flux, $\hat{E}$ the electric field, $\hat{J}^e$ the electric dipole current and $\hat{J}^m$ the magnetic dipole current.

Faraday's law [6], all components of this vector are zero except for the x_2-directed component,

$$\partial_3\hat{E}_1 - \partial_1\hat{E}_3 + \zeta\hat{H}_2 = -\hat{J}^m_2, \tag{2.6}$$

In this medium there are two phases, a solid phase and a fluid phase. The equations describing the particle motion can be formulated separately for each phase in the microscopic approach [2] . However, in this representation of the system all equations are averaged over a volume much bigger than the grain size, therefore containing both phases [7] . By averaging the two particle motion equations over this volume and adding them together, a relation is found which describes the motion of the bulk material, which encompasses both fluid as solid phase,

$$s\rho\hat{v}_1^s + s\rho^f\hat{w}_1 - \partial_1\hat{\tau}_{11} - \partial_3\hat{\tau}_{13} = \hat{f}_1^b, \tag{2.7a}$$
$$s\rho\hat{v}_3^s + s\rho^f\hat{w}_3 - \partial_3\hat{\tau}_{33} - \partial_1\hat{\tau}_{31} = \hat{f}_3^b, \tag{2.7b}$$

In equation 2.7 $\hat{\tau}$ denotes the specified component of the traction matrix. The medium parameters ρ and ρ^f, denote the bulk and fluid densities, respectively, and $\hat{f}^b$ denotes the bulk force.

The equation for the averaged relative fluid motion is found by subtracting the averaged solid motion from the fluid motion, scaled by the fluid density, and averaging the result over the fluid phase,

$$s\rho^f\hat{v}_1^s + \frac{\eta}{\hat{k}}\left(\hat{w}_1 - \hat{L}\hat{E}_1\right) + \partial_1\hat{p} = \hat{f}_1^f, \tag{2.8a}$$
$$s\rho^f\hat{v}_3^s + \frac{\eta}{\hat{k}}\left(\hat{w}_3 - \hat{L}\hat{E}_3\right) + \partial_3\hat{p} = \hat{f}_3^f, \tag{2.8b}$$

In equation 2.8 the $\hat{p}$ denotes the pressure and $\hat{f}^f$ the force acting on the fluid phase. An important note is that these two equations of motion 2.7 and 2.8 are simply a result of linearly combining the two modified equations of solid and fluid motion from Biot [2], by either adding or subtracting them, before averaging over the volume. Because of this, all equations describe the physical effects on the bulk.
The volume-averaged deformation matrix equation for the bulk reduces to 4 components in the 2D P-SV-TM system,

$$-s\hat{\tau}_{11} + S_{1111}\partial_1\hat{v}_1^s + S_{1133}\partial_3\hat{v}_3^s + C\left(\partial_1\hat{w}_1 + \partial_3\hat{w}_3\right) = S_{1111}\hat{h}_{11} + S_{1133}\hat{h}_{33} + C\hat{q}, \tag{2.9a}$$

$$-s\hat{\tau}_{33} + S_{3333}\partial_3\hat{v}_3^s + S_{3311}\partial_1\hat{v}_1^s + C\left(\partial_1\hat{w}_1 + \partial_3\hat{w}_3\right) = S_{3333}\hat{h}_{33} + S_{3311}\hat{h}_{11} + C\hat{q}, \tag{2.9b}$$

$$-s\hat{\tau}_{13} + S_{1313}\left(\partial_3\hat{v}_1^s + \partial_1\hat{v}_3^s\right) = 2S_{1313}\hat{h}_{13}, \tag{2.9c}$$

$$-s\hat{\tau}_{31} + S_{3131}\left(\partial_1\hat{v}_3^s + \partial_3\hat{v}_1^s\right) = 2S_{3131}\hat{h}_{31}, \tag{2.9d}$$

The symbol S denotes a component of the stiffness tensor and $\hat{h}$ denotes a strain source. Equations 2.9a and 2.9b represent the two normal components of the stress tensor, active in the x_1- and x_3- directions, respectively. These are in turn coupled to the fluid phase particle velocity by the filtration velocity. Equations 2.9c and 2.9d represent the two shear stress components, which are equal in magnitude, but differ in direction: one is acting on an arbitrary x_1- directed plane in the x_3- direction, and the other is acting on an arbitrary x_3- directed plane in the x_1- direction. The shear stress components are responsible for the independent shear wave propagation (in combination with the equation of motion 2.7), because of their ability to form a rotational acceleration of particles.

Scalar volume-averaged deformation equation for the pressure field in the bulk,

$$s\hat{p} + C\left(\partial_1\hat{v}_1 + \partial_3\hat{v}_3\right) + M\left(\partial_1\hat{w}_1 + \partial_3\hat{w}_3\right) = C\left(\hat{h}_{11} + \hat{h}_{33}\right) + M\hat{q}, \tag{2.10}$$

The elastic medium parameters are denoted by C and M. The volume injection rate is denoted by $\hat{q}$. This equation together with the equation of motion describes the propagation of a diffusive dilational wave, referred to the P-wave of the second kind. The wave equation is derived in paragraph 2.5.3.

2.5.2 The electromagnetic wave equation

By substituting the $\zeta\hat{H}_2$ component of Faraday's law 2.6 into Ampere's law 2.5 the electric field wave equation is obtained, which is coupled to the filtration velocity,

$$\partial_3\left(\partial_1\hat{E}_3 - \partial_3\hat{E}_1\right) + \zeta\left(\hat{\sigma}^e + s\varepsilon - \hat{L}\hat{\xi}\right)\hat{E}_1 + \zeta\hat{\xi}\hat{w}_1 = -\zeta\hat{J}^e_1 + \partial_3\hat{J}^m_2, \tag{2.11a}$$

$$\partial_1\left(\partial_3\hat{E}_1 - \partial_1\hat{E}_3\right) + \zeta\left(\hat{\sigma}^e + s\varepsilon - \hat{L}\hat{\xi}\right)\hat{E}_3 + \zeta\hat{\xi}\hat{w}_3 = -\zeta\hat{J}^e_3 - \partial_1\hat{J}^m_2, \tag{2.11b}$$

By taking the divergence of equation 2.11 it can be shown that ,

$$\left(\hat{\sigma}^e + s\varepsilon - \hat{L}\hat{\xi}\right)\left(\partial_1\hat{E}_1 + \partial_3\hat{E}_3\right) + \hat{\xi}\left(\partial_1\hat{w}_1 + \partial_3\hat{w}_3\right) = -\left(\partial_1\hat{J}^e_1 + \partial_3\hat{J}^e_3\right), \tag{2.12}$$

which shows that in a homogeneous isotropic fluid the electric field, the divergence of electric sources is linearly coupled to the divergence of the filtration velocity. When the electromagnetic sources are omitted this can be understood more intuitively in that a relative fluid motion is opposed by an electric field vector, simply because the relative motion of the surface ions at the EDL results in a electric field gradient in the opposite direction.

Equations 2.11 and 2.12 will be used to show that the elastodynamic wave equations are coupled to the electric wave equation. The filtration velocity plays the key role here.

2.5.3 Dilatational waves of the second kind coupled to electromagnetic waves

The elastodynamic wave equation for the fluid phase is derived by substituting the pressure-strain relation 2.10 into the equation of motion 2.8,

$$s^2\rho^f\hat{v}_1^s - C\partial_1\left(\partial_1\hat{v}_1^s + \partial_3\hat{v}_3^s\right) + s\eta\left(\hat{w}_1 - \hat{L}\hat{E}_1\right)/\hat{k} - M\partial_1\left(\partial_1\hat{w}_1 + \partial_3\hat{w}_3\right)$$
$$= s\hat{f}_1^f - C\partial_1\left(\hat{h}_{11} + \hat{h}_{33}\right) - M\partial_1\hat{q}, \quad (2.13a)$$

$$s^2\rho^f\hat{v}_3^s - C\partial_3\left(\partial_1\hat{v}_1^s + \partial_3\hat{v}_3^s\right) + s\eta\left(\hat{w}_3 - \hat{L}\hat{E}_3\right)/\hat{k} - M\partial_3\left(\partial_1\hat{w}_1 + \partial_3\hat{w}_3\right)$$
$$= s\hat{f}_3^f - C\partial_3\left(\hat{h}_{11} + \hat{h}_{33}\right) - M\partial_3\hat{q}. \quad (2.13b)$$

The filtration velocity and its divergence in 2.13 are eliminated by substituting electric field equations 2.11 and 2.12. This results in a relation which shows the coupling of the electric field strength to the relative particle velocity in the solid,

$$\begin{aligned} &s^2\rho^f\hat{v}_1^s - C\partial_1\left(\partial_1\hat{v}_1^s + \partial_3\hat{v}_3^s\right) \\ &- \frac{s\eta}{\hat{\xi}\hat{k}}\left[\zeta^{-1}\partial_3\left(\partial_1\hat{E}_3 - \partial_3\hat{E}_1\right) + \left(\hat{\sigma}^e + s\varepsilon\right)\hat{E}_1\right] + \frac{M\left(\hat{\sigma}^e + s\varepsilon - \hat{L}\hat{\xi}\right)}{\hat{\xi}}\partial_1\left(\partial_1\hat{E}_1 + \partial_3\hat{E}_3\right) \\ &\quad = s\hat{f}_1^f - C\partial_1\left(\hat{h}_{11} + \hat{h}_{33}\right) - M\partial_1\hat{q} + \frac{s\eta}{\hat{\xi}\hat{k}}\left(\hat{J}_1^e - \zeta^{-1}\partial_3\hat{J}_2^m\right) \\ &\quad\quad - \frac{M}{\hat{\xi}}\partial_1\left(\partial_1\hat{J}_1^e + \partial_3\hat{J}_3^e\right), \end{aligned} \quad (2.14a)$$

$$\begin{aligned} &s^2\rho^f\hat{v}_3^s - C\partial_3\left(\partial_1\hat{v}_1^s + \partial_3\hat{v}_3^s\right) \\ &- \frac{s\eta}{\hat{\xi}\hat{k}}\left[\zeta^{-1}\partial_1\left(\partial_3\hat{E}_1 - \partial_1\hat{E}_3\right) + \left(\hat{\sigma}^e + s\varepsilon\right)\hat{E}_3\right] + \frac{M\left(\hat{\sigma}^e + s\varepsilon - \hat{L}\hat{\xi}\right)}{\hat{\xi}}\partial_3\left(\partial_1\hat{E}_1 + \partial_3\hat{E}_3\right) \\ &\quad = s\hat{f}_3^f - C\partial_3\left(\hat{h}_{11} + \hat{h}_{33}\right) - M\partial_3\hat{q} + \frac{s\eta}{\hat{\xi}\hat{k}}\left(\hat{J}_3^e + \zeta^{-1}\partial_1\hat{J}_2^m\right) \\ &\quad\quad - \frac{M}{\hat{\xi}}\partial_3\left(\partial_1\hat{J}_1^e + \partial_3\hat{J}_3^e\right), \end{aligned} \quad (2.14b)$$

The wave equation for the divergence of the electric field strength coupled to the divergence of the particle velocity is obtained by taking the divergence of 2.14, resulting in a scalar wave equation describing the coupled dilatational wave of the second kind,

$$\begin{aligned} &\left[s^2\rho^f - C\left(\partial_1^2 + \partial_3^2\right)\right]\left(\partial_1\hat{v}_1 + \partial_3\hat{v}_3\right) \\ &- \left[\frac{s\eta}{\hat{\xi}\hat{k}}\left(\hat{\sigma}^e + s\varepsilon\right) - \frac{\left(\hat{\sigma}^e + s\varepsilon - \hat{L}\hat{\xi}\right)M}{\hat{\xi}}\left(\partial_1^2 + \partial_3^2\right)\right]\left(\partial_1\hat{E}_1 + \partial_3\hat{E}_3\right) \\ &\quad = s\left(\partial_1\hat{f}_1^f + \partial_3\hat{f}_3^f\right) - \left(\partial_1^2 + \partial_3^2\right)\left[C\left(\hat{h}_{11} + \hat{h}_{33}\right) + M\hat{q}\right] \\ &\quad\quad \frac{s\eta}{\hat{\xi}\hat{k}}\left(\partial_1\hat{J}_1^e + \partial_3\hat{J}_3^e\right) - \frac{M}{\hat{\xi}}\left(\partial_1^2 + \partial_3^2\right)\left(\partial_1\hat{J}_1^e + \partial_3\hat{J}_3^e\right) \end{aligned} \quad (2.15)$$

In line with Biot [2], the rotation is also applied to the equation describing the wave propagation. In the purely elastodynamic case in Biot's paper [2] the rotation gave zero, because there this equation described the wave propagation in the fluid phase and the perfect fluids are unable to sustain a circulation. To see whether rotational waves exist in the wave equation of the volume averaged form of the relative movement between fluid and solid particles, the curl must be taken of 2.14. This does not result in zero. The curl of the 2.14 results in a vectorial equation, for which the components in x_1- and x_3- directions are zero, but the x_2 component is given by,

$$
\begin{aligned}
s^2\rho^f\left(\partial_3\hat{v}_1^s-\partial_1\hat{v}_3^s\right)-\frac{s\eta}{\hat{\xi}\hat{k}}\left[\zeta^{-1}\left(\partial_1^2+\partial_3^2\right)-\left(\hat{\sigma}^e+s\epsilon\right)\right]\left(\partial_1\hat{E}_3-\partial_3\hat{E}_1\right)& \\
=s\left(\partial_3\hat{f}_1^f-\partial_1\hat{f}_3^f\right)+\frac{s\eta}{\hat{\xi}\hat{k}}\left[\partial_3\hat{J}_1^e-\partial_1\hat{J}_3^e-\zeta^{-1}\left(\partial_1^2+\partial_3^2\right)\hat{J}_2^m\right]& \quad (2.16)
\end{aligned}
$$

When we analyse the left-hand-side terms we see that the electromagnetic wave operator acts on the curl of the electric field. However, no shear wave operator acts on the curl of the particle velocity in the solid. When we would ignore the source terms on the right-hand-side, we would have an independent electromagnetic wave, which induces a dependent circulation of the particles of the solid. This coupling of the electromagnetic wave to this particle circulation depends highly on the fluid viscosity, because this medium parameter is multiplied with the electromagnetic wave equation in 2.16. According to that, an increase of fluid viscosity, when assuming all other parameters remain constant, will yield a stronger rotation in the particle velocity field. This dependent rotational flow, is referred to as the coelectric field. The coelectric field cannot exist without the electromagnetic wave, except at the source location.

2.5.4 Dilatational waves of the first kind and shear waves coupled to electromagnetic waves

The traction vector components in the equation of motion 2.7 are eliminated by substituting the deformation equation 2.9,

$$
\begin{aligned}
s^2\rho\hat{v}_1^s-\partial_1\left(S_{1111}\partial_1\hat{v}_1^s+S_{1133}\partial_3\hat{v}_3^s\right)-S_{1313}\partial_3\left(\partial_3\hat{v}_1^s+\partial_1\hat{v}_3^s\right)& \\
+s^2\rho^f\hat{w}_1-C\partial_1\left(\partial_1\hat{w}_1+\partial_3\hat{w}_3\right)& \\
=s\hat{f}_1-S_{1111}\partial_1\hat{h}_{11}-S_{1133}\partial_1\hat{h}_{33}-2S_{1313}\partial_3\hat{h}_{13}-C\partial_1\hat{q}& \quad (2.17a)
\end{aligned}
$$

$$
\begin{aligned}
s^2\rho\hat{v}_3^s-\partial_3\left(S_{3333}\partial_3\hat{v}_3^s+S_{3311}\partial_1\hat{v}_1^s\right)-S_{3131}\partial_1\left(\partial_1\hat{v}_3^s+\partial_3\hat{v}_1^s\right)& \\
+s^2\rho^f\hat{w}_3-C\partial_3\left(\partial_1\hat{w}_1+\partial_3\hat{w}_3\right)& \\
=s\hat{f}_3-S_{3333}\partial_3\hat{h}_{33}-S_{3311}\partial_3\hat{h}_{11}-2S_{3113}\partial_3\hat{h}_{13}-C\partial_3\hat{q}& \quad (2.17b)
\end{aligned}
$$

From 2.17 the filtration velocity and its divergence are eliminated using again equations 2.11 and 2.12. At the same time the stiffness parameter constants S are substituted for, so that the solid particle velocity and its divergence can be written explicitly. The result is the vectorial wave equation for the electric field coupled to the particle velocity of the bulk, given in equation 2.19. From this equation onwards, the following medium parameter substitution is made in order to simplify the equations,

$$\varsigma = \hat{\sigma}^e + s\varepsilon - \hat{L}\hat{\xi} \tag{2.18}$$

$$\begin{aligned}
s^2\rho\hat{v}_1^s - \left[K_G + G^{(fr)}/3\right]\partial_1\left(\partial_1\hat{v}_1^s + \partial_3\hat{v}_3^s\right) - G^{(fr)}\left(\partial_1^2 + \partial_3^2\right)\hat{v}_1^s \\
- \frac{s^2\rho^f}{\hat{\xi}}\left(\zeta^{-1}\partial_3\left(\partial_1\hat{E}_3 - \partial_3\hat{E}_1\right) + \varsigma\hat{E}_1\right) + \frac{C\varsigma}{\hat{\xi}}\partial_1\left(\partial_1\hat{E}_1 + \partial_3\hat{E}_3\right) \\
= s\hat{f}_1 - S_{1111}\partial_1\hat{h}_{11} - S_{1133}\partial_1\hat{h}_{33} - 2S_{1313}\partial_3\hat{h}_{13} - C\partial_1\hat{q} \\
+ \frac{s^2\rho^f}{\hat{\xi}}\left(\hat{J}_1^e - \zeta^{-1}\partial_3\hat{J}_2^m\right) - \frac{C}{\hat{\xi}}\partial_1\left(\partial_1\hat{J}_1^e + \partial_3\hat{J}_3^e\right)
\end{aligned} \tag{2.19a}$$

$$\begin{aligned}
s^2\rho\hat{v}_3^s - \left[K_G + G^{(fr)}/3\right]\partial_3\left(\partial_1\hat{v}_1^s + \partial_3\hat{v}_3^s\right) - G^{(fr)}\left(\partial_1^2 + \partial_3^2\right)\hat{v}_3^s \\
- \frac{s^2\rho^f}{\hat{\xi}}\left(\zeta^{-1}\partial_1\left(\partial_3\hat{E}_1 - \partial_1\hat{E}_3\right) + \varsigma\hat{E}_3\right) + \frac{C\varsigma}{\hat{\xi}}\partial_3\left(\partial_1\hat{E}_1 + \partial_3\hat{E}_3\right) \\
= s\hat{f}_3 - S_{3333}\partial_3\hat{h}_{33} - S_{3311}\partial_3\hat{h}_{11} - 2S_{3113}\partial_1\hat{h}_{13} - C\partial_3\hat{q} \\
+ \frac{s^2\rho^f}{\hat{\xi}}\left(\hat{J}_3^e + \zeta^{-1}\partial_1\hat{J}_2^m\right) - \frac{C}{\hat{\xi}}\partial_3\left(\partial_1\hat{J}_1^e + \partial_3\hat{J}_3^e\right)
\end{aligned} \tag{2.19b}$$

The wave equation for the divergence of the electric field strength coupled to the divergence of the particle velocity is obtained by taking the divergence of 2.19. This wave equation describes coupled dilational waves of the first kind,

$$\begin{aligned}
\left[s^2\rho - H\left(\partial_1^2 + \partial_3^2\right)\right]\left(\partial_1\hat{v}_1^s + \partial_3\hat{v}_3^s\right) - \frac{\varsigma}{\hat{\xi}}\left[s^2\rho^f - C\left(\partial_1^2 + \partial_3^2\right)\right]\left(\partial_1\hat{E}_1 + \partial_3\hat{E}_3\right) \\
= s\left(\partial_1\hat{f}_1 + \partial_3\hat{f}_3\right) - \partial_1^2\left(S_{1111}\hat{h}_{11} + S_{1133}\hat{h}_{33}\right) - 4S_{1313}\partial_1\partial_3\hat{h}_{13} - \partial_3^2\left(S_{3311}\hat{h}_{11} + S_{3333}\hat{h}_{33}\right) \\
- C\left(\partial_1^2 + \partial_3^2\right)\hat{q} + \xi^{-1}\left[s^2\rho^f - C\left(\partial_1^2 + \partial_3^2\right)\right]\left(\partial_1\hat{J}_1^e + \partial_3\hat{J}_3^e\right)
\end{aligned} \tag{2.20}$$

In order to observe for this wave equation the coupled vertically polarized shear wave as well, the curl must be taken of equation 2.19. In the resulting vector equation only the component in the x_2- direction is non zero,

$$\begin{aligned}
\left[s^2\rho - G^{(fr)}\left(\partial_1^2 + \partial_3^2\right)\right]\left(\partial_3\hat{v}_1^s - \partial_1\hat{v}_3^s\right) \\
- \frac{s^2\rho^f}{\hat{\xi}}\left[\zeta^{-1}\left(\partial_1^2 + \partial_3^2\right) - \varsigma\right]\left(\partial_1\hat{E}_3 - \partial_3\hat{E}_1\right) \\
= s\left(\partial_3\hat{f}_1 - \partial_1\hat{f}_3\right) + 2G\left(\partial_1\partial_3\hat{h}_{33} - \partial_3\partial_1\hat{h}_{11}\right) \\
+ \frac{s^2\rho^f}{\hat{\xi}}\left[\partial_3\hat{J}_1^e - \partial_1\hat{J}_3^e - \zeta^{-1}\left(\partial_1^2 + \partial_3^2\right)\hat{J}_2^m\right]
\end{aligned} \tag{2.21}$$

The curl operation eliminated all divergence terms of the wave equation 2.19, as well as the terms related to the bulk modulus K^G. The equation resembles 2.16, but it contains now an elastic shear wave operator acting on the curl of the particle velocity in the solid and a wave operator, that contains both the electromagnetic parameters and the coupling coefficients, that acts on the curl of the electric field. This is not surprising, because this wave equation is derived from an equation of motion 2.7, which is the volume-averaged form of the fluid and solid equations of motion added together [2], and shear waves can sustain in the solid phase.

What has been done in the preceding paragraphs: first the two elastodynamic vectorial wave equations are derived from the two different equations of motion 2.8 and 2.7. Subsequently the electric field wave equation coupled to the filtration velocity is substituted in the two wave equations. This resulted in coupled particle velocity-electric field vectorial wave equations, 2.14 and 2.19. By taking the divergence of these wave equations the dilatational wave behaviour can be analysed, alternatively the curl can be taken in order to analyse the transversal wave behaviour. In the following paragraphs we continue to simplify these two sets of wave equations to one main wave equation.

2.5.5 Derivation of the P-SV-TM mode Green's function

We use the divergence wave equations 2.15 (electrically coupled P-waves of the second kind) and 2.20 (electrically coupled P-waves of the first kind) to find separate expressions for the divergence of the electric field and the divergence of the particle velocity, in the three-dimensional wavenumber domain. Equations 2.15 and 2.20 in the wavenumber domain are given as,

$$
\begin{aligned}
&\left[s^2\rho^f + C\left(k_1^2+k_3^2\right)\right] i\left(k_1\breve{v}_1 + k_3\breve{v}_3\right) \\
&\qquad - \frac{\varsigma}{\hat{\xi}}\left[\frac{s\eta}{\varsigma\hat{k}}\left(\varsigma + \hat{L}\hat{\xi}\right) + M\left(k_1^2+k_3^2\right)\right] i\left(k_1\breve{E}_1 + k_3\breve{E}_3\right) \\
&\qquad = si\left(k_1\breve{f}_1^f + k_3\breve{f}_3^f\right) - \left(k_1^2+k_3^2\right)\left(C\left(\breve{h}_{11}+\breve{h}_{33}\right) + M\breve{q}\right) \\
&\qquad\qquad + \hat{\xi}^{-1}\left(\frac{s\eta}{\hat{k}} + M\left(k_1^2+k_3^2\right)\right) i\left(k_1\breve{J}_1^e + k_3\breve{J}_3^e\right). \qquad (2.22)
\end{aligned}
$$

$$
\begin{aligned}
&\left[s^2\rho + H\left(k_1^2+k_3^2\right)\right] i\left(k_1\breve{v}_1 + k_3\breve{v}_3\right) \\
&\qquad - \frac{\varsigma}{\hat{\xi}}\left[s^2\rho^f + C\left(k_1^2+k_3^2\right)\right] i\left(k_1\breve{E}_1 + k_3\breve{E}_3\right) \\
&\qquad = si\left(k_1\breve{f}_1 + k_3\breve{f}_3\right) - k_1^2\left(S_{1111}\breve{h}_{11} + S_{1133}\breve{h}_{33}\right) - 4S_{1313}k_1k_3\breve{h}_{13} \\
&\qquad\qquad - k_3^2\left(S_{3311}\breve{h}_{11} + S_{3333}\breve{h}_{33}\right) - C\left(k_1^2+k_3^2\right)\breve{q} \\
&\qquad\qquad + \hat{\xi}^{-1}\left[s^2\rho^f + C\left(k_1^2+k_3^2\right)\right] i\left(k_1\breve{J}_1^e + k_3\breve{J}_3^e\right). \qquad (2.23)
\end{aligned}
$$

Subsequently, the equations 2.22 and 2.23 can be written in matrix form, due to the resemblance between their left-hand-side terms, which contain the divergence of the particle velocity and electric field,

$$
\begin{bmatrix} L_1 & -\varsigma L_2/\hat{\xi} \\ L_3 & -\varsigma L_1/\hat{\xi} \end{bmatrix} \begin{bmatrix} ik_1\breve{v}_1 + ik_3\breve{v}_3 \\ ik_1\breve{E}_1 + ik_3\breve{E}_3 \end{bmatrix} = \begin{bmatrix} X_1 \\ X_2 \end{bmatrix}, \tag{2.24}
$$

Where, $L_1 = s^2\rho^f + C\left(k_1^2 + k_3^2\right)$ and $L_2 = (s^2\rho^E\left(1 + \hat{L}\hat{\xi}/\varsigma\right) + M\left(k_1^2 + k_3^2\right))$ and $L_3 = s^2\rho + H\left(k_1^2 + k_3^2\right)$

The expression 2.24 expresses the divergence of the electric field and the particle velocity in terms of sources and medium parameters. The vectorial wave equations 2.14 and 2.19 contain these divergence terms, which can now be rewritten as source terms and put on the right-hand-side, resulting in the following vectorial wave equations in the wavenumber frequency domain, the relative fluid particle velocity coupled to the electric field,

$$
\begin{aligned}
s^2\rho^f\breve{v}_1 - \frac{s\eta}{\hat{\xi}\hat{k}\zeta}\left(k_1^2 + k_3^2 + \zeta\varsigma + \zeta\hat{\xi}\hat{L}\right)\breve{E}_1 = X_{11,1} \\
= Cik_1\frac{L_1X_1 - L_2X_2}{L_1^2 - L_2L_3} + \xi^{-1}\left(\frac{s\eta}{\zeta k} - M\varsigma\right)ik_1\frac{\xi}{\varsigma}\frac{L_3X_1 - L_1X_2}{L_1^2 - L_2L_3} \\
+ s\breve{f}_1^f + Cik_1\left(\breve{h}_{11} + \breve{h}_{33}\right) + Mik_1\breve{q} \\
+ \frac{s\eta}{\xi k}\left(\breve{J}_1^e + \zeta^{-1}ik_3\breve{J}_2^m\right) + \frac{M}{\xi}k_1\left(k_1\breve{J}_1^e + k_3\breve{J}_3^e\right)
\end{aligned} \tag{2.25a}
$$

$$
\begin{aligned}
s^2\rho^f\breve{v}_3 - \frac{s\eta}{\hat{\xi}\hat{k}\zeta}\left(k_1^2 + k_3^2 + \zeta\varsigma + \zeta\hat{\xi}\hat{L}\right)\breve{E}_3 = X_{11,3} \\
= Cik_3\frac{L_1X_1 - L_2X_2}{L_1^2 - L_2L_3} + \xi^{-1}\left(\frac{s\eta}{\zeta k} - M\varsigma\right)ik_3\frac{\xi}{\varsigma}\frac{L_3X_1 - L_1X_2}{L_1^2 - L_2L_3} \\
+ s\breve{f}_3^f + Cik_3\left(\breve{h}_{11} + \breve{h}_{33}\right) + Mik_3\breve{q} \\
+ \frac{s\eta}{\xi k}\left(\breve{J}_3^e - \zeta^{-1}ik_1\breve{J}_2^m\right) + M\xi^{-1}\left(k_3k_1\breve{J}_1^e + k_3^2\breve{J}_3^e\right)
\end{aligned} \tag{2.25b}
$$

as well as the volume averaged bulk particle velocity coupled to the electric field,

$$
\begin{aligned}
\left(s^2\rho + G^{(fr)}(k_1^2 + k_3^2)\right)\breve{v}_1 - \frac{s^2\rho^f}{\hat{\xi}\zeta}\left(k_1^2 + k_3^2 + \zeta\varsigma\right)\breve{E}_1 = X_{22,1} \\
= \left(K_G + \frac{G^{(fr)}}{3}\right)ik_1\frac{L_1X_1 - L_2X_2}{L_1^2 - L_2L_3} + \xi^{-1}\left(\frac{s^2\rho^f}{\zeta} - C\varsigma\right)ik_1\frac{\xi}{\varsigma}\frac{L_3X_1 - L_1X_2}{L_1^2 - L_2L_3} \\
+ s\breve{f}_1 + ik_1\left(S_{1111}\breve{h}_{11} + S_{1133}\breve{h}_{33}\right) + 2S_{1313}ik_3\breve{h}_{13} + Cik_1\breve{q} \\
+ \frac{s^2\rho^f}{\xi}\left(\breve{J}_1^e + \zeta^{-1}ik_3\breve{J}_2^m\right) + \frac{C}{\xi}k_1\left(k_1\breve{J}_1^e + k_3\breve{J}_3^e\right)
\end{aligned} \tag{2.26a}
$$

$$
\begin{aligned}
&\left(s^2\rho + G^{(fr)}(k_1^2+k_3^2)\right)\breve{v}_3 - \frac{s^2\rho^f}{\hat{\xi}\zeta}\left(k_1^2+k_3^2+\zeta\varsigma\right)\breve{E}_3 = X_{22,3} \\
&\quad = \left(K_G + \frac{G^{(fr)}}{3}\right) ik_3 \frac{L_1X_1 - L_2X_2}{L_1^2 - L_2L_3} + \xi^{-1}\left(\frac{s^2\rho^f}{\zeta} - C\varsigma\right) ik_3 \frac{\xi}{\varsigma}\frac{L_3X_1 - L_1X_2}{L_1^2 - L_2L_3} \\
&\qquad + s\breve{f}_3 + ik_3\left(S_{1111}\breve{h}_{11} + S_{3333}\breve{h}_{33}\right) + 2S_{1313}ik_1\breve{h}_{13} + Cik_3\breve{q} \\
&\qquad\quad + \frac{s^2\rho^f}{\xi}\left(\breve{J}_3^e - \zeta^{-1}ik_1\breve{J}_2^m\right) + \frac{C}{\xi}k_3\left(k_1\breve{J}_1^e + k_3\breve{J}_3^e\right) \qquad (2.26b)
\end{aligned}
$$

X_{11} and X_{22} represent the source terms, including the rewritten divergence terms, which are presented in Appendix B.

By substituting the particle velocity of the relative fluid wave equation into the bulk wave equation, an equation describing the electric field variation is obtained,

$$
\begin{aligned}
&\left(k_1^2+k_3^2+\gamma_S^2\right)\left(k_1^2+k_3^2+\gamma_{EM}^2\right)\breve{E}_{1;3} \\
&\qquad = -\frac{\zeta\hat{L}}{s}\left(k_1^2+k_3^2+\frac{s^2\rho}{G^{(fr)}}\right)X_{11,1;3} + \frac{s\rho^f\zeta\hat{L}}{G^{(fr)}}X_{22,1;3} \qquad (2.27)
\end{aligned}
$$

This equation encompasses the entire set of equations for the 2D SV-P-TM mode, expressed in terms of the electric field component.
The equivalent expression for the particle velocity can be obtained by substituting the electric field vector of the fluid wave equation into the bulk wave equation, which results in,

$$
\begin{aligned}
&\left(k_1^2+k_3^2+\gamma_S^2\right)\left(k_1^2+k_3^2+\gamma_{EM}^2\right)\breve{v}_{1;3} \\
&\qquad = -\frac{\hat{k}s\rho^f}{\eta G^{fr}}\left(k_1^2+k_3^2+\zeta\varsigma\right)X_{11,i} + \frac{1}{G^{fr}}\left(k_1^2+k_3^2+\zeta(\varsigma+\hat{L}\hat{\xi})\right)X_{22,i} \qquad (2.28)
\end{aligned}
$$

This equation encompasses the entire set of equations for the 2D SV-P-TM mode, expressed in terms of the bulk particle velocity field component. Note that the operators in the left-hand-sides of both second order wave equations 2.27 and 2.28 are equal. Therefore, both wave equations have an equal Greens function solution, $\breve{G}$, which represents the total mechanism behind the coupling of SV to TM wave fields. Note that the right-hand-side terms of equations 2.27 and 2.28 are quite different. This difference arises from the fact that the coupling mechanism leading from a certain source to a resulting electric field disturbance occurs in a completely different manner than the coupling mechanism leading from the same source to a solid particle velocity field disturbance. For example a bulk dipole force can yield a mechanical wave field directly, but will never directly generate an electric field. The latter can only happen indirectly via the coupling mechanism at the electric double layer. Therefore, the mechanism leading to the electric field distortion is of a different nature than the mechanism leading to the particle velocity disturbance. These mechanisms can be analysed exactly by deriving the Green's functions describing the E_1 and v_1 field responses due to each different source type. These expressions are obtained in the next section.

2.6 Solutions to the Green's functions for all sources

The expressions describing the horizontal component of the electric and particle velocity impulse field responses due to any specific source type are obtained by setting all other source functions to zero, except for the one in question, which is set to one (Delta dirac function in space-time domain). Furthermore, the total Green's function $\breve{G}$ is substituted, which incorporates the Green's functions for the TM and SV wave fields. The Green's function describing the coupled P-waves, $\breve{G}_{PP}$, is substituted as well. Both resulting expressions for the electric and particle velocity horizontal components contain all possible seismoelectric wave fields of the P-SV-TM system: the fast dilatational, slow dilatational, vertical polarized shear and the transverse magnetic mode of the electromagnetic wave fields. This is because in principal any disturbance of the EDL has the potential to generate these four wave fields. However, the extend in which each of these fields are generated varies depending on the source type and measured field component. In all expressions different weighting factors apply on these four wave fields, which consist of combinations of the medium parameters. The weighting factors can be considered as factors, which define the strength of the coupling of that specific source type to the evaluated field component. In Chapter 4 these coupling factors are analysed exactly by modelling the four different wave fields for each specific source and receiver couple. In this section spatial derivatives acting on the constituent Green's functions of the different expressions are analysed and a physical interpretation is given. Although the expressions are derived only for the horizontal component of the measured field, the vertical component of the field is occasionally discussed as well. In most cases the structure of this vertical component can be easily derived from the horizontal component field by simply changing the component of the spatial derivatives or adding extra terms. To see the details of this redundancy between components, as well as the specification of the coupling factors active on the Green's functions, refer to Appendix B. For notational convenience, the 'solid particle velocity' is referred to as the 'particle velocity' and is denoted without the subscript 's', as v, from this point onward.

2.6.1 The force acting on the bulk

The reaction of the x-component of the particle velocity as well as the electric field strength to a force acting on the bulk phase of the medium is analysed here. This mechanical force behaves like a dipole. The bulk refers to the volume-averaged combination of both the solid and the fluid phases in the medium, therefore in principle this force is acting on both phases.

The x_1-component of the bulk particle velocity field generated by an x_1-directed force acting on the bulk is given by,

$$\begin{aligned}\breve{G}^{v_1,f_1} =& C_{S1}^{v1,f} ik_1 ik_1 \breve{G}_S + C_{EM1}^{v1,f} ik_1 ik_1 \breve{G}_{EM} + C_{Ps}^{v1,f} ik_1 ik_1 \breve{G}_{Ps} + C_{Pf}^{v1,f} ik_1 ik_1 \breve{G}_{Pf}\\ & C_{S2}^{v1,f1} \breve{G}_S + C_{EM2}^{v1,f1} \breve{G}_{EM}\end{aligned} \tag{2.29}$$

The same field component generated by a x_3-directed force acting on the bulk,

$$\breve{G}^{v_1,f_3} = C_{S1}^{v1,f} ik_3 ik_1 \breve{G}_S + C_{EM1}^{v1,f} ik_3 ik_1 \breve{G}_{EM} + C_{Ps}^{v1,f} ik_3 ik_1 \breve{G}_{Ps} + C_{Pf}^{v1,f} ik_3 ik_1 \breve{G}_{Pf} \quad (2.30)$$

Observe that both force components generate the divergence of all four wave fields. Due to the horizontal spatial variation of this divergence the particles of the bulk are brought into a horizontal movement. The vertical component of the particle velocity vector would be activated due to the vertical spatial variation of this divergence. Note that only the horizontal component of the bulk force has the ability to generate an isotropic shear wave and an electromagnetic wave. This is visible in equation 2.29, which contains two scalar SV and EM Green's functions, which are not present in equation 2.32. In fact, the vertical component of the force vector also contributes to these two wave fields, but only to the vertical component of the particle velocity. No spatial variation is required when the force acts parallel to the receiver direction. The structure of the Green's function relating the bulk force components to the horizontal electric component is equivalent to the particle velocity relation,

$$\begin{aligned}\breve{G}^{E_1,f_1} =& C_{S1}^{E1,f1} ik_1 ik_1 \breve{G}_S + C_{EM1}^{E1,f1} ik_1 ik_1 \breve{G}_{EM} + C_{Ps}^{E1,f1} ik_1 ik_1 \breve{G}_{Ps} + C_{Ps}^{E1,f1} ik_1 ik_1 \breve{G}_{Pf} \\ &+ C_{S2}^{E1,f1} \breve{G}_S + C_{EM2}^{E1,f1} \breve{G}_{EM} \qquad (2.31)\end{aligned}$$

$$\breve{G}^{E_1,f_3} = C_{S}^{E1,f3} ik_1 ik_3 \breve{G}_S + C_{EM}^{E1,f3} ik_1 ik_3 \breve{G}_{EM} + C_{Pf}^{E1,f3} ik_1 ik_3 \breve{G}_{Ps} + C_{Pf}^{E1,f3} ik_1 ik_3 \breve{G}_{Pf} \qquad (2.32)$$

The difference lies in the constants operating on the intrinsic Green's function. The question is whether this electric field is a dominated by the coseismic field, generated by the particle motion induced by the bulk force by the process discussed for equation 2.29 and 2.30, or whether it is dominated by an actual electromagnetic wave field which is generated directly at the source location, due to source to field conversion. In Chapter 4 on Green's function analysis the different contributions per field will be modelled in order to constrain this.

2.6.2 The force acting on the fluid phase

This dipole force is in reality not an independent force, because it is in fact an intrinsic part of the bulk force. However, it is still of interest to examine it separately in theory. Note that the structure of the Green's functions due to the fluid phase force and the bulk force are the same. This is not unexpected considering that the fluid force forms a part of the bulk force. The actual difference between the effects of these forces can only be analysed exactly in the modelling experiment in Chapter 4

The particle velocity field due to this force acting on the fluid is given by,

$$\begin{aligned}\breve{G}^{v1,f_1^f} =& C_{S1}^{v1,ff} ik_1 ik_1 \breve{G}_S + C_{EM1}^{v1,ff} ik_1 ik_1 \breve{G}_{EM} + C_{Ps}^{v1,ff} ik_1 ik_1 \breve{G}_{Ps} + C_{Pf}^{v1,ff} ik_1 ik_1 \breve{G}_{Pf} \\ &+ C_{S2}^{v1,ff} \breve{G}_S + C_{EM2}^{v1,ff} \breve{G}_{EM} \qquad (2.33)\end{aligned}$$

$$\breve{G}^{v1,f_3^f} = C_{S1}^{v1,ff} ik_1 ik_3 \breve{G}_S + C_{EM1}^{v1,ff} ik_1 ik_3 \breve{G}_{EM} + C_{Ps}^{v1,ff} ik_1 ik_3 \breve{G}_{Ps} + C_{Pf}^{v1,ff} ik_1 ik_3 \breve{G}_{Pf} \tag{2.34}$$

The electric field strength is given by,

$$\begin{aligned} \breve{G}^{E1,f_1^f} &= C_{S1}^{E1,ff} ik_1 ik_1 \breve{G}_S + C_{EM1}^{E1,ff} ik_1 ik_1 \breve{G}_{EM} + C_{Ps}^{E1,ff} ik_1 ik_1 \breve{G}_{Ps} + C_{Pf}^{E1,ff} ik_1 ik_1 \breve{G}_{Pf} \\ &+ C_{S2}^{E1,ff} \breve{G}_S + C_{EM2}^{E1,ff} \breve{G}_{EM} \end{aligned} \tag{2.35}$$

$$\breve{G}^{E1,f_3^f} = C_{S1}^{E1,ff} ik_1 ik_3 \breve{G}_S + C_{EM1}^{E1,ff} ik_1 ik_3 \breve{G}_{EM} + C_{Ps}^{E1,ff} ik_1 ik_3 \breve{G}_{Ps} + C_{Pf}^{E1,ff} ik_1 ik_3 \breve{G}_{Pf} \tag{2.36}$$

2.6.3 Volume injection rate

This source type encompasses an injection of mass into the medium, which results in a source of a monopole nature. This implies that this source does not have a certain specified direction, as is the case for dipole source. The particle velocity field component is coupled to this source type as follows,

$$\breve{G}^{v1,q} = C_S^{v1,q} ik_1 \breve{G}_S + C_{EM}^{v1,q} ik_1 \breve{G}_{EM} + C_{Ps}^{v1,q} ik_1 \breve{G}_{Ps} + C_{Pf}^{v1,q} ik_1 \breve{G}_{Pf} \tag{2.37}$$

The vertical particle velocity component has a similar structure as this equation, but for the fact that the horizontal spatial derivative acting on each of the four wave fields as we seen in 2.37 would be replaced by a vertical one. Therefore, the total particle velocity wave field is coupled to this volume injection via the generated divergence of all wave fields. In other words, due the omnidirectional character of this volume injection the EDL is moved in all directions in the 2D medium, thereby generating all four wave fields. Except for the difference in the coupling factors, the electric field component shows the same structure as the particle velocity,

$$\breve{G}^{E1,q} = C_S^{E1,q} ik_1 \breve{G}_S + C_{EM}^{E1,q} ik_1 \breve{G}_{EM} + C_{Ps}^{E1,q} ik_1 \breve{G}_{Ps} + C_{Pf}^{E1,q} ik_1 \breve{G}_{Pf} \tag{2.38}$$

2.6.4 The shear strain sources

As explained in section 2.5.1 there are two strain sources h_{13} and h_{31} which together deform the framework of the bulk in a rotational sense. The resulting particle velocity component is related to the generated fields as follows,

$$
\begin{aligned}
\breve{G}^{v_1,h_{13}} &= C_{S1}^{v1,h13} ik_1 ik_1 ik_3 \breve{G}_S + C_{EM1}^{v1,h13} ik_1 ik_1 ik_3 \breve{G}_{EM} + \\
& C_{Ps}^{v1,h13} ik_1 ik_1 ik_3 \breve{G}_{Ps} + C_{Pf}^{v1,h13} ik_1 ik_1 ik_3 \breve{G}_{Pf} \\
& + C_{S2}^{v1,h13} ik_3 \breve{G}_S + C_{EM2}^{v1,h13} ik_3 \breve{G}_{EM}
\end{aligned} \tag{2.39}
$$

As well for the electric component, which has the same structure,

$$
\begin{aligned}
\breve{G}^{E_1,h_{13}} &= C_{S1}^{E1,h13} ik_1 ik_1 ik_3 \breve{G}_S + C_{EM1}^{E1,h13} ik_1 ik_1 ik_3 \breve{G}_{EM} \\
& + C_{Ps}^{E1,h13} ik_1 ik_1 ik_3 \breve{G}_{Ps} + C_{Pf}^{E1,h13} ik_1 ik_1 ik_3 \breve{G}_{Pf} \\
& + C_{S2}^{E1,h13} ik_3 \breve{G}_S + C_{EM2}^{E1,h13} ik_3 \breve{G}_{EM}
\end{aligned} \tag{2.40}
$$

In both equations the rotational deformation is coupled to the horizontal field components via the vertical spatial variation of the SV and EM wave fields. The field components seem to be coupled as well via the divergence of the double rotation of all four wave fields generated at the EDL. This can be interpreted from the $ik_1 ik_1 ik_3$ terms acting on all constituting Green's functions. These terms would be substituted by $ik_3 ik_1 ik_3$ when we would be looking at the vertical component of the measured fields.

2.6.5 The tensile strain source

The tensile strain source deforms the medium framework in perpendicular directions, without any angular deformation. The generated fields due to both components of the tensile strain source are analysed here. The effect of the horizontal component on the particle velocity wave field is as follows,

$$
\begin{aligned}
\breve{G}^{v1,h11} = C_{Ps}^{v1,h11} ik_1 \breve{G}_{Ps} + C_{Pf}^{v1,h11} ik_1 \breve{G}_{Pf} + C_{SV}^{v1,h11} ik_1 \breve{G}_S + C_{EM}^{v1,h11} ik_1 \breve{G}_{EM} \\
+ C_{*Ps_k1}^{v1} ik_1 ik_1 ik_1 \breve{G}_{Ps} + C_{*Ps_k3}^{v1} ik_3 ik_3 ik_1 \breve{G}_{Ps} \\
+ C_{*Pf_k1}^{v1} ik_1 ik_1 ik_1 \breve{G}_{Pf} + C_{*Pf_k3}^{v1} ik_3 ik_3 ik_1 \breve{G}_{Pf} \\
+ C_{*SV_k1}^{v1} ik_1 ik_1 ik_1 \breve{G}_{SV} + C_{*SV_k3}^{v1} ik_3 ik_3 ik_1 \breve{G}_{SV} \\
+ C_{*EM_k1}^{v1} ik_1 ik_1 ik_1 \breve{G}_{EM} + C_{*EM_k3}^{v1} ik_3 ik_3 ik_1 \breve{G}_{EM}
\end{aligned}
$$

For the operators on the shear terms in the h_{33} source greens function, the double k terms simply have to be switched, the rest stays the same.

$$
\begin{aligned}
\breve{G}^{v1,h33} = {} & C_{Ps}^{v1,h11} ik_1 \breve{G}_{Ps} + C_{Pf}^{v1,h11} ik_1 \breve{G}_{Pf} + C_{SV}^{v1,h11} ik_1 \breve{G}_{S} + C_{EM}^{v1,h11} ik_1 \breve{G}_{EM} \\
& + C_{*Ps_k 3}^{v1} ik_1 ik_1 ik_1 \breve{G}_{Ps} + C_{*Ps_k 1}^{v1} ik_3 ik_3 ik_1 \breve{G}_{Ps} \\
& + C_{*Pf_k 3}^{v1} ik_1 ik_1 ik_1 \breve{G}_{Pf} + C_{*Pf_k 1}^{v1} ik_3 ik_3 ik_1 \breve{G}_{Pf} \\
& + C_{*SV_k 3}^{v1} ik_1 ik_1 ik_1 \breve{G}_{SV} + C_{*SV_k 1}^{v1} ik_3 ik_3 ik_1 \breve{G}_{SV} \\
& + C_{*EM_k 3}^{v1} ik_1 ik_1 ik_1 \breve{G}_{EM} + C_{*EM_k 1}^{v1} ik_3 ik_3 ik_1 \breve{G}_{EM}
\end{aligned}
$$

The field due to both components consists of the horizontal part of the divergence of all wave fields, because when we would measure the vertical particle velocity field these single horizontal derivatives would be replaced by single vertical derivatives. Therefore, this part of the field expression has a similar structure as the field generated by a volume injection. This is as expected, because a tensile deformation of the medium affects the volume, for example strain acting equally from all sides on the system would result in a total volume decrease. If the strain would be of an extensional nature their acting would result in a volume increase, which is comparable to a volume injection into the system. However, the total of 8 extra terms containing third order spatial derivatives indicate that the tensile deformation of the framework is of a more complex nature than the volume injection and therefore quite unique. These terms are also dependent on the direction of the tensile deformation: the constants acting on the $ik_3ik_3ik_1$ terms in the h_{11} field act on the $ik_1ik_1ik_1$ terms in the h_{33} field, and vice versa. The electric field component generated by this tensile deformation has the same structure as its particle velocity equivalent,

$$
\begin{aligned}
\breve{G}^{E1,h11} = {} & C_{Ps}^{E1,h11} ik_1 \breve{G}_{Ps} + C_{Pf}^{E1,h11} ik_1 \breve{G}_{Pf} + C_{SV}^{E1,h11} ik_1 \breve{G}_{S} + C_{EM}^{E1,h11} ik_1 \breve{G}_{EM} \\
& + C_{*Ps_k 1}^{E1} ik_1 ik_1 ik_1 \breve{G}_{Ps} + C_{*Ps_k 3}^{E1} ik_3 ik_3 ik_1 \breve{G}_{Ps} \\
& + C_{*Pf_k 1}^{E1} ik_1 ik_1 ik_1 \breve{G}_{Pf} + C_{*Pf_k 3}^{E1} ik_3 ik_3 ik_1 \breve{G}_{Pf} \\
& + C_{*SV_k 1}^{E1} ik_1 ik_1 ik_1 \breve{G}_{SV} + C_{*SV_k 3}^{E1} ik_3 ik_3 ik_1 \breve{G}_{SV} \\
& + C_{*EM_k 1}^{E1} ik_1 ik_1 ik_1 \breve{G}_{EM} + C_{*EM_k 3}^{E1} ik_3 ik_3 ik_1 \breve{G}_{EM}
\end{aligned}
$$

$$
\begin{aligned}
\breve{G}^{E1,h33} = {} & C_{Ps}^{E1,h11} ik_1 \breve{G}_{Ps} + C_{Pf}^{E1,h11} ik_1 \breve{G}_{Pf} + C_{SV}^{E1,h11} ik_1 \breve{G}_{S} + C_{EM}^{E1,h11} ik_1 \breve{G}_{EM} \\
& + C_{*Ps_k 3}^{E1} ik_1 ik_1 ik_1 \breve{G}_{Ps} + C_{*Ps_k 1}^{E1} ik_3 ik_3 ik_1 \breve{G}_{Ps} \\
& + C_{*Pf_k 3}^{E1} ik_1 ik_1 ik_1 \breve{G}_{Pf} + C_{*Pf_k 1}^{E1} ik_3 ik_3 ik_1 \breve{G}_{Pf} \\
& + C_{*SV_k 3}^{E1} ik_1 ik_1 ik_1 \breve{G}_{SV} + C_{*SV_k 1}^{E1} ik_3 ik_3 ik_1 \breve{G}_{SV} \\
& + C_{*EM_k 3}^{E1} ik_1 ik_1 ik_1 \breve{G}_{EM} + C_{*EM_k 1}^{E1} ik_3 ik_3 ik_1 \breve{G}_{EM}
\end{aligned}
\tag{2.41}
$$

2.6.6 The electric dipole source

This type of source is a dipole which acts on the bulk, which raises the expectation that the effect of this electric dipole is similar to the force dipole source. Here this similarity will be analysed for the structure of the formula's. The particle velocity field component generated by an electric dipole acting on the bulk is,

$$\begin{aligned}\breve{G}^{v_1,J_1^e} &= C_{Ps}^{v1,J^e} ik_1 ik_1 \breve{G}_{Ps} + C_{Pf}^{v1,J^e} ik_1 ik_1 \breve{G}_{Pf} + C_{S1}^{v1,J^e} ik_1 ik_1 \breve{G}_S + C_{EM1}^{v1,J^e} ik_1 ik_1 \breve{G}_{EM} \\ &\quad + C_{S2}^{v1,J^e} \breve{G}_S + C_{EM2}^{v1,J^e} \breve{G}_{EM} \end{aligned} \tag{2.42}$$

$$\breve{G}^{v_1,J_3^e} = C_{Ps}^{v1,J^e} ik_1 ik_3 \breve{G}_{Ps} + C_{Pf}^{v1,J^e} ik_1 ik_3 \breve{G}_{Pf} + C_{S1}^{v1,J^e} ik_1 ik_3 \breve{G}_S + C_{EM1}^{v1,J^e} ik_1 ik_3 \breve{G}_{EM} \tag{2.43}$$

As expected, the structure is the same as for the field generated by the dipole force in 2.29 and 2.30. The same observation goes for the electric field generated by the electric dipole source,

$$\begin{aligned}\breve{G}^{E_1,J_1^e} &= C_{S1}^{E1,Je} ik_1 ik_1 \breve{G}_{SV} + C_{EM1}^{E1,Je} ik_1 ik_1 \breve{G}_{EM} + C_{Ps}^{E1,Je} ik_1 ik_1 \breve{G}_{Ps} + C_{Pf}^{E1,Je} ik_1 ik_1 \breve{G}_{Pf} \\ &\quad + C_{EM2}^{E1,J1e} \breve{G}_{EM} + C_{S2}^{E1,J1e} \breve{G}_{SV} \end{aligned} \tag{2.44}$$

$$\breve{G}^{E_1,J_3^e} = C_{S1}^{E1,Je} ik_1 ik_3 \breve{G}_{SV} + C_{EM1}^{E1,Je} ik_1 ik_3 \breve{G}_{EM} + C_{Ps}^{E1,Je} ik_1 ik_3 \breve{G}_{Ps} + C_{Pf}^{E1,Je} ik_1 ik_3 \breve{G}_{Pf} \tag{2.45}$$

However, here only the structure with respect to the abundance of the various fields and the spatial derivatives acting on each of them are analysed. The effects of the medium parameter operators will be shown in Chapter 4.

2.6.7 The magnetic dipole source

The magnetic source is particularly interesting for this 2D medium, because it acts in the horizontal direction which is invariant here, the x_2- direction. However, due to the fact that the flux of a magnetic field has the intrinsic property to generate an electric field which circulates this magnetic flux vector, the effects of this specific source are quite significant. Because of this, the magnetic source is not directly affecting the medium, but via the generation of this rotating electric field. The structure of the generated particle velocity field is as follows,

$$\breve{G}^{v_1,J_2^m} = \frac{\hat{L}}{G^{fr}} s^2 \rho^f ik_3 \frac{\breve{G}_{EM} - \breve{G}_S}{\gamma_S^2 - \gamma_{EM}^2}$$

Note that in this case only two wave fields are generated, the electromagnetic wave field and the vertical polarized shear wave field, which are the only two divergence-free wave fields. This is because the effective source in this case is the rotation of an electric dipole. This source is of a rotational nature and therefore only has the ability to generate rotational wave fields such as the EM and SV wave fields. However, due to this rotational nature this source does not have the ability to generate dilatational P-waves, which are curl-free wave fields. In fact, when we would analyse the effect of this source on the vertical field component as wel we would observe that the vertical derivative is replaced by the negative horizontal derivative. In other words, the magnetic dipole generates the rotation of these two wave fields. For the particle velocity field the amplitudes of the EM and SV waves are the same strength, but have opposite polarity. The generated electric field component shows the same structure, but the amplitudes of the two fields cannot be as easily evaluated as for the particle velocity case. The electric field due to a magnetic dipole is as follows,

$$\breve{G}^{E_1,J_2^m} = ((s^2\rho/G^{(fr)} - \gamma_S^2) - \hat{k}s^2(\rho^{(f)})^2/(\eta G^{(fr)}))\frac{\breve{G}_S - \breve{G}_{EM}}{\gamma_S^2 - \gamma_{EM}^2} \tag{2.46}$$

The difference between these amplitude factors will be analysed in the Chapter 4.

Chapter 3

Interferometric Green's function recovery for the 2D P-SV-TM mode

In this chapter the theory of interferometry is briefly outlined. An interferometric relation for the P-SV-TM mode in a homogeneous, dissipative 2D medium is derived for the first order equations system according to the mathematical scheme presented by Wapenaar in 2004 [15]. The Green's functions as derived in the previous chapter are used to model this interferometric relation. The result of this interferometric retrieval is showed at the end of this chapter.

3.1 Interferometry

To understand where the concept of interferometry comes from, it is worth to evaluate a simple optic laser beam interferometry problem before we proceed to the application of this basic theory in seismoelectric wave fields. Useful characteristics of a laser beam are that the propagation path of its energy is constricted to a specific direction in the form of a Gaussian beam, as well as that its frequency spectrum is limited to a single frequency, which remains constant over a significant length of the laser beam, referred to as the 'coherence length'. This gives us the advantage to analyse the behaviour of only one monochromatic ray, in stead of having to deal with a full omnidirectional wave field. Additionally, the refraction of the monochromatic laser beam will also not result in an omnidirectional wave field, due to the monochromatic properties of the laser. Schuster et al. [10] addressed a simple optical example of a laser light beam illuminating an irregularly shaped lens from below (figure 3.1). As the beam propagates through the lens, it leaves the lens at point A. However, part of the energy of the beam is reflected at position A, as well as at position r at the bottom of the lens, resulting in the beam leaving the lens again at position B. Of course, part of the laser beam can continue to form multiple reflections until all of its energy has been attenuated, but here we only evaluate the laser beams leaving at positions A and B. When these two laser beams leaving at A and B were to interfere together they will produce an interferogram, also referred to as the intensity of the summed wave fields. The form of this interferogram is only dependent on the phase difference between the beams leaving at A and B. This phase difference is caused by the fact that the beam at B experienced two reflections in the lens as well as a longer propagation path through it than the beam leaving at A. In other words, the interferogram is a measure of the difference between the propagation paths of A and B. In addition, because these paths propagate through the lens, this interferogram can provide us useful information about the properties of the lens, for example its thickness as well as its properties that control the speed of the light beams, without requiring any information about the emitted source laser beam [10]. In 2004 Wapenaar [12] proved that this principle of interferometry can also be applied to the complex seismic world. Before I continue to explain this concept introduced by Wapenaar [15], a few analogies will be shown between interferometry of this simple optic experiment and the complex seismic world [12]. The emitting laser beam is replaced by a seismic source, for example a point source of volume injection. The acoustic wave field emitted by this source travels through a homogeneous, isotropic, acoustic medium and is measured at two different positions at the boundary of the medium, resulting in trace recordings A and B. Instead of a single ray path leaving the medium at two different positions, we have now a full diverging wave field of which we sample two ray paths at receiver positions A and B. We produce an interferogram of these two sampled ray paths by simply cross-correlating the two traces. In the frequency domain this effectively comes down to a multiplication of the spectrum of one trace with the complex conjugate of the spectrum of the other [14]. This process results in a trace which reflects only the phase difference between the two received rays and is not at all depending on the position of the source. This effectively comes down to a subtraction of one ray path from the other, leaving only that part which the two ray paths do not have in common. Depending on which trace is conjugated in the frequency domain, cross-correlation yields either the causal or the a-causal version of this phase difference, because it is a non-commutative process [18] . For a more intuitive understanding, refer to figure 3.1 from Schuster [10], where two direct raypaths received at A and B are depicted. Subtracting one from the other results in a vector pointing from A to B, which is effectively the same as a direct wave measured at B, due to a virtual source at A.

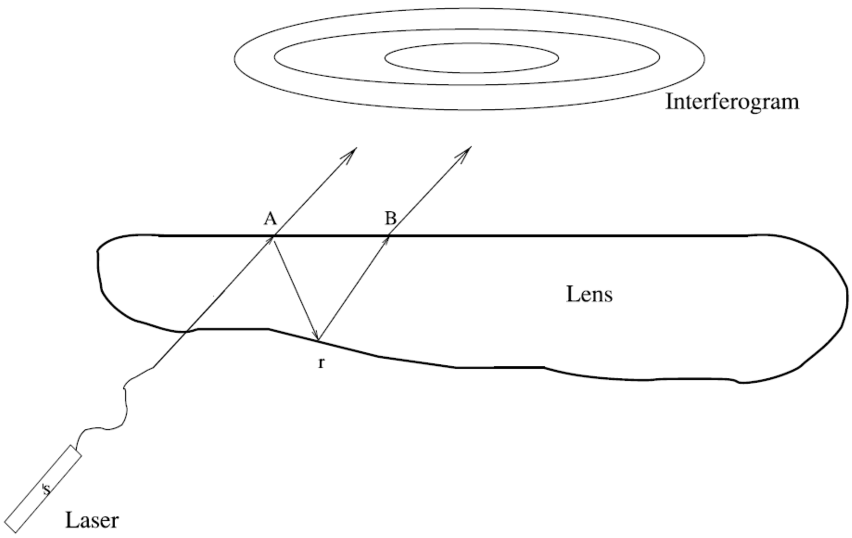

Figure 3.1: Concept of creating an interferogram from a direct arrival at position A and the reflected arrival at position B. Figure obtained from Schuster, 2004 [10]

3.2 The reciprocity theorem of the correlation type

In 2006 Wapenaar and Slob [16] developed the concept of the interferometric Green's function retrieval, based on the reciprocity theorem of the correlation type. I will address this theorem now by linking it to Schuster's [10] interferometric theory as described above. Imagine, a heterogeneous, lossless domain D of arbitrary shape bounded by boundary ∂D. Within this domain two receivers are present, which measure field responses coming from sources anywhere inside as well as on the boundary of the domain (figure 3.2). This case is very complicated compared to the laser beam case where we had only one source location as well as only two ray paths to compare. The objective for the complicated case we have here is to obtain from the total measured field, the direct response at one of the receivers due to a point source at the other receiver position. This is in fact the same as quantifying the phase difference between the total fields measured at both receiver positions. In order to end up with this phase difference, it is required to cross-correlate the two received signals due to each source present in the domain. The cross-correlation of the responses to all sources, measured at the two receiver locations, are summed up, resulting in a stack of the total retrieval. This is done by integrating the cross-correlated fields over the entire domain. A practical advantage of this method is the fact that we sum all the cross-correlations, resulting in a high signal-to-noise ratio. It is therefore desirable to have a large amount of sources. In the case of a passive measurement, when noise sources are used, a great number of sources is achieved by measuring over a sufficiently long time. In Appendix C the reciprocity theorem of the correlation type is derived. Here it is also shown how an interferometric relation can be derived from that theorem for the retrieval of a specific Green's function. In the next section this interferometric relation will be used to model the interferometric retrieval of the causal Green's function which relates the horizontal component of the particle velocity field impulse response at a receiver position to the horizontal directed electric dipole impulse source. For this retrieval, the particle velocity responses as well as the time reversed electric field responses to all source types derived in the previous Chapter 2, are required.

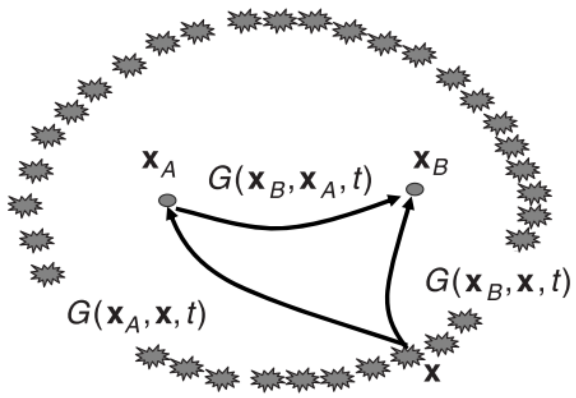

Figure 3.2: Concept of creating an interferogram from a direct arrival at receivers A and B, due to sources spread out over the entire domain. Here, only the sources on the boundary are depicted. Figure is obtained from Wapenaar et al. 2011 [17]

3.3 Interferometry relation

In Appendix C the full derivation of a specific interferometric relation C.29 from the reciprocity theorem of the correlation type is given. This interferometry relation is modelled by inserting the Green's function solutions, as derived in Chapter 2, into the boundary integral of this relation. This has been done with success before in 1D for the other SH-TE mode by de Ridder in 2007 [5]. An important finding of this research was that the domain integral is not required for the retrieval, because it only gave a slight amplitude error. Based on this finding, the same assumption is made that the domain integral is negligible. De Ridder also discovered that the mechanical sources form the strongest contribution to the boundary integral [5]. Due to erroneous results concerning the field responses to the tensile strain sources, these specific Green's functions are left out. These adjustments change the interferometry relation C.29 into the following approximation of the relation,

$$
\begin{aligned}
&G^{E_1,f_1}(\bar{x}_B,\bar{x}_A,\omega) + G^{*v_1,J_1^e}(\bar{x}_A,\bar{x}_B,\omega) \\
&\approx -\oint_{\partial D} [n_3 \hat{G}^{*v_1,J_2^m}_{\bar{x}_A,\bar{x}} \hat{G}^{E_1,J_1^e}_{\bar{x}_B,\bar{x}} - n_1 \hat{G}^{*v_1,J_2^m}_{\bar{x}_A,\bar{x}} \hat{G}^{E_1,J_3^e}_{\bar{x}_B,\bar{x}} + n_3 \hat{G}^{*v_1,J_1^e}_{\bar{x}_A,\bar{x}} \hat{G}^{E_1,J_2^m}_{\bar{x}_B,\bar{x}} - n_1 \hat{G}^{*v_1,J_3^e}_{\bar{x}_A,\bar{x}} \hat{G}^{E_1,J_2^m}_{\bar{x}_B,\bar{x}} \\
&+ n_3 \hat{G}^{*v_1,2h_{31}}_{\bar{x}_A,\bar{x}} \hat{G}^{E_1,f_1}_{\bar{x}_B,\bar{x}} + n_1 \hat{G}^{*v_1,2h_{31}}_{\bar{x}_A,\bar{x}} \hat{G}^{E_1,f_3}_{\bar{x}_B,\bar{x}} + n_3 \hat{G}^{*v_1,f_1}_{\bar{x}_A,\bar{x}} \hat{G}^{E_1,2h_{31}}_{\bar{x}_B,\bar{x}} + n_1 \hat{G}^{*v_1,f_3}_{\bar{x}_A,\bar{x}} \hat{G}^{E_1,2h_{31}}_{\bar{x}_B,\bar{x}} + n_1 \hat{G}^{*v_1,Cq}_{\bar{x}_A,\bar{x}} \hat{G}^{E_1,f_1^{(f)}}_{\bar{x}_B,\bar{x}} \\
&+ n_3 \hat{G}^{*v_1,Cq}_{\bar{x}_A,\bar{x}} \hat{G}^{E_1,f_3^{(f)}}_{\bar{x}_B,\bar{x}} + n_1 \hat{G}^{*v_1,f_1^f}_{\bar{x}_A,\bar{x}} \hat{G}^{E_1,Cq}_{\bar{x}_B,\bar{x}} + n_3 \hat{G}^{*v_1,f_3^f}_{\bar{x}_A,\bar{x}} \hat{G}^{E_1,Cq}_{\bar{x}_B,\bar{x}}] \,\mathrm{d}\bar{x} \qquad (3.1)
\end{aligned}
$$

3.4 Reciprocity theorem of the convolution type

The paper by Wapenaar 2004 [15] can also be used to derive a reciprocity relation of the convolution type. However, in this section the reciprocity relation will be derived according to the method presented in the paper by Wapenaar in 2005 [13]. This approach starts out with the following seismoelectric interaction quantity in 3D,

$$
\partial_j \left[\varepsilon_{ijk} \hat{E}_{i,A} \hat{H}_{k,B} - \varepsilon_{ijk} \hat{H}_{k,A} \hat{E}_{i,B} - \hat{v}^s_{i,A} \hat{\tau}^b_{ij,B} + \hat{\tau}^b_{ij,A} \hat{v}^s_{i,B} + \hat{w}_{j,A} \hat{p}_B - \hat{p}_A \hat{w}_{j,B} \right] \qquad (3.2)
$$

The product rule for partial differentiation is applied to this quantity. Subsequently, the first order seismoelectric coupled equations for the 3D system are substituted in this interaction quantity [13]. The domain integral is taken of this interaction quantity and the assumption is made that the medium parameters are the same for both states,

$$
\oint_{\partial D} \left[\varepsilon_{ijk} \hat{E}_{i,A} \hat{H}_{k,B} - \varepsilon_{ijk} \hat{H}_{k,A} \hat{E}_{i,B} - \hat{v}^s_{i,A} \hat{\tau}^b_{ij,B} + \hat{\tau}^b_{ij,A} \hat{v}^s_{i,B} + \hat{w}_{j,A} \hat{p}_B - \hat{p}_A \hat{w}_{j,B} \right] = \qquad (3.3)
$$

$$
\int_D \left[\hat{J}^m_{k,A} \hat{H}_{k,B} - \hat{H}_{k,A} \hat{J}^m_{k,B} - \hat{J}^e_{i,A} \hat{E}_{i,B} + \hat{E}_{i,A} \hat{J}^e_{i,B} - \hat{f}^b_{i,A} \hat{v}^s_{i,B} + \hat{v}^s_{i,A} \hat{f}^b_{i,B} - \hat{f}^f_{j,A} \hat{w}_{j,B} + \hat{w}_{j,A} \hat{f}^f_{j,B} \right] d^3x \qquad (3.4)
$$

The boundary integral on the left-hand side vanishes when we assume that the medium is isotropic, homogeneous as well as unbounded. The relation is further simplified when we assume we have a 2D domain with a line boundary, which contains two states in which we specify only the sources or wave fields of interest of the P-SV-TM mode. In state A a particle velocity field is active due to an electric dipole source at position x_A. In state B an electric field is generated by a bulk force at position x_B. All source and field have the same orientation. This results in the following integral relation,

$$\int_D \hat{J}^e_{m,A}\hat{E}_{m,B}d^2x = \int_D \hat{v}^s_{n,A}\hat{f}^b_{n,B}d^2x \tag{3.5}$$

If the sources of both states are replaced by impulse sources, the fields in each state change into Greens functions generated by this impulse source at the location x_A or x_B. For example, by changing the electric dipole source in state A into an impulse source at location x_A turns the particle velocity field in state A into a Green's function due to this specific electric impulse at x_A. The same happens for the field and source in state B, which gives the following reciprocity relation,

$$\hat{G}^{E_1,f^b_1}(x_A,x_B) = \hat{G}^{v^s_1,J^e_1}(x_B,x_A) \tag{3.6}$$

Note that the electric field Green's function is only nonzero at x_A and the particle velocity Green's function is only non-zero at x_B, which is due to the fact that both are multiplied in the integral with the impulse function of the other independent state. This reciprocity relation is of great relevance to the modelling experiment in the next section, because it dictates that the causal and a-causal Green's functions should form together a asymmetric signal around the zero time. This is because in the source function $\hat{s}$ used for the derivation of the interferometric relation the J^e_1 is defined with a minus sign in front, while f^b_1 is positive.

3.5 Modelling of the interferometric Green's function retrieval for a circle boundary

The Green's function representation is modelled for a 2D porous saturated, homogeneous, dissipative and isotropic medium. Thereby, both the left-hand side and the right-hand side are implemented and compared to each other. The success of the interferometric retrieval depends on whether these two implemented expressions coincide. The medium parameters are specified in table D.1 in Appendix D. The boundary of the medium is modelled as a perfect circle with a radius of 500 meters. The receivers x_A and x_B are put at a horizontal offset of 160 meters such that their middle point coincides with the circle's center point (figure 3.3). A total of 3600 uncorrelated sources are equally distributed over the circle boundary. The modelling experiment is conducted in the frequency domain, whereby the Green's functions are each convolved with the same source wavelet, a Ricker wavelet with a radial frequency of 800 radians per second. Thereby, Green's function responses are computed at the two receivers due to impulse sources distributed regularly over the circle boundary. For each source position the horizontal component of the particle velocity response at x_A is cross-correlated with the same component of the electric field response at x_B. Actually, several cross correlation are done for different source types at each position, as is specified in the boundary integral of the relation 3.1. In figure 3.3(a) it is shown what the result is of such a cross-correlation of a single source at the boundary. The boundary integral over all the sources is taken by simply stacking all cross-correlation results. This should hypothetically yield a resultant electric field response at x_B due to an impulse bulk force source at x_A plus a time reversed particle velocity field response at x_A due to an electric dipole. A schematic representation of this is given in figure 3.3(b). The Green's functions used for the interferometric modelling are all convolved with a Ricker wavelet of 800 radians per second. Therefore, the left-hand side is convolved with the square of the Ricker wavelet in order to validate the comparison to the cross-correlated Ricker wavelets in the right-hand side.

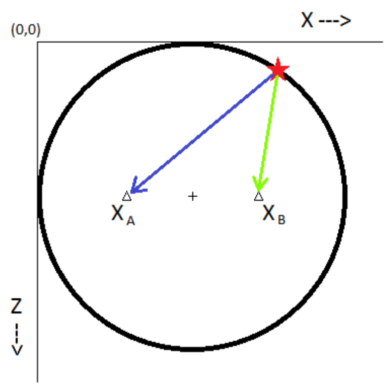

(a)

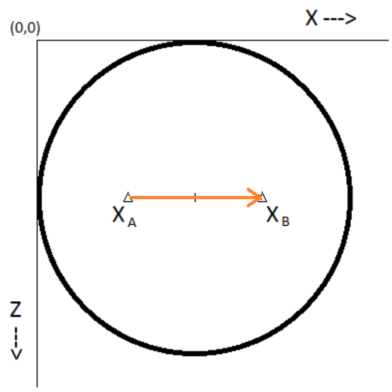

(b)

Figure 3.3: Green's responses are computed at receivers x_A and x_B due to all sources distributed regularly over the circle boundary. In figure 3.3(a) an example is given of a cross-correlation of the two responses at x_A and x_B due to a single source at the boundary. The schematic result of integrating over all cross-correlated source responses is given in 3.3(b), where the orange vector represents the left-hand side of equation 3.1.

3.5.1 Modelling result and interpretation

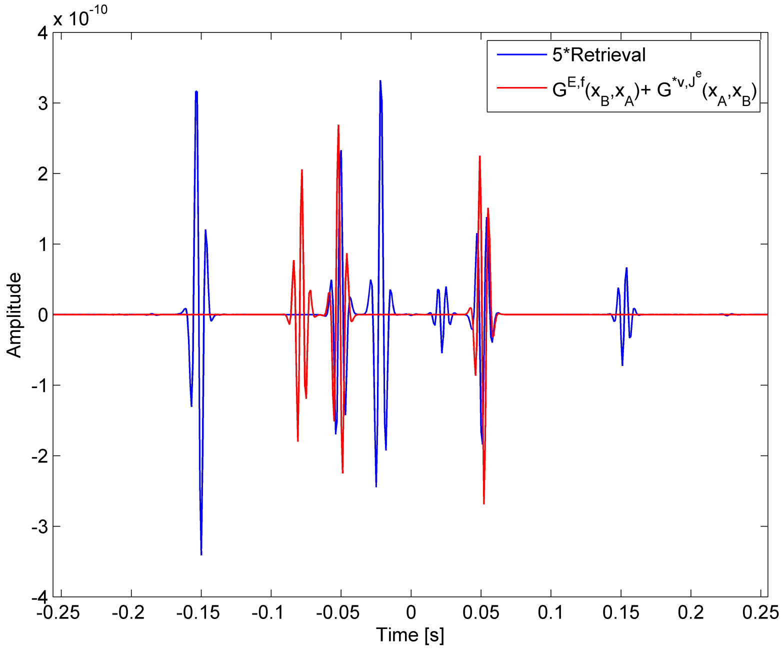

Figure 3.4: Interferometric retrieval is plotted in blue. The retrieval is about five times weaker in amplitude than the left-hand side (red), therefore it is multiplied by a factor of 5.

In figure 3.4 the result of the left-hand side of the implemented equation 3.1 is plotted in red. The two Green's functions in the left-hand side should be exactly reciprocal and therefore symmetric around the point of zero seconds, according to the reciprocity relation 3.6. However, the time-reversed Green's function of the particle velocity response to an electric dipole source contains an extra event at arrival time of 0.08 seconds, which is not visible in the causal Green's function. For the specified distance between x_A and x_B of 160 meters this arrival time corresponds to an SV-wave, which has a speed of $2.027 \cdot 10^3$ ms^{-1} as specified in table D.1. The causal electric field response to a bulk force does not show this extra SV-wave event, which would mean it would have to show a distinct coelectric SV-wave. As described by Pride and Haartssen [8] the coseismic electric field of an SV-wave is much weaker than the coelectric field of a fast P-wave. According to that fact, this Green's function $G^{E_1,f_1}(\bar{x}_B, \bar{x}_A, \omega)$ gives a plausible result. And according to that, the Green's function $G^{*v_1,-J_1^e}(\bar{x}_A, \bar{x}_B, \omega)$ must be incorrect, due to this extra unexpected SV-wave arrival. In order to analyse the rest of the relation further, the reciprocity relation 3.6 is used to substitute for this incorrect Green's function. This changes the relation 3.1 into the following,

$$
\begin{aligned}
&2i\Im\left[\hat{G}^{E_1,f_1}(\bar{x}_B,\bar{x}_A,\omega)\right] \\
&\approx -\oint_{\partial D}[n_3\hat{G}^{*v_1,-J_2^m}_{\bar{x}_A,\bar{x}}\hat{G}^{E_1,-J_1^e}_{\bar{x}_B,\bar{x}} - n_1\hat{G}^{*v_1,-J_2^m}_{\bar{x}_A,\bar{x}}\hat{G}^{E_1,-J_3^e}_{\bar{x}_B,\bar{x}} + n_3\hat{G}^{*E_1,-f_1}_{\bar{x},\bar{x}_A}\hat{G}^{E_1,-J_2^m}_{\bar{x}_B,\bar{x}} - n_1\hat{G}^{*v_1,-J_3^e}_{\bar{x}_A,\bar{x}}\hat{G}^{E_1,-J_2^m}_{\bar{x}_B,\bar{x}} \\
&+n_3\hat{G}^{*v_1,2h_{31}}_{\bar{x}_A,\bar{x}}\hat{G}^{E_1,f_1}_{\bar{x}_B,\bar{x}} + n_1\hat{G}^{*v_1,2h_{31}}_{\bar{x}_A,\bar{x}}\hat{G}^{E_1,f_3}_{\bar{x}_B,\bar{x}} + n_3\hat{G}^{*v_1,f_1}_{\bar{x}_A,\bar{x}}\hat{G}^{E_1,2h_{31}}_{\bar{x}_B,\bar{x}} + n_1\hat{G}^{*v_1,f_3}_{\bar{x}_A,\bar{x}}\hat{G}^{E_1,2h_{31}}_{\bar{x}_B,\bar{x}} + n_1\hat{G}^{*v_1,Cq}_{\bar{x}_A,\bar{x}}\hat{G}^{E_1,f_1^{(f)}}_{\bar{x}_B,\bar{x}} \\
&\qquad + n_3\hat{G}^{*v_1,Cq}_{\bar{x}_A,\bar{x}}\hat{G}^{E_1,f_3^{(f)}}_{\bar{x}_B,\bar{x}} + n_1\hat{G}^{*v_1,f_1^f}_{\bar{x}_A,\bar{x}}\hat{G}^{E_1,Cq}_{\bar{x}_B,\bar{x}} + n_3\hat{G}^{*v_1,f_3^f}_{\bar{x}_A,\bar{x}}\hat{G}^{E_1,Cq}_{\bar{x}_B,\bar{x}}]\,\mathrm{d}\bar{x} \qquad (3.7)
\end{aligned}
$$

This relation 3.7 is implemented in the same model as described for the previous result in 3.3 and results in the interferometric retrieval given in figure 3.5. The causal and a-causal arrivals of the left-hand side at respectively, 0.05 and -0.05 seconds are exactly reciprocal as prescribed by 3.6. This arrival time of 0.05 seconds corresponds to the arrival of a fast P-wave, which has a speed of $3.122 \cdot 10^3$ ms^{-1}. An important observation of these anti-symmetric P-wave arrivals is that they each have a total of 5 zero crossings. The interferometric retrieval is plotted in blue. The retrieval also shows two anti-symmetric events at 0.05 and -0.05 seconds. However, these events each have a total of 4 zero-crossings. Refer to section 3.6.4 for a detailed interpretation of these wavelet shape discrepancies. Another clear observation of figure 3.5 is that the interferometric retrieval contains several extra events which are not present in the left-hand side.

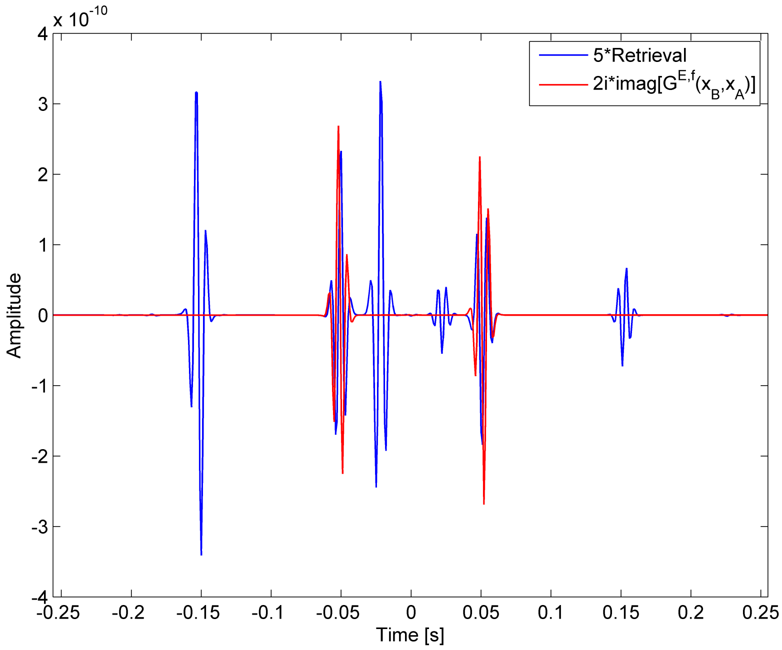

Figure 3.5: The Green's function describing the response of the particle velocity field to the electric dipole source is substituted for by using the reciprocity relation 3.6.

3.6 Differences in contributions to the interferometric retrieval

When analysing the cross-correlation pairs in equation 3.7 it can be observed that only responses to sources of the same character are cross-correlated. For instance, only electromagnetic responses are cross-correlated, never an electromagnetic response with a response to a source acting on the bulk. In fact, we can distinguish three main classes: bulk source, fluid phase source and electromagnetic source responses. In this section the interferometric relation is modelled again, but now only the cross-correlation pairs belonging to one of these three classifications is activated, in order to find out which class of source types form the main contribution.

3.6.1 Electromagnetic sources

For this experiment only the electric and magnetic dipole sources are not set to zero.

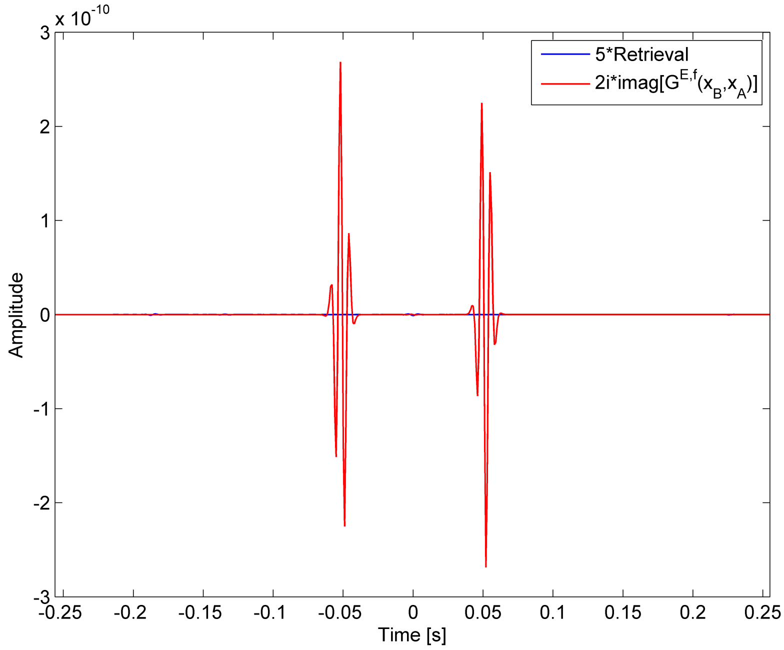

Figure 3.6: The cross-correlation terms containing only responses to electromagnetic sources contributed to the interferometric retrieval here. Note that the contribution hardly existent

The field responses to the electromagnetic sources hardly give a significant contribution to he retrieval of the exact left-hand side.

3.6.2 Fluid phase sources

For this experiment only the dipole force acting on the fluid phase as well as the monopole volume injection source are not set to zero.

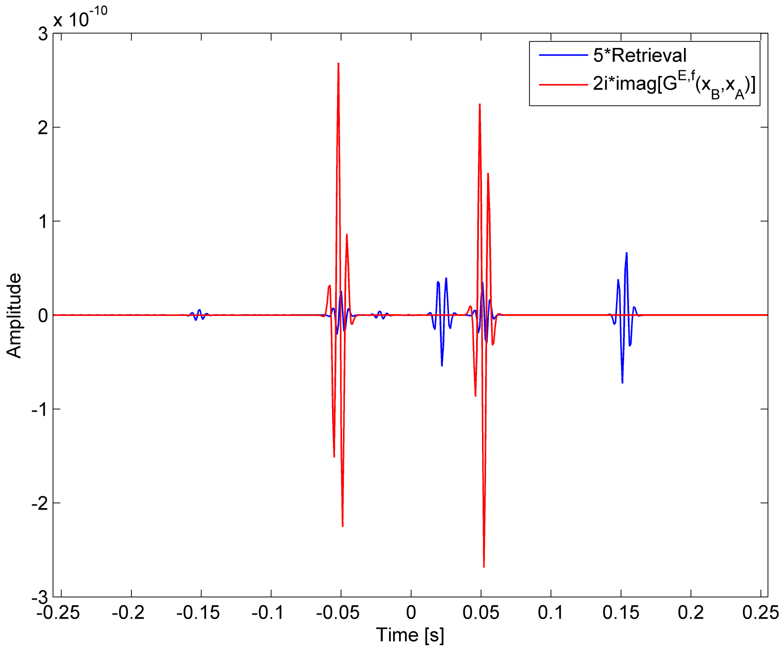

Figure 3.7: Only the cross-correlation terms containing the responses to sources acting on the fluid phase are modelled here. Their contribution is much stronger than the contribution form the electromagnetic source responses as shown in figure 3.6.

The fluid source responses do contribute to the interferometric retrieval of the P-wave arrivals, with an amplitude of the order 10^{-11}. These responses are also contributing to the two causal events at about 0.03 and 0.15 seconds, which are not found in the exact left-hand side signal.

3.6.3 Bulk sources

For this experiment only the dipole shear strain source as well as the dipole force acting on the bulk are not set to zero.

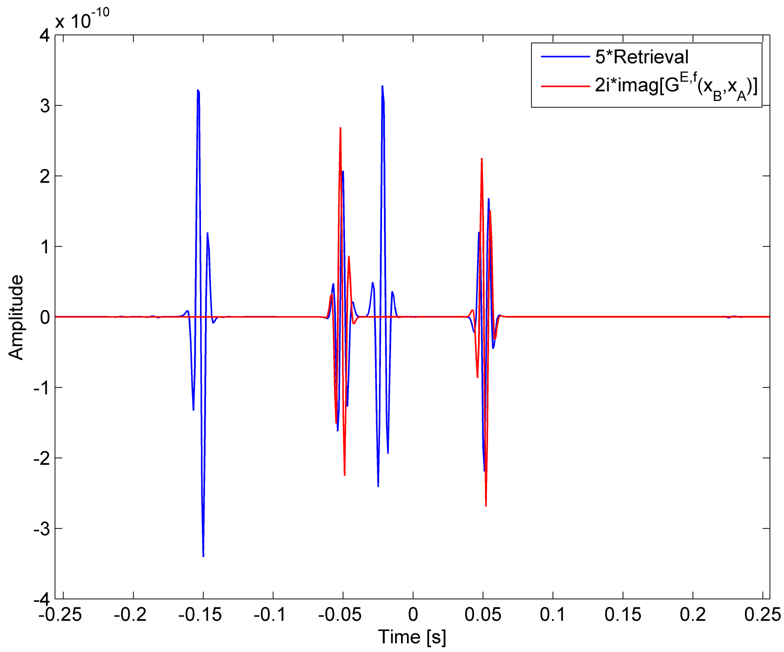

Figure 3.8: Only the cross-correlation terms containing the responses to sources acting on the bulk are modelled here. Their contribution is the strongest to the interferometric retrieval.

When examining figure 3.8 it can be seen that this interferometric retrieval of only the bulk force responses gives the biggest contribution to the left-hand side P-wave arrivals, with an amplitude of the order 10^{-10}. It can also be observed that the bulk forces are responsible for the strong a-causal events at about -0.03 and -0.15 seconds, which are not represented by the left-hand side signal. These a-causal events have a stronger amplitude than their causal equivalents observed in figure 3.6.

Interpretation

The interferometric retrieval did not yield an correct retrieval of the left-hand side of equation 3.7. However, there is still some resemblance, because the retrieval does contain an anti-symmetric signal at arrival times -0.05 and 0.05 seconds just as the exact left-hand side shows as well. However, there is a difference in the wavelet shapes, because the left-hand side contains five zero crossings, while the retrieval contains four. In section 3.6.4 this problem is further explained. The final clear inconsistency between the retrieval and the left-hand side are caused by the four extra events found in the retrieval. The two causal events at about 0.03 and 0.15 seconds are a result of the responses to the sources acting on the fluid phase (figure 3.7). The two a-causal events at about -0.03 and -0.15 seconds are a result of the responses to the sources acting on the bulk (figure 3.8). In Chapter 5 a possible explanation of these extra events is presented, based on the detailed analysis of all field responses which will be undertaken in Chapter 4.

3.6.4 Wavelet shape analysis

Although the interferometric retrieved P-wave events do arrive at the same time as the anti-symmetric left-hand side signal, there is a clear discrepancy visible in the shape of the wavelets between the interferometric retrieval and the left-hand side. The shape of the wavelets in the figure 3.5 can now be compared to the Ricker wavelet and its time derivatives of different orders in order to find out what causes this shape difference. In figure 3.9 a Ricker wavelet is depicted , as well as its first, second and third order derivatives in time. The centre frequency of this Ricker is 100 radians per second, which is 8 times lower than the Ricker used for the modelling. This lower frequency is used for this purpose, because it enables better identification of the specific shape.

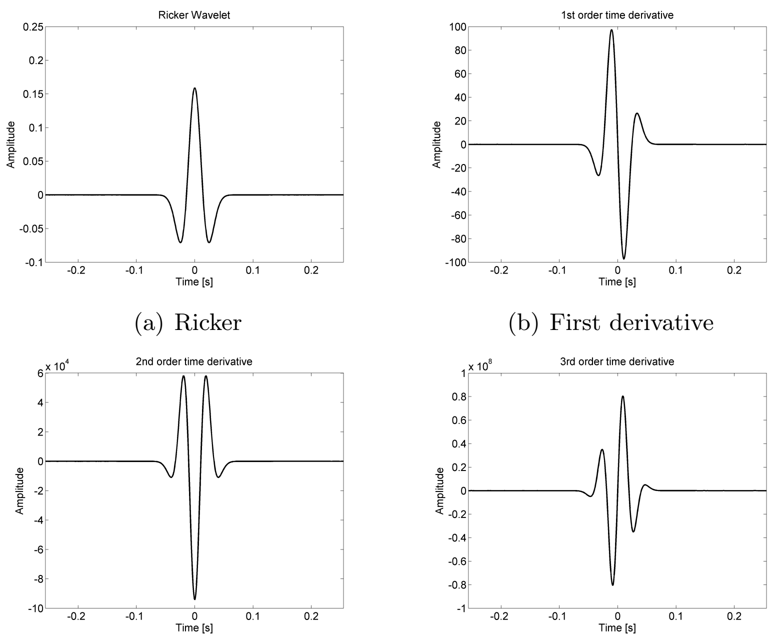

(a) Ricker (b) First derivative

(c) Second derivative (d) Third derivative

Figure 3.9: Ricker wavelet with center frequency of 100 radians per second and its derivative with respect to time for the first, second and third order.

When comparing the left-hand side signal in figure 3.5 with the Ricker wavelets in figure 3.9 it matches best with the shape of the wavelet in figure 3.9(d). It has the same amount of peaks and is asymmetric as well. Therefore, the left-hand side anti-symmetric fast P-waves can be interpreted as third order time derivatives of the Ricker wavelet. The shape of the interferometric retrieved P-wave arrivals resembles the shape of the wavelet in figure 3.9(c) most. It has the same amount of peaks and shows symmetry. Therefore, the interferometric retrieved P-wave arrivals resemble the second order time derivative of the Ricker wavelet. This is not in accordance with the interpretation that the left-hand side is the third order derivative of the source wavelet. The conclusion is that the interferometric retrieval matches the left-hand side only in that it shows as well two anti-symmetric P-wave arrivals. But the amplitude of the retrieval is 5 times too low and it seems that its differential order is one too low compared to the left-hand side. Another discrepancy is that the interferometric retrieval shows several extra artefacts, which are not represented by the left-hand side. The only way to discover where these difficulties are coming from is by evaluating the cross-correlated terms separately. In the next Chapter 4 all Green's functions contributing to the interferometric retrieval will be analysed separately in order to discover where the difficulties arise from.

Chapter 4

Analysis of the 2D homogeneous Green's function solutions for the P-SV-TM mode

In the hope to shed light on the discrepancies encountered during the interferometric modelling in the previous chapter, a detailed analysis is undertaken of the relevant Green's functions used there. In section 2.5, the analysis of the Green's functions showed that in principal every source type has the ability to generate all four P-SV-TM mode wave fields, except for the magnetic dipole which does not generate P-waves. However, from the structure of the Green's functions alone it could not be established which of the constituent wave fields are actually detectable. By modelling the responses separately the actual effect of the different sources on the horizontal component of the electric and particle velocity wave fields of the P-SV-TM mode can be analysed. The modelled 2D medium is of a dissipative, homogeneous, isotropic and saturated porous nature and can be regarded as a surface spanned in the horizontal x_1- and vertical x_3-directions. The medium parameters used for this experiment and the wave speeds are denoted in Table D.1. The horizontal component of the field response due to a single source is modelled at a single receiver in three different configuration set-ups. This means that the receiver represents for all situations a horizontal receiver vector. The source vector is either directed in the horizontal or the vertical direction, with an exception for the volume injection source, which is a monopole source, and the magnetic source vector, which only has a component in the direction perpendicular to the model plane. The source and the receiver are placed at a distance of 200 meters at a horizontal offset, a vertical offset and a diagonal offset, as is defined more precisely with coördinates in (figure 4.1). For this configuration and the specified medium parameters the arrival times corresponding to the fast P-wave and the SV-wave are 0.065 and 0.1 seconds, respectively. The electromagnetic wave field is always observed as an instantaneous arrival, due to its significantly larger wave speed compared to the other wave fields (table D.1). The slow P-wave is not displayed nor discussed, because it is negligibly small in all cases with an amplitude of the order 10^{-154}. The Green's functions are convolved with a Ricker wavelet with a center angular frequency of 600 radians per second. Additionally, an interpretation will be made of these modelling results. Amplitude radiation maps of only the detectable constituent wave fields are shown additionally to support the interpretation of the field responses. In an amplitude radiation map the maximum of the absolute value of the amplitude is given of the field response as

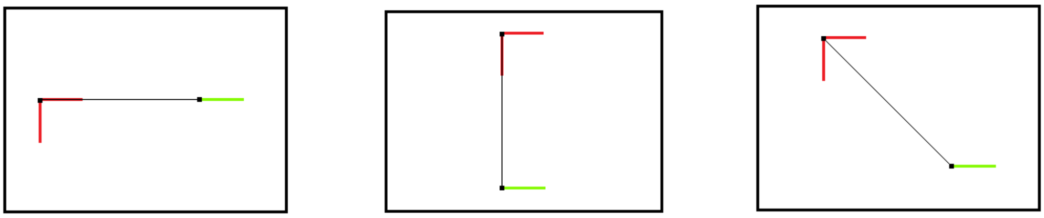

(a) Horizontal configuration (b) Vertical configuration (c) Diagonal configuration

Figure 4.1: The red lines indicate the two possible source directions analysed here, the horizontal and the vertical component. The coördinates of the source position are (0,0) for all configurations. The green line represents the receiver vector. The black line represents the offset between source and receiver, which is 200 meters for all configurations. Receiver coördinates for 4.1(a) are (200,0) and for 4.1(b) (0,200). For the diagonal configuration in 4.1(c) the offset is diagonal and the corresponding receiver coördinates are (141.42,141.42)

a function of the angle of the offset vector between source and receiver. Therefore, when looking at this polar plot the source can be imagined to remain at the center of the polar plot while the receiver is varied along the circle boundary. The maximum amplitude values for the angles of 0, 90 and 315 degrees correspond to the configurations of the horizontal, vertical and diagonal offset as described in figure 4.1.

4.1 Analysis of the horizontal component of the particle velocity response

In this section the response of the horizontal component of the particle velocity vector to all relevant source are analysed.

4.1.1 Modelled response to a bulk force

The bulk force is a source of a dipole nature. It is active on both the solid framework and the fluid phase of the medium. The effects of the horizontal as well as the vertical component of the force on the horizontal component of the solid particle velocity field are analysed here.

When the receiver is aligned with the horizontally directed force, two events can be distinguished in figure 4.2(a). One event arrives at 0.067 seconds, which corresponds to a fast P-wave arrival. The second arrival corresponds to an SV-wave, because it arrives at 0.1 seconds. When the receiver is put at a vertical offset only, the P-wave reduces to an almost insignificant amplitude compared to the SV-wave (factor of 1000 smaller), which remains unchanged (4.2(b)). In the case of an offset at 45 degrees, both events can be distinguished again (4.2(c)). However, in this case the P-wave has a smaller amplitude than in figure 4.2(a). The SV-wave retains the same amplitude strength of about $1 \cdot 10^{-9}$ $ms^{-1}$for all configurations. In the case of a vertically directed force, for both horizontal and vertical offsets this force has no influence at all on the horizontal component of the particle velocity field (figures 4.3(a) and 4.3(b)). However, for the diagonal configuration both a P-wave and an SV-wave arrival can be distinguished (4.3(c)). The amplitude of the SV-wave is about 10 times smaller than the amplitude of this wave in the case of a horizontally directed force for the same configuration (4.2(c)). However, the P-wave has the same amplitude as the P-wave event in figure 4.2(c).

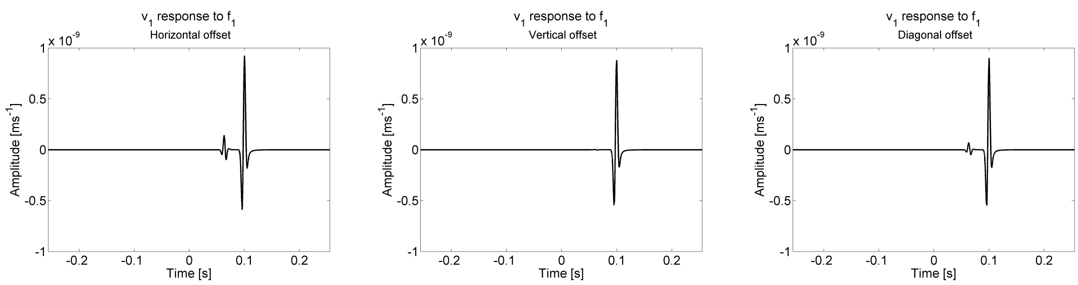

(a) (b) (c)

Figure 4.2: Particle velocity field response to the horizontal component of the bulk force

Interpretation of the observations on the bulk force response

The horizontal directed force generates an SV-wave which is detectable at all three different receiver positions. This implies that this force generates an SV-wave with a horizontal polarization. The horizontal force also generates a fast P-wave, however this P-wave does not influence the particle velocity field for the vertical offset configuration. In fact, it has a maximum amplitude for the horizontal offset and a smaller amplitude for the diagonal

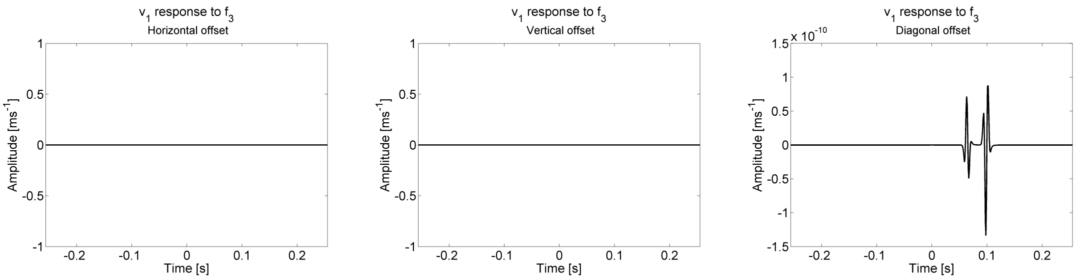

(a) (b) (c)

Figure 4.3: Particle velocity field response to the vertical component of the bulk force

offset. This specific fast P-wave field is examined further by looking at its radiation pattern in figure 4.4(a). This figure shows a typical dipole field. The effect of the dilatational particle motion decreases for an increase in the alignment angle, and indeed becomes zero for a vertical offset at 90 degrees, which is in line with are modelled results. The results for the vertical component of the bulk force are quite different, in that it only generates a horizontal particle movement when the receiver is positioned in the diagonal configuration. For this configuration both a dilatational P-wave and a transversal SV-wave are detected. In the radiation pattern of the fast P-wave field can be observed that this vertical force on the bulk does not generate any horizontal movement at source-receiver alignments of either 0 or 90 degrees, which corresponds to the horizontal and vertical offset configuration (4.4(b)). The influence on the horizontal particle movement increases for angle values in between the horizontal and vertical offset angles. For the SV-wave radiation pattern, the same interpretation holds as for the P-wave (figure 4.4(c)).

4.1.2 Modelled response to a force acting only on the fluid phase

This dipole force acts purely on the fluid phase of the medium, which is different from the bulk force, which acts on both the fluid and the solid phase.

The horizontal component of the force acting on the fluid phase generates only a detectable SV-wave for all configurations. The amplitude of the SV-wave arrival varies with the orientation of the source-receiver alignment. The amplitude is strongest in the case of the horizontal offset configuration, with a value of approximately $3 \cdot 10^{-9}$ ms^{-1} (4.5(a)). For the vertical offset configuration, the amplitude diminishes to the order of 10^{-11} (4.5(b)). For the diagonal configuration the amplitude is about half of the amplitude modelled for the horizontal offset (4.5(c)). The vertical component of the force acting on the fluid phase also generates only a detectable SV-wave. This wave field only affects the particle velocity field when the receiver is placed in the diagonal offset configuration (4.6(c)).

Interpretation of the observations on the response to the fluid phase force

The force acting only on the fluid phase is actually not a source type which can be simulated in reality, because applying a force to a medium will always affect the solid phase as well. However, theoretically it is interesting to look at this force type, because if it acts only on the fluid phase it can be seen as a microscopic acceleration of only the mobile fluid layer of the EDL inside the pore spaces. Our observations of the horizontal component

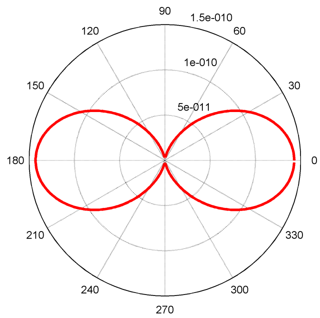

(a)

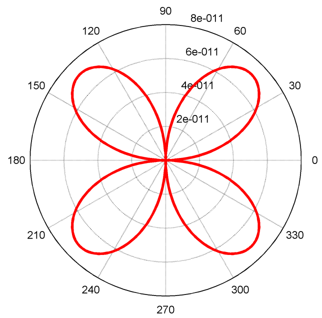

(b)

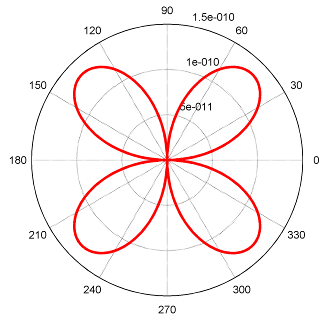

(c)

Figure 4.4: Radiation patterns for the particle velocity field are shown: in (a) the radiation pattern of the P-wave field generated by the horizontal force component, in (b) the radiation pattern of the P-wave field generated by the vertical force component and in (c) the pattern of the SV-wave field generated by the vertical force component.

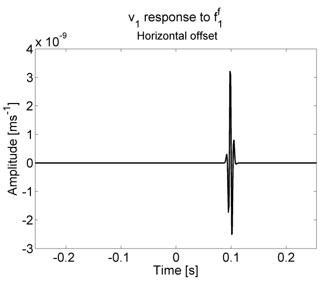

(a)

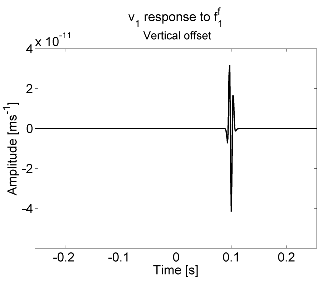

(b)

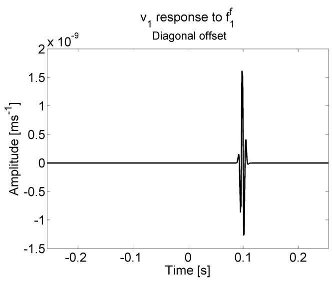

(c)

Figure 4.5: Particle velocity field response to the horizontal component of the fluid force

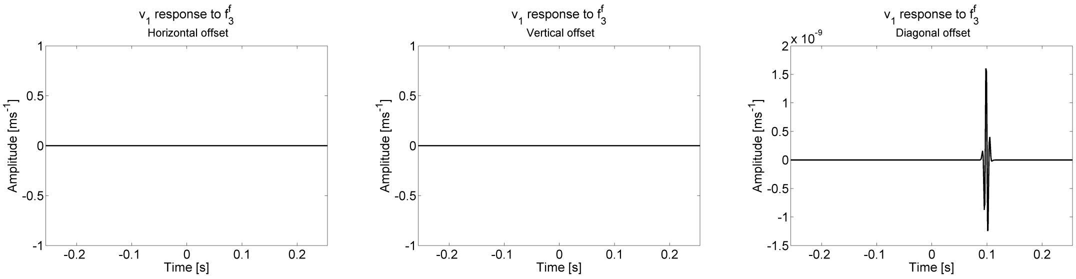

(a) (b) (c)

Figure 4.6: Particle velocity field response to the vertical component of the fluid force

of this force indicate that accelerating the EDL in the horizontal direction generates an SV-wave with a horizontal polarization. In the radiation pattern of this SV-wave field can be seen that the amplitude of this polarization is strongest in the direction of the force. A possible explanation of this SV-wave field is that the force acting in the horizontal direction on the fluid EDL causes an acceleration in that direction. Due to the fact that all equations are volume averaged over a volume containing both fluid as solid phases, a directional acceleration purely in the fluid phase can be translated directly to the solid phase, in the same direction. In the case of the force acting on the EDL in the vertical direction the same thing would happen, because of the isotropic and homogeneous nature of the medium. However, the vertical particle velocity is not modelled here. But we do see that this vertical directed source does have the ability to generate horizontal particle motion, because this wave field is observed in figure 4.6(c). This can be explained by the fact that any displacement of the elastic framework in a certain direction can induce a displacement in a perpendicular direction, due to the interconnectivity of this elastic solid framework.

4.1.3 Modelled response to a volume injection rate

This source can be regarded as a literal injection of volume into the fluid phase of the medium at the source location. It is the only source of monopole nature discussed in this thesis.

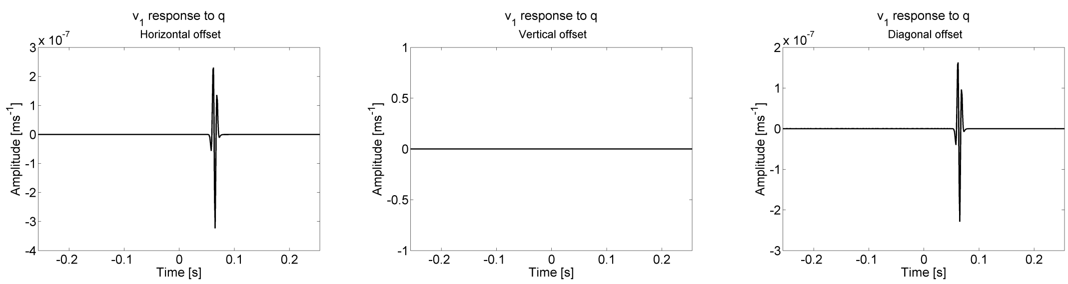

(a) (b) (c)

Figure 4.7: Particle velocity field response to the volume injection

This source only induces a detectable horizontal particle velocity wave field of the P-wave type. This P-wave is however not detectable in the case of the vertical offset configuration (4.7(b)). The amplitude is strongest in the case of the horizontal offset configuration (4.7(a)) with a value of approximately $2.5 \cdot 10^{-7}$ ms^{-1}. In the other configuration in figure 4.7(c) the amplitude is a bit less with a value of about $1.5 \cdot 10^{-7}$ ms^{-1}.

Interpretation of the observations on the volume injection response

In the modelling results we observed that the volume injection only generates a detectable dilatational movement of the horizontal component of the particle velocity field. In fact, the total wave field generated by this source is a purely radially orientated dilatational wave field. Therefore, the particle velocity displacement vector has in the whole medium this radial orientation. This behaviour is caused by the monopole or isotropic nature of the volume injection source, which we also observed in equation 2.37, which showed us that the wave field is composed of the divergence of all constituent wave field types. This also explains why this movement was not detectable when the receiver was placed at a vertical offset: the particle velocity induced by this source is directed in the vertical direction here, which is perpendicular to the receiver which measures the horizontal component only.

4.1.4 Modelled response to a shear strain source

This source deforms the medium by way of rotational shearing it at the source location.

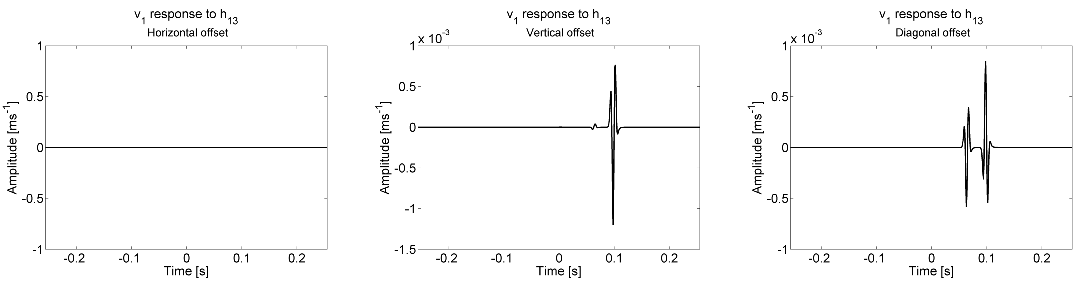

(a) (b) (c)

Figure 4.8: Particle velocity field response to the horizontal component of the shear strain source

For the horizontal offset configuration this source has no influence on the horizontal component of the particle velocity field (4.8(a)). At a vertical offset a shear wave with an amplitude of the order of 10^{-3} is generated, as well as a P-wave with a considerably lower amplitude of the order 10^{-4}. For the diagonal configuration there is also an SV-wave generated, however its polarity is reversed in this case. The amplitude of the P-wave is much stronger for this configuration. A close examination of the P-wave for both figures 4.8(b) and 4.8(c), shows that there occurs a polarity switch for the P-wave as well.

Interpretation of the observations on the response to the shear strain source

In the section on the shear strain source in Chapter 2 I discussed the complicated third order spatial derivatives acting on the constituent Green's functions. In the modelling results we observed a polarity switch between the vertical and diagonal offset for both the P-wave as the SV-wave. This polarity switch could be explained by the third order spatial derivatives active on both P and SV-waves, as seen in the Green's function 2.39. This complicated pattern arises, due to the fact that the SV-wave field is actually a combination of a vertical spatial derivative and a third order spatial derivative term (equation 2.39). In figure 4.9(a) just the vertical derivative of the SV-wave field is shown. This tells us that this term is not detectable at positions horizontally aligned with the source. In figure 4.9(b) the third order spatial derivative of the SV-wave is shown. These radiation patterns together yield the total pattern of the SV wavefield (figure 4.9(c)), which shows six lobes, each distanced at 60 degrees from each other. From our observations of 4.8(c) we know that the polarity switches for the diagonal configuration, which is at 315 degrees in the radiation pattern, which could imply that the entire lobe at this angle is of opposite polarity with respect to the lobe at 90 degrees. This radiation pattern is of a much more complex nature than for instance in the case of a dipole force, which showed just four lobes of the same polarity (4.4(c)). This increase of complexity arises from the fact that this source generates a double rotation of the fields of which the divergence results in the particle velocity field.

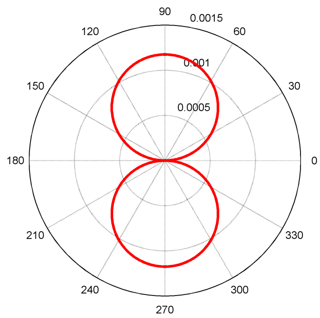

(a)

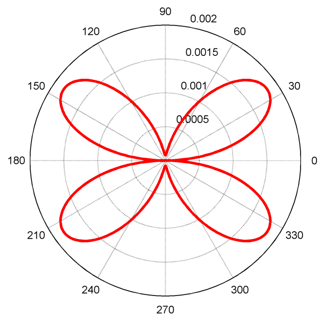

(b)

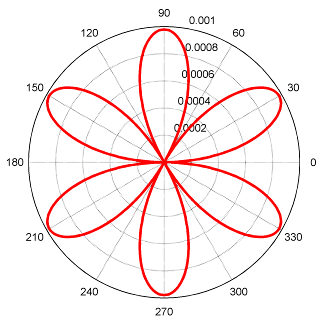

(c)

Figure 4.9: In figure (a) the SV radiation pattern purely due to the vertical derivative is shown. In (b) the SV radiation pattern due to the third order derivative is shown. In figure (c) the total SV radiation patterns is given, which is simply the summation of patterns in (a) and (b).

4.1.5 Modelled response to a magnetic dipole

The magnetic dipole source is analysed here. This source is directed perpendicular to the 2D medium surface.

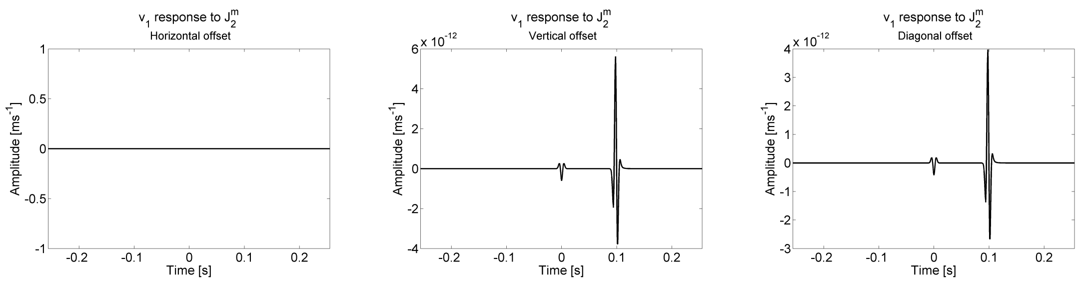

(a) (b) (c)

Figure 4.10: Particle velocity field response to the magnetic dipole

In figure 4.10(b) and 4.10(c) the arrival of an EM-wave with an amplitude of the order of 10^{-13} as well as an SV-wave with an amplitude of the order 10^{-13} are distinguishable. However, for the horizontal configuration given in figure 4.10(a) there is no detectable horizontal particle velocity.

Interpretation of the observations on the response to the magnetic dipole

According to Faraday's law, the spatial rotation of the electric field is induced by a temporal variation in the magnetic flux. Faraday's law dictates that the orientation of the curl of the electric field is opposite to the magnetic flux vector. The magnetic dipole source generates a a magnetic flux varying in time in the direction perpendicular to the 2D medium. According to Faraday's law, this results in an electric field which varies in a rotational manner in the plane of the 2D medium. A schematic representation of this is given in figure 4.11, where the magnetic flux direction is given by the black outward pointing vector and the generated electric field direction is indicated by the red arrows. These electric field vectors generate

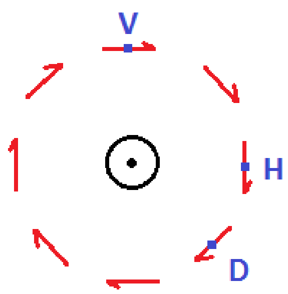

Figure 4.11: This figure illustrates the effects of Faraday's law [6]. The magnetic dipole source is denoted by the black outward pointing vector and the induced rotational electric field is denoted by the red field vectors. In yellow the positions of the receiver for the three different configurations are denoted by H (horizontal offset), D (diagonal offset) and V (vertical offset).

the electromagnetic wave field with a polarization which is parallel to these red vectors in figure 4.11. In turn this electric field generates as well a particle velocity motion with the same spatial orientation. The effect of this could result in outward propagating SV-waves. This could be better captured when looking at the schematic representation in figure 4.11. Here, point H represents the receiver position in the case of the horizontal set up. For this set up, the electric field vector is orientated in the vertical direction and this could be an explanation why no horizontal component of the SV-wave is measured for this configuration. When we look at the other set ups, denoted by points D (diagonal setup) and V (vertical setup), the electric field vector clearly has a horizontal component. This could also explain why for the vertical configuration the amplitude of the SV-wave is bigger than for the diagonal configuration, because at point V, the full electric field vector points in the horizontal direction, while for point D only a part of the field vector is horizontally directed. The same interpretation goes for the EM-wave which has the same polarization direction as the SV-wave, but is detected by the particle velocity receiver as the coelectric field.

4.2 Analysis of the horizontal component of the electric response

In this section the response of the horizontal component of the electric field is analysed for the same sources as in the previous section. The electric dipole, which was not considered in the previous section due to erroneous results, is included for this case.

4.2.1 Modelled response to a bulk force

When examining the electric field response to the horizontally directed bulk force in figure 4.12, a P-wave arrival can be observed for all three configurations. The amplitude of the P-wave is about $3 \cdot 10^{-7}$ Vm^{-1} for the horizontal offset configuration (4.12(a)). For the vertical configuration the amplitude decreases to a value of about $7 \cdot^{1} 0{-}9$ Vm^{-1}. For the diagonal configuration the amplitude is about half the amplitude of the P-wave for the horizontal configuration. There is also a detectable EM-wave observable in figures 4.12(a) and 4.12(b). The amplitude is the same in both case, with an absolute value of about $3 \cdot 10^{-9}$Vm^{-1}. However, the polarity of the EM-wave in 4.12(a) is negative as opposed to the positive polarity observed for the EM-wave in 4.12(b). The vertical directed bulk force only generates a horizontal directed electric field when the receiver is placed in the diagonal configuration (4.13(c)). It generates a fast P-wave with amplitude of a bit less than $2 \cdot 10^{-7}$ Vm^{-1}. Additionally, an EM-wave is detected with an amplitude of approximately $3 \cdot 10^{-9}$ Vm^{-1} and a reversed polarity with respect to the EM-wave seen in figure 4.12(b).

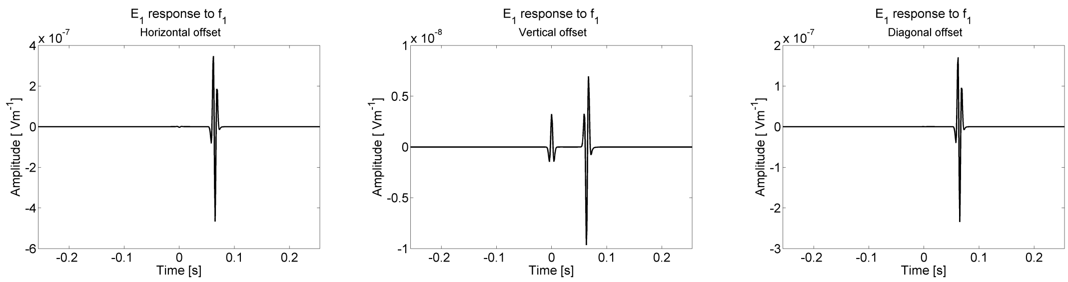

(a) (b) (c)

Figure 4.12: Electric field response to the horizontal component of the bulk force

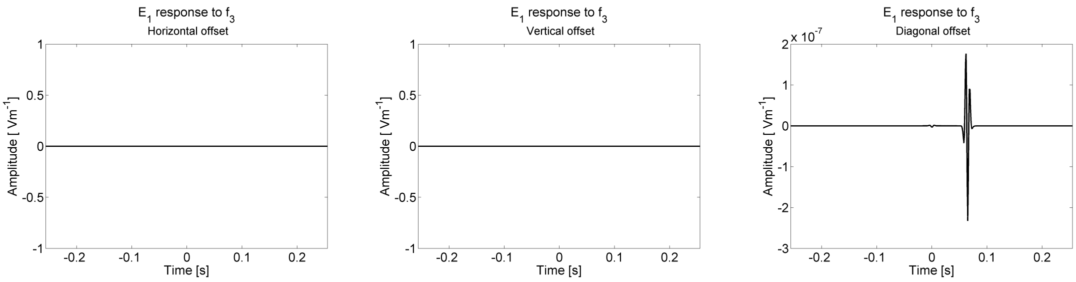

(a) (b) (c)

Figure 4.13: Electric field response to the vertical component of the bulk force

Interpretation

From the observations can be seen that the horizontal component of the bulk force generates a dominant fast P-wave. The coseismic field, which travels intrinsically with this P-wave, is detected by the horizontal electric field receiver for all configurations. The strongest response is measured when the source and receiver are aligned. It is interesting to compare this observation with the particle velocity field response to the same bulk force component in section 4.1.1. In figure 4.2 could be seen that the SV-wave is the dominant field in all configurations and the P-wave is of a much smaller amplitude. Apparently, the electric receiver detects no coseismic field of this strong SV-wave, but instead measures the coseismic field of the much weaker P-wave of 4.2. This is consistent with Pride's theory [8], which states that in general a shear wave generates a much weaker co-moving electric field compared to the co-moving electric field generated by a P-wave, as discussed in Chapter 2. The same explanation goes for the effect of the vertical component on the horizontal component of the electric field for the diagonal configuration. The detection of an EM-wave event for the vertical configuration, implies that the horizontal component of the bulk force causes direct conversion into an EM-wave field. It is useful to examine a radiation pattern of this field, because the amplitude variations of this field are difficult to analyse when plotted together with the much more dominant coseismic P-wave field. In the radiation pattern of figure 4.14(a) can be seen that the generated EM-wave creates the same electric field amplitude for both the horizontal and the vertical configuration. The reason why we cannot see the EM-wave event in 4.2(a) as clear as in 4.2(b) is caused by the fact that the fast P-wave is much stronger in figure 4.2(a). Note that from the observation of the polarity reversal of the EM-wave in figures 4.12(a) an 4.12(b) can be inferred that the polarity of the lobe at zero degrees is reversed with respect to the lobe at 90 degrees. An interpretation of this radiation pattern could be that this force generates an EM-wave field which is equivalent to an EM-wave field which would be generated by a pure electric dipole with the same orientation. Due to the prevalence of the charged mobile EDL layer, the bulk force has the ability to convert into an electric dipole. This interpretation can be verified further by looking at the radiation pattern of the EM-wave field due to an actual electric dipole later in this section (figure 4.22(a)).

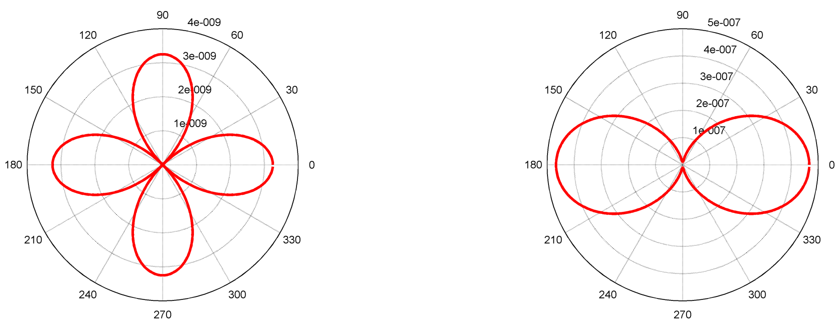

(a) (b)

Figure 4.14: The EM radiation pattern for the response of the horizontal electric field component to the horizontal component of the bulk force

4.2.2 Modelled response to a force acting only on the fluid phase

This dipole force acts purely on the fluid phase of the medium. The horizontal component of the force acting on the fluid generates both a fast P-wave as an SV-wave for all configurations. The amplitude of the SV-wave arrival is for all configurations bigger than the P-wave. For the horizontal offset the P- and SV-wave amplitudes are about $1 \cdot 10^{-4}$ and $1.5 \cdot 10^{-4}$ Vm^{-1}, respectively (figure 4.15(a)). For the vertical configuration both amplitudes decrease with about a factor of 100 (4.15(b)). For the diagonal configuration in figure 4.15(c) the amplitudes are about half the amplitude as seen for the horizontal configuration in figure 4.15(a). The vertical component of the fluid force only generates a detectable P- and SV-wave for the diagonal configuration in figure 4.15(c) with amplitudes of about $5 \cdot 10^{-5}$ Vm^{-1} and $7 \cdot 10^{-5}$ Vm^{-1}, respectively.

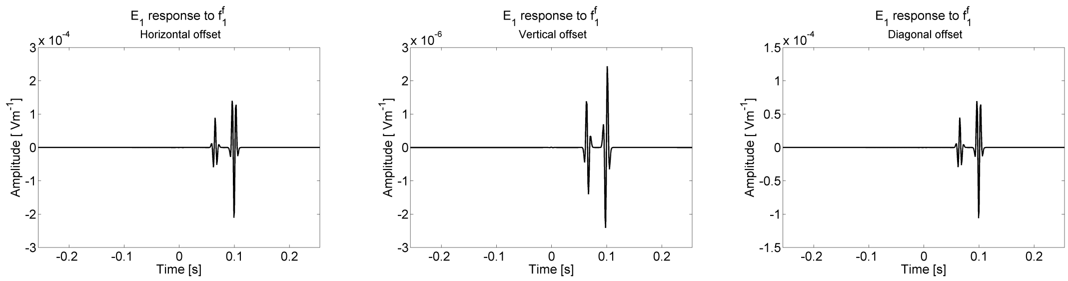

(a) (b) (c)

Figure 4.15: Electric field response to the horizontal component of the fluid force

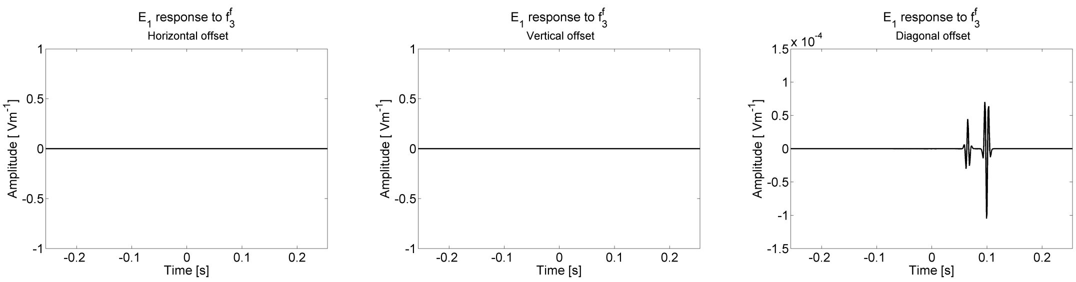

(a) (b) (c)

Figure 4.16: Electric field response to the vertical component of the fluid force

Interpretation of the observations on the effect of the fluid force

As opposed to the observation for the effect of the bulk force, we do observe for the force acting on the fluid phase a coseismic electric field of the SV-wave field. In section 4.1.2 was observed that the fluid force generates a detectable SV-wave in the particle velocity field. No fast P-wave was detected in the particle velocity field. However, the coseismic electric fields of both an SV-wave and a fast P-wave are detected as seen in figures 4.15 and 4.16. This indicates that the coseismic field of the P-wave is apparently so much stronger than the SV-wave that even when the fast P-wave is insignificantly small compared to the SV-wave field, it is still detected. This is in line with the observations and interpretation for the bulk force in section 4.2.1

4.2.3 Modelled response to a volume injection rate

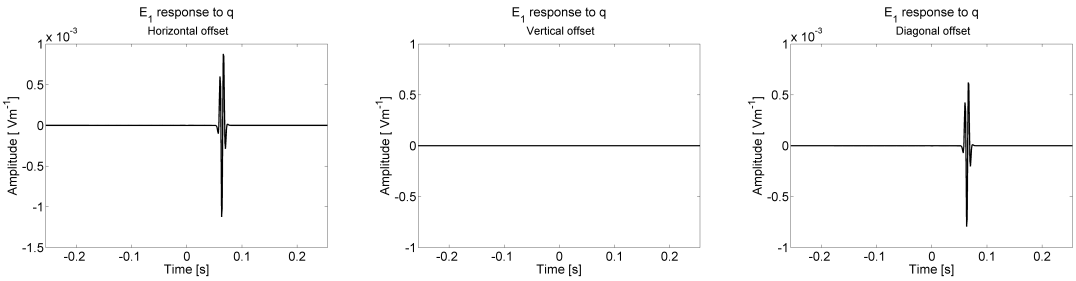

(a) (b) (c)

Figure 4.17: Electric field response to the volume injection

Examination of figure 4.17 shows us that the volume injection generates a fast P-wave for both the horizontal (figure 4.17(a)) and the diagonal configuration (4.17(c)). The amplitude of this P-wave is in both cases of the same order. However, the amplitude is a bit lower for the diagonal configuration with $6 \cdot 10^{-4}$ Vm^{-1} compared to $8 \cdot 10^{-4}$ Vm^{-1} for the horizontal configuration. No wave field is detected for the vertical configuration (figure 4.17(b)).

Interpretation of the observation of the response to the volume injection

The monopole volume injection source generates a purely dilatational P-wave, which is equipartitioned in all directions in this isotropic medium, as already explained in detail in section 4.1.3. The coseismic field of this same dilatational field is detected by the electric field receiver. This is simply because the charged particles contained in the mobile part of the EDL move along with the dilatational P-wave, thus generating a variation in the electric field strength in the same direction as the P-wave polarization.

4.2.4 Modelled response to a shear strain source

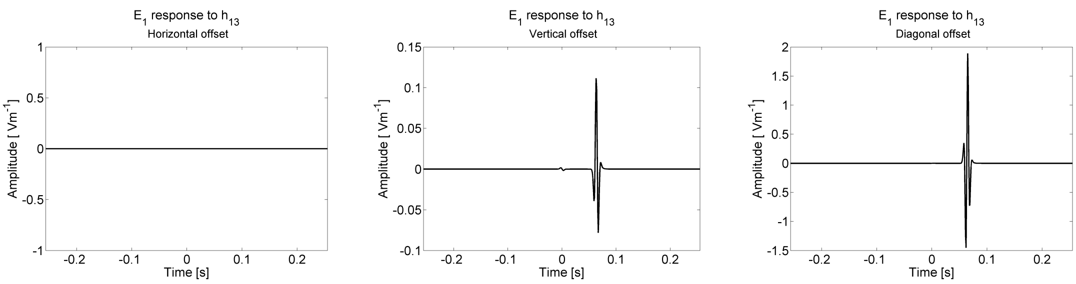

(a) (b) (c)

Figure 4.18: Electric field response to the horizontal component of the shear strain source

For the horizontal configuration, the shear strain source does not generate any wave field which affects the horizontal electric field component (figure 4.18(a)). However, for the vertical configuration a distinct fast P-wave is visible with an amplitude of about $1 \cdot 10^{-1}$ Vm^{-1} (figure 4.18(b)). Also a much smaller EM-wave can be distinguished with amplitude of the order 10^{-2}. Note that the shape of the EM wavelet is asymmetrical. For the diagonal configuration in figure 4.18(c), a fast P-wave is observed with an amplitude about twice as strong as in figure 4.18(a). No EM-wave is distinguishable here.

Interpretation of the observation of the response to the shear strain source

In section 4.1.4 we observed that this shear strain source generates a fast P-wave and an SV-wave, affecting the particle velocity field, for the vertical and diagonal configurations. Although both wave fields were of the same order, the shear wave appeared to be stronger than the P-wave, especially for the vertical configuration. Here, for the electric field (figure 4.18), we observed as well no field disturbances for the horizontal configuration. However, only the coseismic electric field is detected of the fast P-wave and not of the SV-wave. This is because the fast P-wave generates a much stronger co-moving electric field compared to the SV-wave, as already explained for the effects of the bulk force in section 4.2.1, where a similar phenomenon was observed. The small EM wavelet observed for the vertical configuration in figure 4.18(b) is interesting because of its asymmetrical shape. This asymmetry for the vertical configuration indicates that the field is generated via a spatial derivative in the vertical direction of the source. In equation 2.40 in Chapter 2 can be seen that this distinct EM wavelet for the vertical configuration could arise either from the third order spatial derivative term or the first order vertical spatial derivative term. By examining the radiation patterns in figure 4.19, generated by each of the terms separately, it can be observed that for the angle of 90 degrees the third order spatial derivative term (figure 4.19(b)) yields a 10^6 times stronger amplitude than the first order term. Therefore, it can be concluded that the EM wavelet in figure 4.18(b) is a result of the third order spatial derivative of the EM Green's function seen in equation 2.40.

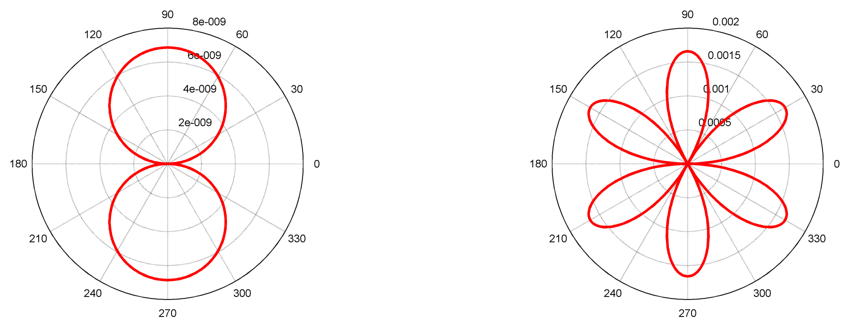

(a) (b)

Figure 4.19: In figure 4.19(a) the vertical spatial derivative term of the EM wave field is shown, where the amplitude is of the order 10^{-9}. In figure 4.19(b) the third order spatial derivative term of the EM wave field is shown, where the amplitude is of the order 10^{-3}.

4.2.5 Modelled response to an electric dipole source

In figure 4.20(a), the electric field response to a horizontal electric dipole is given for the horizontal configuration. A strong EM-wave arrival of positive polarity and an amplitude of about $7 \cdot 10^{-1}$ Vm^{-1}, as well as a weaker fast P-wave arrival with an amplitude of about

$1 \cdot 10^{-1}$ Vm^{-1}, can be observed. For the vertical configuration in figure 4.20(b), only an EM-wave can be distinguished with the same absolute amplitude value as the EM-wave observed in figure 4.20(a). However, the EM-wave is of reversed polarity in this case. For the diagonal configuration only a fast P-wave can be detected with an amplitude of about $5 \cdot 10^{-2}$ Vm^{-1}. For the vertical component of the electric dipole can be observed that it does not generate any disturbance in the electric field for both horizontal and vertical configurations (figures 4.21(a) and 4.21(b)). For the diagonal set up, an EM-wave with an amplitude of about $7 \cdot 10^{-1}$ Vm^{-1} is generated, as well as a weaker fast P-wave with an amplitude of about $4 \cdot 10^{-2}$ Vm^{-1}.

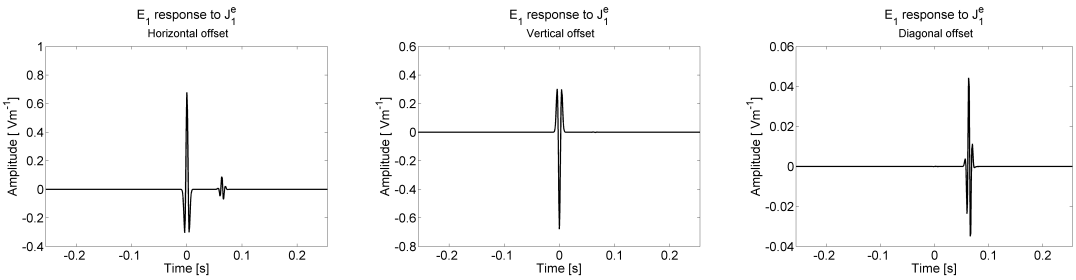

(a) (b) (c)

Figure 4.20: Electric field response to the horizontal component of the electric dipole

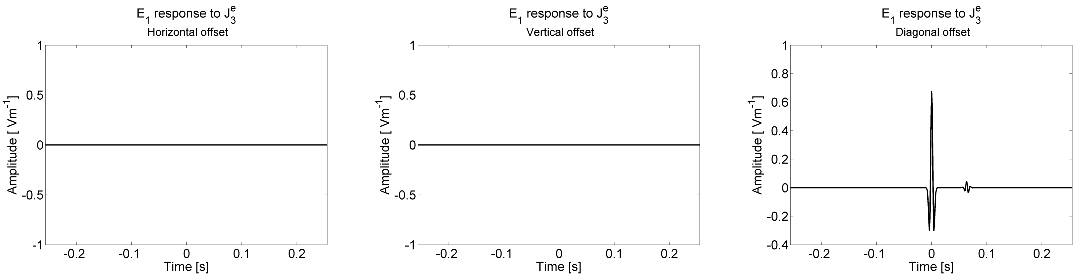

(a) (b) (c)

Figure 4.21: Electric field response to the vertical component of the electric dipole

Interpretation of the observation of the response to the electric dipole

The horizontal component of the electric dipole source generates both an EM-wave and a fast P-wave. The radiation pattern of the EM-wave generated by the horizontal component of the electric dipole is given in figure 4.22(a). In section 4.2.1, the idea that the bulk force has the ability to act as an electric dipole was introduced. This can be verified by comparing the radiation pattern of the EM-wave of the horizontal bulk force in that section in figure 4.14(a) with the radiation pattern for the same wave due to the same component of the electric dipole here in figure 4.22(a). The shape of the radiation patterns are indeed the same, except for the much lower amplitude in the case of the bulk force. This lower amplitude can be explained by the energy loss caused by the coupling of the mechanical force field into an electric field. However, the idea that the bulk force can generate the same EM wave as an electric dipole seems plausible. The question is now whether this idea also works the other way round, in other words whether an electric dipole source also has the ability to act as a bulk force and generate a similar fast P-wave field. The radiation patterns of the fast P-wave field generated by the electric dipole in figure 4.22(b) and the bulk force in figure 4.14(b) are compared. The shapes of the two radiation patterns turn out to be the same. However, the electric dipole generates a fast P-wave with a much stronger coseismic electric field than the coseismic field of the fast P-wave generated by the bulk force. This is remarkable, because one would expect that the electric dipole generates a weaker fast P-wave than the bulk force, because of energy loss during conversion. However, a possible explanation could be that an electric dipole has in general a much stronger effect on this type of medium than a bulk force.

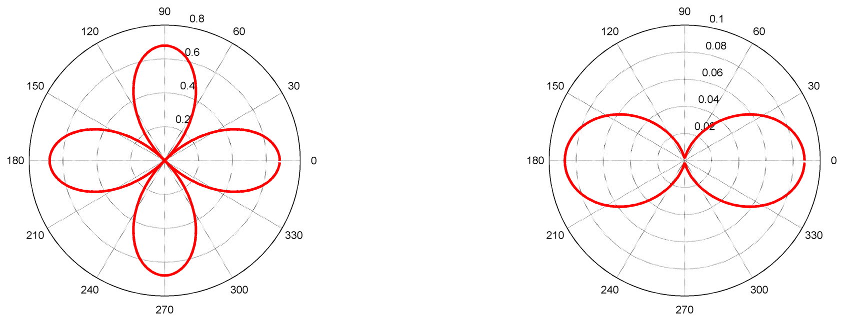

(a) (b)

Figure 4.22: The EM radiation pattern for the response of the horizontal electric field component to the horizontal component of the electric dipole is given in 4.22(a). Note the resemblance to the radiation pattern in figure 4.14(a). There is also a resemblance between the radiation pattern of the fast P-wave field in figure 4.22(b) due to the horizontal electric dipole and the radiation pattern in figure 4.14(b).

4.2.6 Modelled response to a magnetic dipole

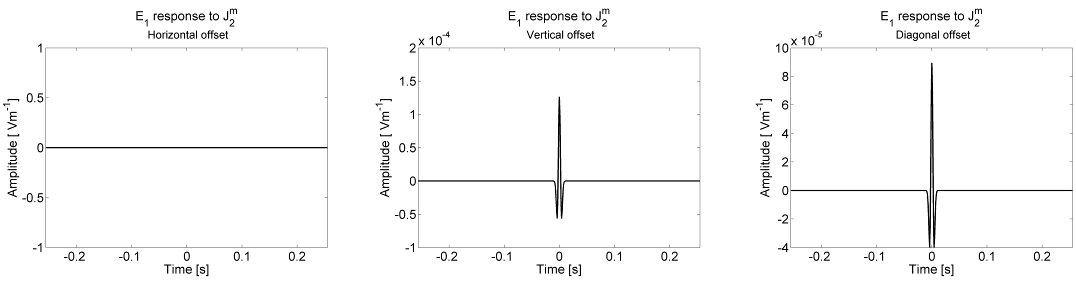

(a) (b) (c)

Figure 4.23: Electric field response to the magnetic dipole

In figures 4.23(a) and 4.23(c) can be observed that the magnetic dipole vector only affects the electric field for the vertical and diagonal configurations with amplitude values of $13 \cdot 10^{-5}$ Vm^{-1} and $9 \cdot 10^{-5}$ Vm^{-1}, respectively. For the horizontal configuration there is no electric field response to this source (figure 4.23(a)).

Interpretation of the observation of the response to the magnetic dipole

The particle velocity response to this source type yields both an EM-wave and an SV-wave for the horizontal and diagonal configurations as discussed in section 4.1.5. The amplitudes of these fields were in the order of 10^{-12}. In the case of the electric field response to this source type (figure 4.23) only an EM-wave is detected, because the coseismic electric field of the SV-wave is insignificantly small.

Chapter 5

Discussion of results

In this thesis the first steps are take to retrieve a Green's function by interferometry of the P-SV-TM mode in 2D. Each dipole source type generates four fields, fast and slow P-waves, a vertically polarized S-wave and a TM-mode electromagnetic field. The magnetic source generates only an SV-wave and a TM-mode field. To better understand the contributions from the different constituents per source type, a Green's function analysis of this complicated P-SV-TM mode has been performed. All field responses necessary for the interferometric Green's retrieval, as specified in equation 3.7, which is repeated here as equation 5.1, were analysed for different configurations. By considering the effect of cross-correlation on these field responses, the analysis of Chapter 4 can now be used to evaluate the results found in Chapter 3.

$$
\begin{aligned}
&2i\Im\left[\hat{G}^{E_1,f_1}(\bar{x}_B,\bar{x}_A,\omega)\right] \\
&= -\oint_{\partial D}[n_3\hat{G}^{*v_1,J_2^m}_{\bar{x}_A,\bar{x}}\hat{G}^{E_1,J_1^e}_{\bar{x}_B,\bar{x}} - n_1\hat{G}^{*v_1,J_2^m}_{\bar{x}_A,\bar{x}}\hat{G}^{E_1,J_3^e}_{\bar{x}_B,\bar{x}} + n_3\hat{G}^{*E_1,f_1}_{\bar{x},\bar{x}_A}\hat{G}^{E_1,J_2^m}_{\bar{x}_B,\bar{x}} - n_1\hat{G}^{*v_1,J_3^e}_{\bar{x}_A,\bar{x}}\hat{G}^{E_1,J_2^m}_{\bar{x}_B,\bar{x}} \\
&+n_3\hat{G}^{*v_1,2h_{31}}_{\bar{x}_A,\bar{x}}\hat{G}^{E_1,f_1}_{\bar{x}_B,\bar{x}}+n_1\hat{G}^{*v_1,2h_{31}}_{\bar{x}_A,\bar{x}}\hat{G}^{E_1,f_3}_{\bar{x}_B,\bar{x}}+n_3\hat{G}^{*v_1,f_1}_{\bar{x}_A,\bar{x}}\hat{G}^{E_1,2h_{31}}_{\bar{x}_B,\bar{x}}+n_1\hat{G}^{*v_1,f_3}_{\bar{x}_A,\bar{x}}\hat{G}^{E_1,2h_{31}}_{\bar{x}_B,\bar{x}}+n_1\hat{G}^{*v_1,Cq}_{\bar{x}_A,\bar{x}}\hat{G}^{E_1,f_1^{(f)}}_{\bar{x}_B,\bar{x}} \\
&\qquad + n_3\hat{G}^{*v_1,Cq}_{\bar{x}_A,\bar{x}}\hat{G}^{E_1,f_3^{(f)}}_{\bar{x}_B,\bar{x}} + n_1\hat{G}^{*v_1,f_1^f}_{\bar{x}_A,\bar{x}}\hat{G}^{E_1,Cq}_{\bar{x}_B,\bar{x}} + n_3\hat{G}^{*v_1,f_3^f}_{\bar{x}_A,\bar{x}}\hat{G}^{E_1,Cq}_{\bar{x}_B,\bar{x}}]\,\mathrm{d}\bar{x} \qquad (5.1)
\end{aligned}
$$

5.1 Possible explanations for the discrepancies observed in the interferometric retrieval

The exact left hand-side of equation 3.7 results in an anti-symmetrical signal of P-waves as observed in figure 3.5 . The interferometric retrieval of these P-wave arrivals, arises from the cross-correlation of the coseismic field of the P-wave received at electric receiver B, with the seismic P-wave received at the particle velocity receiver A (refer to figure 3.3 for the model configuration). However, the responses at these receivers do not always consist purely of a dominant P-wave arrival. On the contrary, as observed in Chapter 2, all sources, except for the magnetic dipole, have the ability to generate all three wave fields. On top of that, in Chapter 4, all these three wave fields were indeed observed, however which field was actually detectable turned out to depend strongly on the source type as well as on the geometry of the configuration. We think that the extra retrieved events as observed in figure 3.5 could be caused by the cross-correlation of P-waves with SV-waves. In order to verify that, the time lags need to be known, which would result from cross-correlating these two wave types, for different illumination angles. In table 5.1 these various time lags are shown accordingly. As observed from the final interferometric retrieval the extra events occur at ± 0.15 and ± 0.03 seconds. In the table 5.1, can be observed that these arrival times could result from cross-correlating signals which arise from sources at a horizontal offset orientation. When increasing this angle of illumination from horizontal to finally the vertical orientation, these two time lags will converge to the same time lag value of 0.09 seconds. The vertical configurations are not considered further in this discussion, because no retrieved event at ± 0.09 seconds is observed in figure 3.5. It will be assumed that the time lag values as shown in table 5.1 will not change significantly as the angle of illumination is varied between 0 to 30 degrees. Another assumption is that responses due to the diagonal configuration (offset angle of 45 degrees) as observed in Chapter 4 are comparable to configuration with an offset angle of 30 degrees. These assumptions enable the examination of both horizontal and diagonal configurations from Chapter 4, for the purpose of finding an explanation for the extra retrieved events.

Table 5.1: In this table the resulting time lag values by cross-correlating the specified wave types coming from either sides of the circle are given in seconds. With 'illumination right' or 'illumination left', is meant that the sources are located on the right- or left- half side of the modelled circle boundary, respectively. With 'horizontal' is meant an illumination angle range of 330-30 degrees and 150-210 degrees, for the right and left sides of the circle boundary, respectively.

Cross-correlated wave types	Horizontal illumination right	Horizontal illumination left
$P_B \otimes SV_A$	-0.15 s	-0.03 s
$SV_B \otimes P_A$	0.03 s	0.15 s

5.1.1 Cross-correlation terms containing responses to the bulk sources

In figure 3.8 could be observed that the bulk source responses contribute significantly to the P-wave retrieval. Except of the fact that the retrieval signal is of a different wavelet shape as discussed in section 3.6.4. The bulk responses also contribute to the a-causal artefacts at -0.03 and -0.15 seconds. It will be investigated now, from which of the four bulk source cross-correlation pairs in equation 5.1 these artefacts could arise from.

The cross-correlation pair, which compares the particle velocity response to a shear strain with the electric field response to a vertical bulk force is given by,

$$n_1 \hat{G}^{*v_1,2h_{31}}_{\bar{x}_A,\bar{x}} \hat{G}^{E_1,f_3}_{\bar{x}_B,\bar{x}} \tag{5.2}$$

The electric field response due to a vertical bulk source is only non-zero for the diagonal configuration. Therefore, the contribution of this term will only come from the areas of the circle which are neither exactly vertically nor horizontally orientated with respect to the receivers. Therefore, only sources from the diagonally orientated parts of the circle boundary will contribute to this term. The particle velocity response to the shear source for the diagonal configuration results in dominant P- and SV-waves of the order of 10^{-3} (figure 4.8(c)). The electric field yields a dominant P-wave of the order 10^{-7}, but the SV-wave is of an undetectable amplitude (figure 4.13(c)). The result of cross-correlating the P-waves of both responses will be the phase difference between the P-wave arrivals, which is due to the receiver offset, with an amplitude around the order of 10^{-10}. However, the extra SV-wave event in the particle velocity response causes extra artefacts in the resulting cross-correlation. This is due to the extra phase difference which exists between P- and SV- wave arrivals. From table 5.1 can be seen that the cross-correlation of a P-wave received at B with a SV-wave received at A would result in a time lag of -0.15 and -0.03 seconds for sources located at the right and left sides of the circle, respectively.

The cross-correlation pair, which compares the particle velocity response to a shear strain with the electric field response to a horizontal bulk force is given by,

$$n_3 \hat{G}^{*v_1,2h_{31}}_{\bar{x}_A,\bar{x}} \hat{G}^{E_1,f_1}_{\bar{x}_B,\bar{x}} \tag{5.3}$$

For the diagonal configuration the particle velocity response to a strain source shows dominant P- and SV-waves of the order of 10^{-3} (figure 4.8(c)). For the same configuration the electric field response to the horizontal bulk force yields only a P-wave of amplitude order 10^{-7}. This would yield the same result as the cross-correlation pair 5.2, but the contribution is probably much less because the n_3- component is very low for the horizontal illumination angle range and zero for a purely horizontal illumination.

The cross-correlation pair, which compares the particle velocity response to a horizontal bulk force with the electric field response to a shear strain is given by,

$$n_3 \hat{G}^{*v_1,f_1}_{\bar{x}_A,\bar{x}} \hat{G}^{E_1,2h_{31}}_{\bar{x}_B,\bar{x}} \tag{5.4}$$

For the vertical offset, the electric field response shows a dominant coseismic field of a P-wave with an amplitude of the order 10^{-1}. The velocity field shows an SV-wave of amplitude of order 10^{-9}, but no detectable P-wave. I expect that cross-correlating this coseismic P-wave with a seismic SV-wave has no significant contribution, because there is no artefact observable at 0.09 seconds, which is the expected time lag for vertical configurations. For the diagonal configuration the particle velocity field, a dominant SV-wave is observed as well, but this configuration does also yield a detectable P-wave with an amplitude of the order 10^{-10} (figure 4.2(c)). The P-wave detected for the same configuration for the electric field is of the order 10^{1} (figure 4.18(c)). Cross-correlation of the responses would therefore yield a P-wave arrival with an amplitude of the order 10^{-10}, but due to the much stronger SV-wave in the particle velocity field, bigger contributions will be made to the a-causal artefacts at -0.03 and -0.15 seconds.

The cross-correlation pair which compares the particle velocity response to a vertical bulk force with the electric field response to a shear strain is given by,

$$n_1 \hat{G}^{*v_1,f_3}_{\bar{x}_A,\bar{x}} \hat{G}^{E_1,2h_{31}}_{\bar{x}_B,\bar{x}} \tag{5.5}$$

Only the diagonal offset orientation has the ability to generate a particle velocity field due to the vertical bulk force, as observed from figure 4.3, therefore the cross-correlation only has a contribution for non-vertical and non-horizontal offset orientations. For the diagonal offset, the particle velocity response yields both a fast P-wave as an SV-wave of amplitude order 10^{-10}. In the case of the electric field response to the shear strain source for this particular configuration (figure 4.18(c)), only the fast P-wave gives a dominant contribution of order 10^{1}. Cross-correlation of these two responses would yield a P-wave arrival of the order 10^{-10}. However, the dominant SV-wave in the particle velocity trace again contributes significantly to the a-causal artefacts.

5.1.2 Cross-correlation terms containing responses to the fluid sources

In figure 3.7 could be seen that the cross-correlation of responses to volume injection and force acting on the fluid phase contribute to the anti-symmetric P-wave retrieval, but not as strongly as the bulk force responses did, as observed from figure 3.8. The fluid source responses contribute mainly to the causal artefacts at 0.03 and 0.15 seconds, but also show a slight contribution to the a-causal equivalents.

The cross-correlation pair, which compares the particle velocity response to a volume injection source to the electric field response to the horizontal component of the fluid force,

$$n_1 \hat{G}^{*v_1,Cq}_{\bar{x}_A,\bar{x}} \hat{G}^{E_1,f_1^{(f)}}_{\bar{x}_B,\bar{x}} \tag{5.6}$$

The particle velocity field induced by the volume injection source produces for both the horizontal and the diagonal configuration a P-wave amplitude of the order of 10^{-7} (figures 4.7(a) and 4.7(c)). The electric field response to the horizontal component of the force acting on the fluid phase yields a P-wave amplitude of the order of 10^{-4} for both configurations (figures 4.15(a) and 4.15(c)). The co-seicmic field of an SV-wave of the same order is detected as well. The cross-correlation of these two field responses would yield a P-wave arrival with amplitude of the order 10^{-11} due to sources located at horizontal diagonal offsets. However, the extra SV-wave event observed in the electric field response will affect the cross-correlation result. Nevertheless, it will not contribute to the a-causal artefacts as was observed for the bulk force cross-correlation pairs, for which SV-waves were observed in the particle velocity fields (which is the conjugate part of the cross-correlation pair). Due to the fact that the SV-wave occurs for the fluid force cross-correlation pairs as a coseismic in the non-conjugated electric field response, the resulting artefacts will now occur only in the causal part of the resulting signal. Therefore, the coseismic SV-wave will contribute to the causal artefacts observed in figure 3.7 at 0.03 and 0.15 seconds.

The cross-correlation pair, which compares the particle velocity response to a volume injection source to the electric field response to the vertical component of the fluid force,

$$n_3 \hat{G}^{*v_1,Cq}_{\bar{x}_A,\bar{x}} \hat{G}^{E_1,f_3^{(f)}}_{\bar{x}_B,\bar{x}} \tag{5.7}$$

The particle velocity field response is zero for the vertical configuration (figure 4.7(b)). Therefore, only the diagonal configuration needs to be discussed here, which shows a detectable P-wave with an amplitude of the order 10^{-7} for the particle velocity response (figure 4.7(c)). The electric field response to the vertical component of the bulk force yields a detectable P-wave as well, of the order 10^{-4}. It also shows a detectable SV-wave of the same order. Cross-correlation of these two responses would yield a P-wave arrival with amplitude of the order 10^{-11} for diagonal offset orientations only. The extra coseismic SV-wave event will contribute to the causal artefacts at 0.025 and 0.16 seconds.

The cross-correlation pair which compares the particle velocity response to a volume injection source to the electric field response to the horizontal component of the fluid force, is given by

$$n_1 \hat{G}^{*v_1,f_1^f}_{\bar{x}_A,\bar{x}} \hat{G}^{E_1,Cq}_{\bar{x}_B,\bar{x}} \tag{5.8}$$

For the horizontal and diagonal configurations the particle velocity response to the horizontal component of the fluid force is dominated by an SV-wave with an amplitude of the order 10^{-9} (figures 4.5(a) and 4.5(c)). For the same configurations, the electric field response to a volume injection is dominated by the coseismic field of P-waves of the order of 10^{-3}. The correlation between these two wave field responses will only result in a-causal artefacts, because here we cross-correlate a coseismic P-wave with a seismic SV-wave. In figure 3.7 you can see a slight contribution to the a-causal artefacts, which I think arise from this specific cross-correlation.

The cross-correlation pair, which compares the particle velocity response to a volume injection source to the electric field response to the horizontal component of the fluid force,

$$n_3 \hat{G}^{*v_1,f_3^f}_{\bar{x}_A,\bar{x}} \hat{G}^{E_1,Cq}_{\bar{x}_B,\bar{x}} \tag{5.9}$$

Only for the diagonal configuration, the particle velocity gives a response to the vertical component of the fluid force (figure 4.6). This response shows a dominant seismic SV-wave of the amplitude order 10^{-9}. The electric field response to the volume injection source yields a coseismic P-wave of the amplitude order of 10^{-3}. As was the case for the cross-correlation term, $n_1 \hat{G}^{*v_1,f_1^f}_{\bar{x}_A,\bar{x}} \hat{G}^{E_1,Cq}_{\bar{x}_B,\bar{x}}$, this term will also result in a contribution to the a-causal artefacts.

Chapter 6

Conclusions

The original goal of this thesis was to obtain an interferometric retrieval of the exact left hand-side. The resulting retrieval showed some resemblances to the exact left-hand side, because the exact anti-symmetric P-wave signal was observed as well for the retrieval. However, the retrieval amplitude was about five times lower and its shape indicates that it is a second order derivative of a Ricker wavelet, in stead of a third order derivative as is indicated by the shape of the left-hand side. The retrieval also showed four extra events, which were not represented by the left hand-side. The detailed analysis conducted in Chapter 4 made it possible to determine which source responses give the strongest contribution to the desired exact retrieval and which contribute to the unwanted extra events.

The cross-correlation pairs which contain the field responses to sources acting on the bulk give the strongest contribution to the interferometric retrieval. The cross-correlation pairs containing the responses to the sources acting purely on the fluid phase have less contribution to the retrieval, but not as negligible as the pairs containing the responses to electromagnetic sources. The anti-symmetric P-wave arrivals which characterize the Green's function on the left hand-side of the interferometric relation 5.1, are retrieved by cross-correlation of the electric coseismic fields of P-waves with seismic P-waves. As was observed from the analysis in Chapter 4 these P-waves are quite abundant in most of the responses. However, due to the abundance of SV-waves as well, the causal and a-causal artefacts arise. The a-causal artefacts of the interferometric retrieval arise from cross-correlating coseismic fields of P-waves received at x_B with seismic SV-waves received at x_A, which are generated by sources acting on the bulk. The causal artefacts arise from cross-correlating electric coseismic fields of SV-waves received at x_B with seismic P-waves received at x_A, generated by sources acting on the fluid phase. Therefore, the fact that dominant seismic or coseismic SV-waves occur in several field responses results in the observed artefacts in the interferometric retrieval. The causality of these artefacts depend on whether this SV-wave event is observed in the particle velocity field, which forms the conjugate of the pair, or as a coseismic in the electric field, which forms the non-conjugate of the pair. Whether the artefact appears at the absolute travel time of 0.15 seconds or at 0.03 seconds depends on from which side the receivers are illuminated.

Suggestions for future research

The field responses to the shear strain sources turned out to contribute most significantly to the interferometric retrieval modelled in this thesis. In spite of this strong contribution, the retrieval's amplitude was five times weaker than the exact left hand-side. This could be due to the fact that the other source terms of the strain tensor, the tensile strain sources h_{11} and h_{33}, were not modelled in this thesis. It can be expected that these sources will have a very strong contribution to the retrieval and therefore it is recommended to include them in any future attempt to model the interferometric retrieval of a seismoelectric P-SV-TM mode wave field. Another assumption made in this interferometric modelling experiment, was that the domain integral of the interferometry relation is negligible. Including this volume integral in the model could present a possible solution for the encountered inconsistencies in the results.

Appendix A

Spatial derivatives of the Bessel function K_0

$$\hat{G}^{2D}(x_R, x_S, s) = \hat{G}^{2D}(r, s) = \frac{1}{2\pi} K_0(\gamma r) \tag{A.1}$$

$$\tag{A.2}$$

Where, $\gamma = \frac{s}{c}$ and $r = \sqrt{(x_{1,R} - x_{1,S})^2 + (x_{3,R} - x_{3,S})^2}$. The receiver position is the variable coordinate. The derivatives of the modified Bessel function of second kind and order zero are given (Abramowitz and Stegun, 1972),

$$\frac{2n}{z} e^{in\pi} K_n(z) = e^{i(n-1)\pi} K_{n-1}(z) - e^{i(n+1)\pi} K_{n+1}(z) \tag{A.3}$$

$$2e^{in\pi} K_n'(z) = e^{i(n-1)\pi} K_{n-1}(z) + e^{i(n+1)\pi} K_{n+1}(z) \tag{A.4}$$

$$K_n'(z) = \frac{n}{z} K_n(z) - K_{n+1}(z) \tag{A.5}$$

$$\begin{aligned} \partial_3^R K_0(\gamma r) &= \gamma \frac{x_{3,R} - x_{3,S}}{r} K_0'(\gamma r) \\ &= -\gamma \frac{x_{3,R} - x_{3,S}}{r} K_1(\gamma r) \end{aligned} \tag{A.6}$$

$$\begin{aligned} \partial_1^R K_0(\gamma r) &= \gamma \left[\frac{x_{1,R} - x_{1,S}}{r} K_0'(\gamma r) \right] \\ &= -\gamma \left[\frac{x_{1,R} - x_{1,S}}{r} K_1(\gamma r) \right] \end{aligned}$$

$$
\begin{aligned}
\partial_1^R\partial_1^R K_0(\gamma r) &= \partial_1^R\gamma\left[\frac{x_{1,R}-x_{1,S}}{r}K_0'(\gamma r)\right] = -\partial_1^R\gamma\left[\frac{x_{1,R}-x_{1,S}}{r}K_1(\gamma r)\right] \\
&= -\gamma\left[\left(\frac{1}{r}-\frac{(x_{1,R}-x_{1,S})^2}{r^3}\right)K_1(\gamma r)+\gamma\frac{(x_{1,R}-x_{1,S})^2}{r^2}K_1'(\gamma r)\right] \\
&= -\gamma^2\left[\left(1-\frac{(x_{1,R}-x_{1,S})^2}{r^2}\right)\frac{K_1(\gamma r)}{\gamma r}+\frac{(x_{1,R}-x_{1,S})^2}{r^2}K_1'(\gamma r)\right] \\
&= \gamma^2\left[-\frac{K_1(\gamma r)}{\gamma r}+\frac{(x_{1,R}-x_{1,S})^2}{r^2}\left(\frac{K_1(\gamma r)}{\gamma r}-K_1'(\gamma r)\right)\right] \\
&= \gamma^2\left[\frac{(x_{1,R}-x_{1,S})^2}{r^2}K_2(\gamma r)-\frac{K_1(\gamma r)}{\gamma r}\right]
\end{aligned}
\tag{A.7}
$$

$$
\begin{aligned}
&\partial_1^R\partial_1^R\partial_1^R K_0(\gamma r) = \gamma^2\partial_1^R\left[\frac{(x_{1,R}-x_{1,S})^2}{r^2}K_2(\gamma r)\right]-\gamma\partial_1^R\left[\frac{K_1(\gamma r)}{r}\right] \\
&= \gamma^2\left[2(\frac{x_{1,R}-x_{1,S}}{r^2}-\frac{(x_{1,R}-x_{1,S})^3}{r^4})K_2(\gamma r)-\gamma\frac{(x_{1,R}-x_{1,S})^3}{2r^3}\left(K_1(\gamma r)+K_3(\gamma r)\right)\right] \\
&-\gamma\partial_1^R\left[\frac{K_1(\gamma r)}{r}\right] \\
&= \gamma^2\left[2(\frac{x_{1,R}-x_{1,S}}{r^2}-\frac{(x_{1,R}-x_{1,S})^3}{r^4})K_2(\gamma r)-\gamma\frac{(x_{1,R}-x_{1,S})^3}{2r^3}\left(K_1(\gamma r)+K_3(\gamma r)\right)\right] \\
&+\gamma\left[\frac{K_1(\gamma r)}{r^3}(x_{1,R}-x_{1,S})+\frac{\gamma}{2r}(x_{1,R}-x_{1,S})\left(K_0(\gamma r)+K_2(\gamma r)\right)\right]
\end{aligned}
\tag{A.8}
$$

$$
\begin{aligned}
&\partial_3^R\partial_1^R\partial_1^R K_0(\gamma r) = \gamma\frac{x_{3,R}-x_{3,S}}{r^3}K_1(\gamma r)+\gamma^2\frac{x_{3,R}-x_{3,S}}{2r^2}(K_0(\gamma r)+K_2(\gamma r)) \\
&-(x_{1,R}-x_{1,S})^2\left(\frac{\gamma}{r^2}\right)^2\left[2(x_{3,R}-x_{3,S})K_2(\gamma r)+\frac{\gamma}{2}r(x_{3,R}-x_{3,S})\left(K_1(\gamma r)+K_3(\gamma r)\right)\right]
\end{aligned}
\tag{A.9}
$$

$$
\begin{aligned}
&\partial_3^R\partial_1^R K_0(\gamma r) = \partial_3^R\gamma\left[\frac{x_{1,R}-x_{1,S}}{r}K_0'(\gamma r)\right] \\
&= -\partial_3^R\gamma\left[\frac{x_{1,R}-x_{1,S}}{r}K_1(\gamma r)\right] \\
&= -\gamma\left[-\frac{(x_{1,R}-x_{1,S})(x_{3,R}-x_{3,S})}{r^3}K_1(\gamma r)+\gamma\frac{(x_{1,R}-x_{1,S})(x_{3,R}-x_{3,S})}{r^2}K_1'(\gamma r)\right] \\
&= \gamma^2\left[\left(\frac{K_1(\gamma r)}{\gamma r}-K_1'(\gamma r)\right)\frac{(x_{1,R}-x_{1,S})(x_{3,R}-x_{3,S})}{r^2}\right] \\
&= \gamma^2\left[K_2(\gamma r)\frac{(x_{1,R}-x_{1,S})(x_{3,R}-x_{3,S})}{r^2}\right]
\end{aligned}
\tag{A.10}
$$

$$\partial_3^R \partial_3^R \partial_1^R K_0(\gamma r) =$$
$$\gamma^2 (x_{1,R} - x_{1,S}) \left[\frac{K_2(\gamma r)}{r^2} - \frac{2(x_{3,R} - x_{3,S})^2 K_2(\gamma r)}{r^4} - \frac{\gamma}{2} \frac{(x_{3,R} - x_{3,S})^2}{r^2} (K_1(\gamma r) + K_3(\gamma r)) \right] \tag{A.11}$$

Appendix B

Green's function representations of 2D P-SV-TM mode wave fields

The full expressions for all Green's functions discussed in Chapter 2 are given here. These functions are found by substituting the relevant source type into the source terms of the two second order wave equations B.5 and B.6.

B.1 Wave equations and source functions

The two second order wave equations 2.27 and 2.28 derived in Chapter 2 are repeated here, respectively,

$$\left(k_1^2 + k_3^2 + \gamma_S^2\right)\left(k_1^2 + k_3^2 + \gamma_{EM}^2\right)\breve{E}_{1;3} = \\ -\frac{\zeta\hat{L}}{s}\left(k_1^2 + k_3^2 + \frac{s^2\rho}{G^{fr}}\right)X_{11,1;3} + \frac{s\rho^f\zeta\hat{L}}{G^{fr}}X_{22,1;3} \tag{B.1}$$

$$\left(k_1^2 + k_3^2 + \gamma_S^2\right)\left(k_1^2 + k_3^2 + \gamma_{EM}^2\right)\breve{v}_{1;3} = \\ -\frac{\hat{k}s\rho^f}{\eta G^{fr}}\left(k_1^2 + k_3^2 + \zeta\varsigma\right)X_{11,1;3} + \frac{1}{G^{fr}}\left(k_1^2 + k_3^2 + \zeta(\varsigma + \hat{L}\hat{\xi})\right)X_{22,1;3} \tag{B.2}$$

The full seismoelectric Green's function consists of a coupled electromagnetic and elastodynamic transveral Green's function, $\breve{G}_{EM}$ and $\breve{G}_S$, respectively,

$$\begin{aligned}\breve{G} &= \frac{1}{\left(k_1^2 + k_3^2 + \gamma_S^2\right)\left(k_1^2 + k_3^2 + \gamma_{EM}^2\right)} \\ &= \frac{\breve{G}_{EM} - \breve{G}_S}{\gamma_S^2 - \gamma_{EM}^2} \\ &= \frac{\breve{G}_{EM}}{\gamma_S^2 - \gamma_{EM}^2} - \frac{\breve{G}_S}{\gamma_S^2 - \gamma_{EM}^2}\end{aligned} \tag{B.3}$$

$$
\begin{aligned}
(k_1^2 + k_3^2)\breve{G} &= \frac{(k_1^2 + k_3^2)\breve{G}_{EM} - (k_1^2 + k_3^2)\breve{G}_S}{\gamma_S^2 - \gamma_{EM}^2} \\
&= \frac{1 - \gamma_{EM}^2\breve{G}_{EM} - 1 + \gamma_S^2\breve{G}_S}{\gamma_S^2 - \gamma_{EM}^2} \\
&= \frac{\gamma_S^2\breve{G}_S - \gamma_{EM}^2\breve{G}_{EM}}{\gamma_S^2 - \gamma_{EM}^2}
\end{aligned} \tag{B.4}
$$

The second order wave equation for both the horizontal as vertical component of the electric field, which can be selected by choosing either the 1 or the 3, respectively,

$$
\begin{aligned}
&\breve{E}_{1;3} = \\
&\quad -\frac{\zeta\hat{L}}{s}\left(k_1^2 + k_3^2 + \frac{s^2\rho}{G^{fr}}\right)\breve{G}X_{11,1;3} + \frac{s\rho^f\zeta\hat{L}}{G^{fr}}\breve{G}X_{22,1;3} \\
&\quad = -\frac{\zeta\hat{L}}{s}\left(k_1^2 + k_3^2\right)\breve{G}X_{11,1;3} - \frac{\zeta\hat{L}}{s}\breve{G}X_{11,1;3} + \frac{s\rho^f\zeta\hat{L}}{G^{fr}}\breve{G}X_{22,1;3} \\
&\quad = -\frac{\zeta\hat{L}}{s}\left(\frac{\gamma_S^2\breve{G}_S - \gamma_{EM}^2\breve{G}_{EM}}{\gamma_S^2 - \gamma_{EM}^2}\right)X_{11,1;3} - \frac{s^2\rho\zeta\hat{L}}{sG^{fr}}\left(\frac{\breve{G}_{EM}}{\gamma_S^2 - \gamma_{EM}^2} - \frac{\breve{G}_S}{\gamma_S^2 - \gamma_{EM}^2}\right)X_{11,1;3} \\
&\quad + \frac{s\rho^f\zeta\hat{L}}{G^{fr}}\left(\frac{\breve{G}_{EM}}{\gamma_S^2 - \gamma_{EM}^2} - \frac{\breve{G}_S}{\gamma_S^2 - \gamma_{EM}^2}\right)X_{22,1;3} \\
&\quad = -\frac{\zeta\hat{L}}{sG^{fr}}\left(\frac{G^{fr}\gamma_S^2\breve{G}_S - G^{fr}\gamma_{EM}^2\breve{G}_{EM} + s^2\rho\breve{G}_{EM} - s^2\rho\breve{G}_S}{\gamma_S^2 - \gamma_{EM}^2}\right)X_{11,1;3} \\
&\quad + \frac{s\rho^f\zeta\hat{L}}{G^{fr}}\left(\frac{\breve{G}_{EM}}{\gamma_S^2 - \gamma_{EM}^2} - \frac{\breve{G}_S}{\gamma_S^2 - \gamma_{EM}^2}\right)X_{22,1;3}
\end{aligned}
$$

$$
\begin{aligned}
&\quad = \zeta\hat{L}\frac{s^2\rho - \gamma_s^2G^{fr}}{sG^{fr}}\frac{1}{\gamma_S^2 - \gamma_{EM}^2}\breve{G}_SX_{11,1;3} \\
&\quad + \zeta\hat{L}\frac{\gamma_{EM}^2G^{fr} - s^2\rho}{sG^{fr}}\frac{1}{\gamma_S^2 - \gamma_{EM}^2}\breve{G}_{EM}X_{11,1;3} \\
&\quad - \frac{\zeta\hat{L}s\rho^f}{G^{fr}}\frac{1}{\gamma_S^2 - \gamma_{EM}^2}\breve{G}_SX_{22,1;3} \\
&\quad + \frac{\zeta\hat{L}s\rho^f}{G^{fr}}\frac{1}{\gamma_S^2 - \gamma_{EM}^2}\breve{G}_{EM}X_{22,1;3}
\end{aligned} \tag{B.5}
$$

The second order wave equation for both the horizontal as vertical component of the particle velocity field, which can be selected by choosing either the 1 or the 3, respectively,

$$
\begin{aligned}
&\breve{v}_{1;3} = \\
&\quad - \frac{\hat{k}s\rho^f}{\eta G^{fr}} \left(k_1^2 + k_3^2 + \zeta \hat{L} \right) \breve{G} X_{11,1;3} + \frac{1}{G^{fr}} \left(k_1^2 + k_3^2 + \zeta(\varsigma + \hat{L}\hat{\xi}) \right) \breve{G} X_{22,1;3} \\
&= - \frac{\hat{k}s\rho^f}{\eta G^{fr}} \left(k_1^2 + k_3^2 \right) \breve{G} X_{11,1;3} - \frac{\hat{k}s\rho^f}{\eta G^{fr}} (\zeta\varsigma) \breve{G} X_{11,1;3} \\
&\quad + \frac{1}{G^{fr}} \left(k_1^2 + k_3^2 \right) \breve{G} X_{22,1;3} + \frac{1}{G^{fr}} \left(\zeta(\varsigma + \hat{L}\hat{\xi}) \right) \breve{G} X_{22,1;3} \\
&= - \frac{\hat{k}s\rho^f}{\eta G^{fr}} \left(\frac{\gamma_S^2 \breve{G}_S - \gamma_{EM}^2 \breve{G}_{EM}}{\gamma_S^2 - \gamma_{EM}^2} \right) X_{11,1;3} - \frac{\hat{k}s\rho^f}{\eta G^{fr}} (\zeta\varsigma) \left(\frac{\breve{G}_{EM}}{\gamma_S^2 - \gamma_{EM}^2} - \frac{\breve{G}_S}{\gamma_S^2 - \gamma_{EM}^2} \right) X_{11,1;3} \\
&\quad + \frac{1}{G^{fr}} \left(\frac{\gamma_S^2 \breve{G}_S - \gamma_{EM}^2 \breve{G}_{EM}}{\gamma_S^2 - \gamma_{EM}^2} \right) X_{22,1;3} + \frac{1}{G^{fr}} \left(\zeta(\varsigma + \hat{L}\hat{\xi}) \right) \left(\frac{\breve{G}_{EM}}{\gamma_S^2 - \gamma_{EM}^2} - \frac{\breve{G}_S}{\gamma_S^2 - \gamma_{EM}^2} \right) X_{22,1;3} \\
&= - \frac{\hat{k}s\rho^f}{\eta G^{fr}} \left(\frac{\gamma_S^2 \breve{G}_S}{\gamma_S^2 - \gamma_{EM}^2} \right) X_{11,1;3} + \frac{\hat{k}s\rho^f}{\eta G^{fr}} \left(\frac{\gamma_{EM}^2 \breve{G}_{EM}}{\gamma_S^2 - \gamma_{EM}^2} \right) X_{11,1;3} \\
&\quad - \frac{\hat{k}s\rho^f}{\eta G^{fr}} (\zeta\varsigma) \left(\frac{\breve{G}_{EM}}{\gamma_S^2 - \gamma_{EM}^2} \right) X_{11,1;3} + \frac{\hat{k}s\rho^f}{\eta G^{fr}} (\zeta\varsigma) \left(\frac{\breve{G}_S}{\gamma_S^2 - \gamma_{EM}^2} \right) X_{11,1;3} \\
&\quad + \frac{1}{G^{fr}} \left(\frac{\gamma_S^2 \breve{G}_S}{\gamma_S^2 - \gamma_{EM}^2} \right) X_{22,1;3} - \frac{1}{G^{fr}} \left(\frac{\gamma_{EM}^2 \breve{G}_{EM}}{\gamma_S^2 - \gamma_{EM}^2} \right) X_{22,1;3} \\
&\quad + \frac{1}{G^{fr}} \left(\zeta(\varsigma + \hat{L}\hat{\xi}) \right) \left(\frac{\breve{G}_{EM}}{\gamma_S^2 - \gamma_{EM}^2} \right) X_{22,1;3} - \frac{1}{G^{fr}} \left(\zeta(\varsigma + \hat{L}\hat{\xi}) \right) \left(\frac{\breve{G}_S}{\gamma_S^2 - \gamma_{EM}^2} \right) X_{22,1;3} \\
&= + \frac{s\rho^f k}{\eta G^{fr}} \frac{\zeta\varsigma - \gamma_S^2}{\gamma_S^2 - \gamma_{EM}^2} \breve{G}_S X_{11,1;3} \\
&\quad + \frac{s\rho^f k}{\eta G^{fr}} \frac{\gamma_{EM}^2 - \zeta\varsigma}{\gamma_S^2 - \gamma_{EM}^2} \breve{G}_{EM} X_{11,1;3} \\
&\quad + \frac{1}{G^{fr}} \frac{\gamma_S^2 - \zeta(\varsigma + \hat{L}\hat{\xi})}{\gamma_S^2 - \gamma_{EM}^2} \breve{G}_S X_{22,1;3} \\
&\quad + \frac{1}{G^{fr}} \frac{\zeta(\varsigma + \hat{L}\hat{\xi}) - \gamma_{EM}^2}{\gamma_S^2 - \gamma_{EM}^2} \breve{G}_{EM} X_{22,1;3}
\end{aligned} \tag{B.6}
$$

The specification of the source terms $X_{11,1}$ and $X_{22,1}$ are given in the next section.

B.2 Specification of the source terms affecting the horizontal component of the field vectors

$$
\begin{aligned}
X_{11,1}^{f_{1;3}} =& -\frac{C}{C^2 - HM} ik_1 s^3 \rho^E (1 + \frac{\hat{\xi}\hat{L}}{\varsigma}) \breve{G}_{PP} ik_{1;3} \breve{f}_{1;3} \\
& - \frac{C}{C^2 - HM} ik_1 s M \frac{\gamma_{Ps}^2 \breve{G}_{Ps} - \gamma_{Pf}^2 \breve{G}_{Pf}}{\gamma_{Ps}^2 - \gamma_{Pf}^2} ik_{1;3} \breve{f}_{1;3} \\
& - \frac{\frac{s\eta}{\zeta\hat{k}\varsigma} - M}{C^2 - HM} ik_1 s^3 \rho^f \breve{G}_{PP} ik_{1;3} \breve{f}_{1;3} \\
& - \frac{\frac{s\eta}{\zeta\hat{k}\varsigma} - M}{C^2 - HM} ik_1 s C \frac{\gamma_{Ps}^2 \breve{G}_{Ps} - \gamma_{Pf}^2 \breve{G}_{Pf}}{\gamma_{Ps}^2 - \gamma_{Pf}^2} ik_{1;3} \breve{f}_{1;3}
\end{aligned} \tag{B.7}
$$

$$
\begin{aligned}
X_{22,1}^{f_{1;3}} =& -\frac{K_G + G^{fr}/3}{C^2 - HM} ik_1 s^3 \rho^E (1 + \frac{\hat{\xi}\hat{L}}{\varsigma}) \breve{G}_{PP} ik_{1;3} \breve{f}_{1;3} \\
& - \frac{K_G + G^{fr}/3}{C^2 - HM} ik_1 s M \frac{\gamma_{Ps}^2 \breve{G}_{Ps} - \gamma_{Pf}^2 \breve{G}_{Pf}}{\gamma_{Ps}^2 - \gamma_{Pf}^2} ik_{1;3} \breve{f}_{1;3} \\
& - \frac{\frac{s^2\rho^f}{\zeta\varsigma} - C}{C^2 - HM} ik_1 s^3 \rho^f \breve{G}_{PP} ik_{1;3} \breve{f}_{1;3} \\
& - \frac{\frac{s^2\rho^f}{\zeta\varsigma} - C}{C^2 - HM} ik_1 s C \frac{\gamma_{Ps}^2 \breve{G}_{Ps} - \gamma_{Pf}^2 \breve{G}_{Pf}}{\gamma_{Ps}^2 - \gamma_{Pf}^2} ik_{1;3} \breve{f}_{1;3} \\
& + s \breve{f}_{1;-}
\end{aligned} \tag{B.8}
$$

$$
\begin{aligned}
X_{11,1}^{f_{1;3}^f} =& \frac{C}{C^2 - HM} ik_1 s^3 \rho^f \breve{G}_{PP} ik_{1;3} \breve{f}_{1;3}^f \\
& + \frac{C}{C^2 - HM} ik_1 s C \frac{\gamma_{Ps}^2 \breve{G}_{Ps} - \gamma_{Pf}^2 \breve{G}_{Pf}}{\gamma_{Ps}^2 - \gamma_{Pf}^2} ik_{1;3} \breve{f}_{1;3}^f \\
& + \frac{\frac{s\eta}{\zeta\hat{k}\varsigma} - M}{C^2 - HM} ik_1 s^3 \rho \breve{G}_{PP} ik_{1;3} \breve{f}_{1;3}^f \\
& + \frac{\frac{s\eta}{\zeta\hat{k}\varsigma} - M}{C^2 - HM} ik_1 s H \frac{\gamma_{Ps}^2 \breve{G}_{Ps} - \gamma_{Pf}^2 \breve{G}_{Pf}}{\gamma_{Ps}^2 - \gamma_{Pf}^2} ik_{1;3} \breve{f}_{1;3}^f \\
& + s \breve{f}_{1;-}^f
\end{aligned} \tag{B.9}
$$

$$
\begin{aligned}
X_{22,1}^{f_{1;3}^{f}} =& \frac{K_G + G^{fr}/3}{C^2 - HM} ik_1 s^3 \rho^f \breve{G}_{PP} ik_{1;3} \breve{f}_{1;3}^{f} \\
&+ \frac{K_G + G^{fr}/3}{C^2 - HM} ik_1 sC \frac{\gamma_{Ps}^2 \breve{G}_{Ps} - \gamma_{Pf}^2 \breve{G}_{Pf}}{\gamma_{Ps}^2 - \gamma_{Pf}^2} ik_{1;3} \breve{f}_{1;3}^{f} \\
&+ \frac{\frac{s^2 \rho^f}{\zeta\varsigma} - C}{C^2 - HM} ik_1 s^3 \rho \breve{G}_{PP} ik_{1;3} \breve{f}_{1;3}^{f} \\
&+ \frac{\frac{s^2 \rho^f}{\zeta\varsigma} - C}{C^2 - HM} ik_1 sH \frac{\gamma_{Ps}^2 \breve{G}_{Ps} - \gamma_{Pf}^2 \breve{G}_{Pf}}{\gamma_{Ps}^2 - \gamma_{Pf}^2} ik_{1;3} \breve{f}_{1;3}^{f}
\end{aligned} \tag{B.10}
$$

$$
\begin{aligned}
X_{11,1}^{h_{11;33}} =& - \frac{C}{C^2 - HM} ik_1 Cs^2 \rho^f \frac{\gamma_{Ps}^2 \breve{G}_{Ps} - \gamma_{Pf}^2 \breve{G}_{Pf}}{\gamma_{Ps}^2 - \gamma_{Pf}^2} \breve{h}_{11;33} \\
&- \frac{C}{C^2 - HM} ik_1 C^2 \frac{\gamma_{Ps}^2 \breve{G}_{Ps} - \gamma_{Pf}^2 \breve{G}_{Pf}}{\gamma_{Ps}^2 - \gamma_{Pf}^2} (1 - \gamma_{00}^2 \breve{G}^{00}) \breve{h}_{11;33} \\
&+ \frac{C}{C^2 - HM} ik_1 s^2 C_1 K_G \frac{\gamma_{Ps}^2 \breve{G}_{Ps} - \gamma_{Pf}^2 \breve{G}_{Pf}}{\gamma_{Ps}^2 - \gamma_{Pf}^2} \breve{h}_{11;33} \\
&+ \frac{C}{C^2 - HM} ik_1 s^2 C_1 G^{fr} (\frac{4}{3} k_{1;3}^2 - \frac{2}{3} k_{3;1}^2) \breve{G}_{PP} \breve{h}_{11;33} \\
&+ \frac{C}{C^2 - HM} ik_1 M K_G (1 - \gamma_{00}^2 \breve{G}^{00}) \frac{\gamma_{Ps}^2 \breve{G}_{Ps} - \gamma_{Pf}^2 \breve{G}_{Pf}}{\gamma_{Ps}^2 - \gamma_{Pf}^2} \breve{h}_{11;33} \\
&+ \frac{C}{C^2 - HM} ik_1 M G^{fr} (\frac{4}{3} k_{1;3}^2 - \frac{2}{3} k_{3;1}^2) \frac{\gamma_{Ps}^2 \breve{G}_{Ps} - \gamma_{Pf}^2 \breve{G}_{Pf}}{\gamma_{Ps}^2 - \gamma_{Pf}^2} \breve{h}_{11;33} \\
&- \frac{\frac{s\eta}{\zeta\hat{k}\varsigma} - M}{C^2 - HM} ik_1 s^2 \rho C \frac{\gamma_{Ps}^2 \breve{G}_{Ps} - \gamma_{Pf}^2 \breve{G}_{Pf}}{\gamma_{Ps}^2 - \gamma_{Pf}^2} \breve{h}_{11;33} \\
&- \frac{\frac{s\eta}{\zeta\hat{k}\varsigma} - M}{C^2 - HM} ik_1 CH \frac{\gamma_{Ps}^2 \breve{G}_{Ps} - \gamma_{Pf}^2 \breve{G}_{Pf}}{\gamma_{Ps}^2 - \gamma_{Pf}^2} (1 - \gamma_{00}^2 \breve{G}^{00}) \breve{h}_{11;33} \\
&+ \frac{\frac{s\eta}{\zeta\hat{k}\varsigma} - M}{C^2 - HM} ik_1 s^2 \rho^f K_G \frac{\gamma_{Ps}^2 \breve{G}_{Ps} - \gamma_{Pf}^2 \breve{G}_{Pf}}{\gamma_{Ps}^2 - \gamma_{Pf}^2} \breve{h}_{11;33} \\
&+ \frac{\frac{s\eta}{\zeta\hat{k}\varsigma} - M}{C^2 - HM} ik_1 s^2 \rho^f G^{fr} (\frac{4}{3} k_{1;3}^2 - \frac{2}{3} k_{3;1}^2) \breve{G}_{PP} \breve{h}_{11;33} \\
&+ \frac{\frac{s\eta}{\zeta\hat{k}\varsigma} - M}{C^2 - HM} ik_1 C K_G (1 - \gamma_{00}^2 \breve{G}^{00}) \frac{\gamma_{Ps}^2 \breve{G}_{Ps} - \gamma_{Pf}^2 \breve{G}_{Pf}}{\gamma_{Ps}^2 - \gamma_{Pf}^2} \breve{h}_{11;33} \\
&+ \frac{\frac{s\eta}{\zeta\hat{k}\varsigma} - M}{C^2 - HM} ik_1 C G^{fr} (\frac{4}{3} k_{1;3}^2 - \frac{2}{3} k_{3;1}^2) \frac{\gamma_{Ps}^2 \breve{G}_{Ps} - \gamma_{Pf}^2 \breve{G}_{Pf}}{\gamma_{Ps}^2 - \gamma_{Pf}^2} \breve{h}_{11;33} \\
&+ Cik_1 \breve{h}_{11;33}
\end{aligned} \tag{B.11}
$$

$$
\begin{aligned}
X_{22,1}^{h_{11;33}} =& - \frac{K_G + G^{fr}/3}{C^2 - HM} ik_1 C s^2 \rho^f \frac{\gamma_{Ps}^2 \breve{G}_{Ps} - \gamma_{Pf}^2 \breve{G}_{Pf}}{\gamma_{Ps}^2 - \gamma_{Pf}^2} \breve{h}_{11;33} \\
& - \frac{K_G + G^{fr}/3}{C^2 - HM} ik_1 C^2 \frac{\gamma_{Ps}^2 \breve{G}_{Ps} - \gamma_{Pf}^2 \breve{G}_{Pf}}{\gamma_{Ps}^2 - \gamma_{Pf}^2} (1 - \gamma_{00}^2 \breve{G}^{00}) \breve{h}_{11;33} \\
& + \frac{K_G + G^{fr}/3}{C^2 - HM} ik_1 s^2 C_1 K_G \frac{\gamma_{Ps}^2 \breve{G}_{Ps} - \gamma_{Pf}^2 \breve{G}_{Pf}}{\gamma_{Ps}^2 - \gamma_{Pf}^2} \breve{h}_{11;33} \\
& + \frac{K_G + G^{fr}/3}{C^2 - HM} ik_1 s^2 C_1 G^{fr} (\frac{4}{3} k_{1;3}^2 - \frac{2}{3} k_{3;1}^2) \breve{G}_{PP} \breve{h}_{11;33} \\
& + \frac{K_G + G^{fr}/3}{C^2 - HM} ik_1 M K_G (1 - \gamma_{00}^2 \breve{G}^{00}) \frac{\gamma_{Ps}^2 \breve{G}_{Ps} - \gamma_{Pf}^2 \breve{G}_{Pf}}{\gamma_{Ps}^2 - \gamma_{Pf}^2} \breve{h}_{11;33} \\
& + \frac{K_G + G^{fr}/3}{C^2 - HM} ik_1 M G^{fr} (\frac{4}{3} k_{1;3}^2 - \frac{2}{3} k_{3;1}^2) \frac{\gamma_{Ps}^2 \breve{G}_{Ps} - \gamma_{Pf}^2 \breve{G}_{Pf}}{\gamma_{Ps}^2 - \gamma_{Pf}^2} \breve{h}_{11;33} \\
& - \frac{\frac{s^2 \rho^f}{\zeta\varsigma} - C}{C^2 - HM} ik_1 s^2 \rho C \frac{\gamma_{Ps}^2 \breve{G}_{Ps} - \gamma_{Pf}^2 \breve{G}_{Pf}}{\gamma_{Ps}^2 - \gamma_{Pf}^2} \breve{h}_{11;33} \\
& - \frac{\frac{s^2 \rho^f}{\zeta\varsigma} - C}{C^2 - HM} ik_1 C H \frac{\gamma_{Ps}^2 \breve{G}_{Ps} - \gamma_{Pf}^2 \breve{G}_{Pf}}{\gamma_{Ps}^2 - \gamma_{Pf}^2} (1 - \gamma_{00}^2 \breve{G}^{00}) \breve{h}_{11;33} \\
& + \frac{\frac{s^2 \rho^f}{\zeta\varsigma} - C}{C^2 - HM} ik_1 s^2 \rho^f K_G \frac{\gamma_{Ps}^2 \breve{G}_{Ps} - \gamma_{Pf}^2 \breve{G}_{Pf}}{\gamma_{Ps}^2 - \gamma_{Pf}^2} \breve{h}_{11;33} \\
& + \frac{\frac{s^2 \rho^f}{\zeta\varsigma} - C}{C^2 - HM} ik_1 s^2 \rho^f G^{fr} (\frac{4}{3} k_{1;3}^2 - \frac{2}{3} k_{3;1}^2) \breve{G}_{PP} \breve{h}_{11;33} \\
& + \frac{\frac{s^2 \rho^f}{\zeta\varsigma} - C}{C^2 - HM} ik_1 C K_G (1 - \gamma_{00}^2 \breve{G}^{00}) \frac{\gamma_{Ps}^2 \breve{G}_{Ps} - \gamma_{Pf}^2 \breve{G}_{Pf}}{\gamma_{Ps}^2 - \gamma_{Pf}^2} \breve{h}_{11;33} \\
& + \frac{\frac{s^2 \rho^f}{\zeta\varsigma} - C}{C^2 - HM} ik_1 C G^{fr} (\frac{4}{3} k_{1;3}^2 - \frac{2}{3} k_{3;1}^2) \frac{\gamma_{Ps}^2 \breve{G}_{Ps} - \gamma_{Pf}^2 \breve{G}_{Pf}}{\gamma_{Ps}^2 - \gamma_{Pf}^2} \breve{h}_{11;33} \\
& + \left[(K_G + \frac{4}{3} G^{fr}); (K_G - \frac{2}{3} G^{fr}) \right] ik_1 \breve{h}_{11;33}
\end{aligned} \tag{B.12}
$$

$$
\begin{aligned}
X_{11,1}^{J^e_{1;3}} =& \frac{C}{C^2-HM} ik_1 \frac{s^3\rho^f\eta}{\hat{\xi}\hat{k}} \breve{G}_{PP} ik_{1;3} \breve{J}^e_{1;3} \\
&+ \frac{C}{C^2-HM} ik_1 \frac{s(s\rho^f M + \eta C/\hat{k})}{\hat{\xi}} \frac{\gamma_{Ps}^2 \breve{G}_{Ps} - \gamma_{Pf}^2 \breve{G}_{Pf}}{\gamma_{Ps}^2 - \gamma_{Pf}^2} ik_{1;3} \breve{J}^e_{1;3} \\
&+ \frac{C}{C^2-HM} ik_1 CM \frac{\gamma_{Ps}^2 \breve{G}_{Ps} - \gamma_{Pf}^2 \breve{G}_{Pf}}{\gamma_{Ps}^2 - \gamma_{Pf}^2} (1-\gamma_{00}^2 \breve{G}_{00}) ik_{1;3} \breve{J}^e_{1;3} \\
&- \frac{C}{C^2-HM} ik_1 \frac{s^4 C_1 \rho^f}{\hat{\xi}} \breve{G}_{PP} ik_{1;3} \breve{J}^e_{1;3} \\
&- \frac{C}{C^2-HM} ik_1 \frac{s^2(CC_1 + M\rho^f)}{\hat{\xi}} \frac{\gamma_{Ps}^2 \breve{G}_{Ps} - \gamma_{Pf}^2 \breve{G}_{Pf}}{\gamma_{Ps}^2 - \gamma_{Pf}^2} ik_{1;3} \breve{J}^e_{1;3} \\
&- \frac{C}{C^2-HM} ik_1 \frac{CM}{\hat{\xi}} \frac{\gamma_{Ps}^2 \breve{G}_{Ps} - \gamma_{Pf}^2 \breve{G}_{Pf}}{\gamma_{Ps}^2 - \gamma_{Pf}^2} (1-\gamma_{00}^2 \breve{G}_{00}) ik_{1;3} \breve{J}^e_{1;3} \\
&+ \frac{\frac{s\eta}{\zeta\hat{k}\varsigma} - M}{C^2-HM} ik_1 \frac{s^3\rho\eta}{\hat{\xi}\hat{k}} \breve{G}_{PP} ik_{1;3} \breve{J}^e_{1;3} \\
&+ \frac{\frac{s\eta}{\zeta\hat{k}\varsigma} - M}{C^2-HM} ik_1 \frac{s(s\rho M + \eta H/\hat{k})}{\hat{\xi}} \frac{\gamma_{Ps}^2 \breve{G}_{Ps} - \gamma_{Pf}^2 \breve{G}_{Pf}}{\gamma_{Ps}^2 - \gamma_{Pf}^2} ik_{1;3} \breve{J}^e_{1;3} \\
&+ \frac{\frac{s\eta}{\zeta\hat{k}\varsigma} - M}{C^2-HM} ik_1 \frac{MH}{\hat{\xi}} \frac{\gamma_{Ps}^2 \breve{G}_{Ps} - \gamma_{Pf}^2 \breve{G}_{Pf}}{\gamma_{Ps}^2 - \gamma_{Pf}^2} (1-\gamma_{00}^2 \breve{G}_{00}) ik_{1;3} \breve{J}^e_{1;3} \\
&- \frac{\frac{s\eta}{\zeta\hat{k}\varsigma} - M}{C^2-HM} ik_1 \frac{(s^2\rho^f)^2}{\hat{\xi}} \breve{G}_{PP} ik_{1;3} \breve{J}^e_{1;3} \\
&- \frac{\frac{s\eta}{\zeta\hat{k}\varsigma} - M}{C^2-HM} ik_1 \frac{2s^2\rho^f C}{\hat{\xi}} \frac{\gamma_{Ps}^2 \breve{G}_{Ps} - \gamma_{Pf}^2 \breve{G}_{Pf}}{\gamma_{Ps}^2 - \gamma_{Pf}^2} ik_{1;3} \breve{J}^e_{1;3} \\
&- \frac{\frac{s\eta}{\zeta\hat{k}\varsigma} - M}{C^2-HM} ik_1 \frac{C^2}{\hat{\xi}} \frac{\gamma_{Ps}^2 \breve{G}_{Ps} - \gamma_{Pf}^2 \breve{G}_{Pf}}{\gamma_{Ps}^2 - \gamma_{Pf}^2} (1-\gamma_{00}^2 \breve{G}_{00}) ik_{1;3} \breve{J}^e_{1;3} \\
&- \frac{M}{\hat{\xi}} ik_1 ik_{1;3} \breve{J}^e_{1;3} + \frac{s\eta}{\hat{\xi}\hat{k}} \breve{J}^e_{1;-}
\end{aligned} \tag{B.13}
$$

$$
\begin{aligned}
X_{22,1}^{J_{1;3}^e} = &+ \frac{K_G + G^{fr}/3}{C^2 - HM} ik_1 \frac{s^3 \rho^f \eta}{\hat{\xi}\hat{k}} \breve{G}_{PP} ik_{1;3} \breve{J}_{1;3}^e \\
&+ \frac{K_G + G^{fr}/3}{C^2 - HM} ik_1 \frac{s(s\rho^f M + \eta C/\hat{k})}{\hat{\xi}} \frac{\gamma_{Ps}^2 \breve{G}_{Ps} - \gamma_{Pf}^2 \breve{G}_{Pf}}{\gamma_{Ps}^2 - \gamma_{Pf}^2} ik_{1;3} \breve{J}_{1;3}^e \\
&+ \frac{K_G + G^{fr}/3}{C^2 - HM} ik_1 CM \frac{\gamma_{Ps}^2 \breve{G}_{Ps} - \gamma_{Pf}^2 \breve{G}_{Pf}}{\gamma_{Ps}^2 - \gamma_{Pf}^2} (1 - \gamma_{00}^2 \breve{G}_{00}) ik_{1;3} \breve{J}_{1;3}^e \\
&- \frac{K_G + G^{fr}/3}{C^2 - HM} ik_1 \frac{s^4 C_1 \rho^f}{\hat{\xi}} \breve{G}_{PP} ik_{1;3} \breve{J}_{1;3}^e \\
&- \frac{K_G + G^{fr}/3}{C^2 - HM} ik_1 \frac{s^2 (CC_1 + M\rho^f)}{\hat{\xi}} \frac{\gamma_{Ps}^2 \breve{G}_{Ps} - \gamma_{Pf}^2 \breve{G}_{Pf}}{\gamma_{Ps}^2 - \gamma_{Pf}^2} ik_{1;3} \breve{J}_{1;3}^e \\
&- \frac{K_G + G^{fr}/3}{C^2 - HM} ik_1 \frac{CM}{\hat{\xi}} \frac{\gamma_{Ps}^2 \breve{G}_{Ps} - \gamma_{Pf}^2 \breve{G}_{Pf}}{\gamma_{Ps}^2 - \gamma_{Pf}^2} (1 - \gamma_{00}^2 \breve{G}_{00}) ik_{1;3} \breve{J}_{1;3}^e \\
&+ \frac{\frac{s^2 \rho^f}{\zeta\varsigma} - C}{C^2 - HM} ik_1 \frac{s^3 \rho \eta}{\hat{\xi}\hat{k}} \breve{G}_{PP} ik_{1;3} \breve{J}_{1;3}^e \\
&+ \frac{\frac{s^2 \rho^f}{\zeta\varsigma} - C}{C^2 - HM} ik_1 \frac{s(s\rho M + \eta H/\hat{k})}{\hat{\xi}} \frac{\gamma_{Ps}^2 \breve{G}_{Ps} - \gamma_{Pf}^2 \breve{G}_{Pf}}{\gamma_{Ps}^2 - \gamma_{Pf}^2} ik_{1;3} \breve{J}_{1;3}^e \\
&+ \frac{\frac{s^2 \rho^f}{\zeta\varsigma} - C}{C^2 - HM} ik_1 \frac{MH}{\hat{\xi}} \frac{\gamma_{Ps}^2 \breve{G}_{Ps} - \gamma_{Pf}^2 \breve{G}_{Pf}}{\gamma_{Ps}^2 - \gamma_{Pf}^2} (1 - \gamma_{00}^2 \breve{G}_{00}) ik_{1;3} \breve{J}_{1;3}^e \\
&- \frac{\frac{s^2 \rho^f}{\zeta\varsigma} - C}{C^2 - HM} ik_1 \frac{(s^2 \rho^f)^2}{\hat{\xi}} \breve{G}_{PP} ik_{1;3} \breve{J}_{1;3}^e \\
&- \frac{\frac{s^2 \rho^f}{\zeta\varsigma} - C}{C^2 - HM} ik_1 \frac{2s^2 \rho^f C}{\hat{\xi}} \frac{\gamma_{Ps}^2 \breve{G}_{Ps} - \gamma_{Pf}^2 \breve{G}_{Pf}}{\gamma_{Ps}^2 - \gamma_{Pf}^2} ik_{1;3} \breve{J}_{1;3}^e \\
&- \frac{\frac{s^2 \rho^f}{\zeta\varsigma} - C}{C^2 - HM} ik_1 \frac{C^2}{\hat{\xi}} \frac{\gamma_{Ps}^2 \breve{G}_{Ps} - \gamma_{Pf}^2 \breve{G}_{Pf}}{\gamma_{Ps}^2 - \gamma_{Pf}^2} (1 - \gamma_{00}^2 \breve{G}_{00}) ik_{1;3} \breve{J}_{1;3}^e \\
&- \frac{C}{\hat{\xi}} ik_1 ik_{1;3} \breve{J}_{1;3}^e + \frac{s^2 \rho^f}{\hat{\xi}} \breve{J}_{1;-}^e
\end{aligned} \tag{B.14}
$$

$$
\begin{aligned}
X^q_{11,1} = &- \frac{C}{C^2 - HM} ik_1 s^2 \rho^f M \frac{\gamma^2_{Ps}\breve{G}_{Ps} - \gamma^2_{Pf}\breve{G}_{Pf}}{\gamma^2_{Ps} - \gamma^2_{Pf}} \breve{q} \\
&- \frac{C}{C^2 - HM} ik_1 CM \frac{\gamma^2_{Ps}\breve{G}_{Ps} - \gamma^2_{Pf}\breve{G}_{Pf}}{\gamma^2_{Ps} - \gamma^2_{Pf}} (1 - \gamma^2_{00}\breve{G}_{00}) \breve{q} \\
&+ \frac{C}{C^2 - HM} ik_1 s^2 C_1 C \frac{\gamma^2_{Ps}\breve{G}_{Ps} - \gamma^2_{Pf}\breve{G}_{Pf}}{\gamma^2_{Ps} - \gamma^2_{Pf}} \breve{q} \\
&+ \frac{C}{C^2 - HM} ik_1 CM \frac{\gamma^2_{Ps}\breve{G}_{Ps} - \gamma^2_{Pf}\breve{G}_{Pf}}{\gamma^2_{Ps} - \gamma^2_{Pf}} (1 - \gamma^2_{00}\breve{G}_{00}) \breve{q} \\
&- \frac{\frac{s\eta}{\zeta\hat{k}\varsigma} - M}{C^2 - HM} ik_1 s^2 \rho M \frac{\gamma^2_{Ps}\breve{G}_{Ps} - \gamma^2_{Pf}\breve{G}_{Pf}}{\gamma^2_{Ps} - \gamma^2_{Pf}} \breve{q} \\
&- \frac{\frac{s\eta}{\zeta\hat{k}\varsigma} - M}{C^2 - HM} ik_1 MH \frac{\gamma^2_{Ps}\breve{G}_{Ps} - \gamma^2_{Pf}\breve{G}_{Pf}}{\gamma^2_{Ps} - \gamma^2_{Pf}} (1 - \gamma^2_{00}\breve{G}_{00}) \breve{q} \\
&+ \frac{\frac{s\eta}{\zeta\hat{k}\varsigma} - M}{C^2 - HM} ik_1 s^2 \rho^f C \frac{\gamma^2_{Ps}\breve{G}_{Ps} - \gamma^2_{Pf}\breve{G}_{Pf}}{\gamma^2_{Ps} - \gamma^2_{Pf}} \breve{q} \\
&+ \frac{\frac{s\eta}{\zeta\hat{k}\varsigma} - M}{C^2 - HM} C^2 \frac{\gamma^2_{Ps}\breve{G}_{Ps} - \gamma^2_{Pf}\breve{G}_{Pf}}{\gamma^2_{Ps} - \gamma^2_{Pf}} (1 - \gamma^2_{00}\breve{G}_{00}) \breve{q} \\
&+ M ik_1 \breve{q}
\end{aligned}
\tag{B.15}
$$

$$
\begin{aligned}
X^q_{22,1} = &- \frac{K_G + G^{fr}/3}{C^2 - HM} ik_1 s^2 \rho^f M \frac{\gamma^2_{Ps}\breve{G}_{Ps} - \gamma^2_{Pf}\breve{G}_{Pf}}{\gamma^2_{Ps} - \gamma^2_{Pf}} \breve{q} \\
&- \frac{K_G + G^{fr}/3}{C^2 - HM} ik_1 CM \frac{\gamma^2_{Ps}\breve{G}_{Ps} - \gamma^2_{Pf}\breve{G}_{Pf}}{\gamma^2_{Ps} - \gamma^2_{Pf}} (1 - \gamma^2_{00}\breve{G}_{00}) \breve{q} \\
&+ \frac{K_G + G^{fr}/3}{C^2 - HM} ik_1 s^2 C_1 C \frac{\gamma^2_{Ps}\breve{G}_{Ps} - \gamma^2_{Pf}\breve{G}_{Pf}}{\gamma^2_{Ps} - \gamma^2_{Pf}} \breve{q} \\
&+ \frac{K_G + G^{fr}/3}{C^2 - HM} ik_1 CM \frac{\gamma^2_{Ps}\breve{G}_{Ps} - \gamma^2_{Pf}\breve{G}_{Pf}}{\gamma^2_{Ps} - \gamma^2_{Pf}} (1 - \gamma^2_{00}\breve{G}_{00}) \breve{q} \\
&- \frac{\frac{s^2\rho^f}{\zeta\varsigma} - C}{C^2 - HM} ik_1 s^2 \rho M \frac{\gamma^2_{Ps}\breve{G}_{Ps} - \gamma^2_{Pf}\breve{G}_{Pf}}{\gamma^2_{Ps} - \gamma^2_{Pf}} \breve{q} \\
&- \frac{\frac{s^2\rho^f}{\zeta\varsigma} - C}{C^2 - HM} ik_1 MH \frac{\gamma^2_{Ps}\breve{G}_{Ps} - \gamma^2_{Pf}\breve{G}_{Pf}}{\gamma^2_{Ps} - \gamma^2_{Pf}} (1 - \gamma^2_{00}\breve{G}_{00}) \breve{q} \\
&+ \frac{\frac{s^2\rho^f}{\zeta\varsigma} - C}{C^2 - HM} ik_1 s^2 \rho^f C \frac{\gamma^2_{Ps}\breve{G}_{Ps} - \gamma^2_{Pf}\breve{G}_{Pf}}{\gamma^2_{Ps} - \gamma^2_{Pf}} \breve{q} \\
&+ \frac{\frac{s^2\rho^f}{\zeta\varsigma} - C}{C^2 - HM} C^2 \frac{\gamma^2_{Ps}\breve{G}_{Ps} - \gamma^2_{Pf}\breve{G}_{Pf}}{\gamma^2_{Ps} - \gamma^2_{Pf}} (1 - \gamma^2_{00}\breve{G}_{00}) \breve{q} \\
&+ C ik_1 \breve{q}
\end{aligned}
\tag{B.16}
$$

$$
\begin{aligned}
X_{11}^{h_{13}} = &-\frac{C}{C^2-HM} ik_1 4s^2 C_1 G^{fr} \breve{G}_{PP} ik_1 ik_3 \breve{h}_{13} \\
&-\frac{C}{C^2-HM} ik_1 4MG^{fr} \frac{\gamma_{Ps}^2 \breve{G}_{Ps} - \gamma_{Pf}^2 \breve{G}_{Pf}}{\gamma_{Ps}^2 - \gamma_{Pf}^2} ik_1 ik_3 \breve{h}_{13} \\
&-\frac{\frac{s\eta}{\zeta\hat{k}\varsigma} - M}{C^2-HM} ik_1 4s^2 \rho^f G^{fr} \breve{G}_{PP} ik_1 ik_3 \breve{h}_{13} \\
&-\frac{\frac{s\eta}{\zeta\hat{k}\varsigma} - M}{C^2-HM} ik_1 4CG^{fr} \frac{\gamma_{Ps}^2 \breve{G}_{Ps} - \gamma_{Pf}^2 \breve{G}_{Pf}}{\gamma_{Ps}^2 - \gamma_{Pf}^2} ik_1 ik_3 \breve{h}_{13}
\end{aligned} \tag{B.17}
$$

$$
\begin{aligned}
X_{22}^{h_{13}} = &-\frac{K_G + G^{fr}/3}{C^2-HM} ik_1 4s^2 C_1 G^{fr} \breve{G}_{PP} ik_1 ik_3 \breve{h}_{13} \\
&-\frac{K_G + G^{fr}/3}{C^2-HM} ik_1 4MG^{fr} \frac{\gamma_{Ps}^2 \breve{G}_{Ps} - \gamma_{Pf}^2 \breve{G}_{Pf}}{\gamma_{Ps}^2 - \gamma_{Pf}^2} ik_1 ik_3 \breve{h}_{13} \\
&-\frac{\frac{s^2\rho^f}{\zeta\varsigma} - C}{C^2-HM} ik_1 4s^2 \rho^f G^{fr} \breve{G}_{PP} ik_1 ik_3 \breve{h}_{13} \\
&-\frac{\frac{s^2\rho^f}{\zeta\varsigma} - C}{C^2-HM} ik_1 4CG^{fr} \frac{\gamma_{Ps}^2 \breve{G}_{Ps} - \gamma_{Pf}^2 \breve{G}_{Pf}}{\gamma_{Ps}^2 - \gamma_{Pf}^2} ik_1 ik_3 \breve{h}_{13} \\
&+ ik_3 G^{fr} \breve{h}_{13}
\end{aligned} \tag{B.18}
$$

$$
X_{11}^{J_2^m} = \frac{s\eta}{\hat{\xi}\hat{k}\zeta} ik_3 \breve{J}_2^m \tag{B.19}
$$

$$
X_{22}^{J_2^m} = \frac{s^2\rho^f}{\hat{\xi}\zeta} ik_3 \breve{J}_2^m \tag{B.20}
$$

By substituting each of these source terms into the $X_{11,1}$ and $X_{22,1}$ expressions for the second order wave equations B.5 and B.6, the impulse response functions to these specific sources can be found. These resulting Green's functions are given in the next section of this Appendix.

B.3 Particle velocity response to the bulk force

$$F_{Ps} = \frac{s\rho^f \hat{k}}{\eta} \frac{sM\gamma_{Ps}^2 C + \left(\frac{s\eta}{\zeta\hat{k}\varsigma} - M\right)(sC\gamma_{Ps}^2 - s^3\rho^f) - Cs^3\rho^E\left(1 + \frac{\hat{\xi}\hat{L}}{\varsigma}\right)}{G^{fr}\left(\gamma_S^2 - \gamma_{EM}^2\right)\left(\gamma_{Ps}^2 - \gamma_{Pf}^2\right)(C^2 - HM)} \tag{B.21}$$

$$F_{Pf} = \frac{s\rho^f \hat{k}}{\eta} \frac{sM\gamma_{Pf}^2 C + \left(\frac{s\eta}{\zeta\hat{k}\varsigma} - M\right)(sC\gamma_{Pf}^2 - s^3\rho^f) - Cs^3\rho^E\left(1 + \frac{\hat{\xi}\hat{L}}{\varsigma}\right)}{G^{fr}\left(\gamma_S^2 - \gamma_{EM}^2\right)\left(\gamma_{Ps}^2 - \gamma_{Pf}^2\right)(C^2 - HM)} \tag{B.22}$$

$$Z_{Ps} = \frac{(H - G^{fr})\left(sM\gamma_{Ps}^2 - s^3\rho^E(1 + \frac{\hat{\xi}\hat{L}}{\varsigma})\right) + \left(sC\gamma_{Ps}^2 - s^3\rho^f\right)(\frac{s^2\rho^f}{\zeta\varsigma} - C)}{G^{fr}\left(\gamma_S^2 - \gamma_{EM}^2\right)\left(\gamma_{Ps}^2 - \gamma_{Pf}^2\right)(C^2 - HM)} \tag{B.23}$$

$$Z_{Pf} = \frac{(H - G^{fr})\left(sM\gamma_{Pf}^2 - s^3\rho^E(1 + \frac{\hat{\xi}\hat{L}}{\varsigma})\right) + \left(sC\gamma_{Pf}^2 - s^3\rho^f\right)(\frac{s^2\rho^f}{\zeta\varsigma} - C)}{G^{fr}\left(\gamma_S^2 - \gamma_{EM}^2\right)\left(\gamma_{Ps}^2 - \gamma_{Pf}^2\right)(C^2 - HM)} \tag{B.24}$$

$$
\begin{aligned}
C_{S1}^{v1,f} &= F_{Pf}\frac{\zeta\varsigma-\gamma_S^2}{\gamma_{Pf}^2-\gamma_S^2} - F_{Ps}\frac{\zeta\varsigma-\gamma_S^2}{\gamma_{Ps}^2-\gamma_S^2} - \frac{Z_{Ps}(\gamma_S^2-\zeta(\varsigma+\hat{L}\hat{\xi}))}{\gamma_{Ps}^2-\gamma_S^2} \\
&+ \frac{Z_{Pf}(\gamma_S^2-\zeta(\varsigma+\hat{L}\hat{\xi}))}{\gamma_{Pf}^2-\gamma_S^2}
\end{aligned} \tag{B.25}
$$

$$
\begin{aligned}
C_{EM1}^{v1,f} &= F_{Pf}\frac{\gamma_{EM}^2-\zeta\varsigma}{\gamma_{Pf}^2-\gamma_{EM}^2} - F_{Ps}\frac{\gamma_{EM}^2-\zeta\varsigma}{\gamma_{Ps}^2-\gamma_{EM}^2} - \frac{Z_{Ps}(\zeta(\varsigma+\hat{L}\hat{\xi})-\gamma_{EM}^2)}{\gamma_{Ps}^2-\gamma_{EM}^2} \\
&+ \frac{Z_{Pf}(\zeta(\varsigma+\hat{L}\hat{\xi})-\gamma_{EM}^2)}{\gamma_{Pf}^2-\gamma_{EM}^2}
\end{aligned} \tag{B.26}
$$

$$
\begin{aligned}
C_{Ps}^{v1,f} &= F_{Ps}\frac{\zeta\varsigma-\gamma_S^2}{\gamma_{Ps}^2-\gamma_S^2} + \frac{Z_{Ps}(\gamma_S^2-\zeta(\varsigma+\hat{L}\hat{\xi}))}{\gamma_{Ps}^2-\gamma_S^2} + F_{Ps}\frac{\gamma_{EM}^2-\zeta\varsigma}{\gamma_{Ps}^2-\gamma_{EM}^2} \\
&+ \frac{Z_{Ps}(\zeta(\varsigma+\hat{L}\hat{\xi})-\gamma_{EM}^2)}{\gamma_{Ps}^2-\gamma_{EM}^2}
\end{aligned} \tag{B.27}
$$

$$
\begin{aligned}
C_{Pf}^{v1,f} &= -F_{Pf}\frac{\zeta\varsigma-\gamma_S^2}{\gamma_{Pf}^2-\gamma_S^2} - \frac{Z_{Pf}(\gamma_S^2-\zeta(\varsigma+\hat{L}\hat{\xi}))}{\gamma_{Pf}^2-\gamma_S^2} - F_{Pf}\frac{\gamma_{EM}^2-\zeta\varsigma}{\gamma_{Pf}^2-\gamma_{EM}^2} \\
&- \frac{Z_{Pf}(\zeta(\varsigma+\hat{L}\hat{\xi})-\gamma_{EM}^2)}{\gamma_{Pf}^2-\gamma_{EM}^2}
\end{aligned} \tag{B.28}
$$

$$
C_{S2}^{v1,f1} = +\frac{(\gamma_S^2-\zeta(\varsigma+\hat{L}\hat{\xi}))}{G^{fr}(\gamma_S^2-\gamma_{EM}^2)}s \tag{B.29}
$$

$$
C_{EM2}^{v1,f} = +\frac{(\zeta(\varsigma+\hat{L}\hat{\xi})-\gamma_{EM}^2)}{G^{fr}(\gamma_S^2-\gamma_{EM}^2)}s \tag{B.30}
$$

$$
\begin{aligned}
\breve{G}^{v_1,f_1} = C_{S1}^{v1,f} ik_1ik_1\breve{G}_S + C_{S2}^{v1,f1}\breve{G}_S + C_{EM1}^{v1,f} ik_1ik_1\breve{G}_{EM} \\
+ C_{EM2}^{v1,f1}\breve{G}_{EM} + C_{Ps}^{v1,f} ik_1ik_1\breve{G}_{Ps} + C_{Pf}^{v1,f} ik_1ik_1\breve{G}_{Pf}
\end{aligned} \tag{B.31}
$$

$$
\breve{G}^{v_1,f_3} = C_{S1}^{v1,f} ik_3ik_1\breve{G}_S + C_{EM1}^{v1,f} ik_3ik_1\breve{G}_{EM} + C_{Ps}^{v1,f} ik_3ik_1\breve{G}_{Ps} + C_{Pf}^{v1,f} ik_3ik_1\breve{G}_{Pf} \tag{B.32}
$$

B.4 Particle velocity response to fluid force

$$F_{Ps} = \frac{s\rho^f \hat{k}}{\eta} \frac{C(sC\gamma_{Ps}^2 - s^3\rho^f) + \left(\frac{s\eta}{\zeta\hat{k}\varsigma} - M\right)(sH\gamma_{Ps}^2 - s^3\rho)}{G^{fr}\left(\gamma_S^2 - \gamma_{EM}^2\right)\left(\gamma_{Ps}^2 - \gamma_{Pf}^2\right)(C^2 - HM)} \tag{B.33}$$

$$F_{Pf} = \frac{s\rho^f \hat{k}}{\eta} \frac{C(sC\gamma_{Pf}^2 - s^3\rho^f) + \left(\frac{s\eta}{\zeta\hat{k}\varsigma} - M\right)(sH\gamma_{Pf}^2 - s^3\rho)}{G^{fr}\left(\gamma_S^2 - \gamma_{EM}^2\right)\left(\gamma_{Ps}^2 - \gamma_{Pf}^2\right)(C^2 - HM)} \tag{B.34}$$

$$Z_{Ps} = \frac{(H - G^{fr})\left(sC\gamma_{Ps}^2 - s^3\rho^f\right) + (\frac{s^2\rho^f}{\zeta\varsigma} - C)\left(sH\gamma_{Ps}^2 - s^3\rho\right)}{G^{fr}\left(\gamma_S^2 - \gamma_{EM}^2\right)\left(\gamma_{Ps}^2 - \gamma_{Pf}^2\right)(C^2 - HM)} \tag{B.35}$$

$$Z_{Pf} = \frac{(H - G^{fr})\left(sC\gamma_{Pf}^2 - s^3\rho^f\right) + (\frac{s^2\rho^f}{\zeta\varsigma} - C)\left(sH\gamma_{Pf}^2 - s^3\rho\right)}{G^{fr}\left(\gamma_S^2 - \gamma_{EM}^2\right)\left(\gamma_{Ps}^2 - \gamma_{Pf}^2\right)(C^2 - HM)} \tag{B.36}$$

$$\begin{aligned} C_{S1}^{v1,f^f} &= \frac{\zeta\varsigma - \gamma_S^2}{\gamma_{Ps}^2 - \gamma_S^2} F_{Ps} - \frac{\zeta\varsigma - \gamma_S^2}{\gamma_{Pf}^2 - \gamma_S^2} F_{Pf} + \frac{Z_{Ps}(\gamma_S^2 - \zeta(\varsigma + \hat{L}\hat{\xi}))}{\gamma_{Ps}^2 - \gamma_S^2} \\ &- \frac{Z_{Pf}(\gamma_S^2 - \zeta(\varsigma + \hat{L}\hat{\xi}))}{\gamma_{Pf}^2 - \gamma_S^2} \end{aligned} \tag{B.37}$$

$$C_{S2}^{v1,f^f} = \frac{\rho^f \hat{k}}{\eta G^{fr}} \frac{\zeta\varsigma - \gamma_S^2}{\gamma_S^2 - \gamma_{EM}^2} \tag{B.38}$$

$$\tag{B.39}$$

$$\begin{aligned} C_{EM1}^{v1,f^f} &= \frac{\gamma_{EM}^2 - \zeta\varsigma}{\gamma_{Ps}^2 - \gamma_{EM}^2} F_{Ps} - \frac{\gamma_{EM}^2 - \zeta\varsigma}{\gamma_{Pf}^2 - \gamma_{EM}^2} F_{Pf} + \frac{Z_{Ps}(\zeta(\varsigma + \hat{L}\hat{\xi}) - \gamma_{EM}^2)}{\gamma_{Ps}^2 - \gamma_{EM}^2} \\ &- \frac{Z_{Pf}(\zeta(\varsigma + \hat{L}\hat{\xi}) - \gamma_{EM}^2)}{\gamma_{Pf}^2 - \gamma_{EM}^2} \end{aligned} \tag{B.40}$$

$$\tag{B.41}$$

$$C_{EM2}^{v1,f^f} = \frac{\rho^f \hat{k}}{\eta G^{fr}} \frac{\gamma_{EM}^2 - \zeta\varsigma}{\gamma_S^2 - \gamma_{EM}^2} \tag{B.42}$$

$$\tag{B.43}$$

$$\begin{aligned} C_{Ps}^{v1,f^f} &= -\frac{\zeta\varsigma - \gamma_S^2}{\gamma_{Ps}^2 - \gamma_S^2} F_{Ps} - \frac{Z_{Ps}(\gamma_S^2 - \zeta(\varsigma + \hat{L}\hat{\xi}))}{\gamma_{Ps}^2 - \gamma_S^2} - \frac{\gamma_{EM}^2 - \zeta\varsigma}{\gamma_{Ps}^2 - \gamma_{EM}^2} F_{Ps} \\ &- \frac{Z_{Ps}(\zeta(\varsigma + \hat{L}\hat{\xi}) - \gamma_{EM}^2)}{\gamma_{Ps}^2 - \gamma_{EM}^2} \end{aligned} \tag{B.44}$$

$$\tag{B.45}$$

$$\begin{aligned} C_{Pf}^{v1,f^f} &= +\frac{s^2\rho - \gamma_S^2 G^{fr}}{\gamma_{Pf}^2 - \gamma_S^2} F_{Pf} + \frac{Z_{Pf}(\gamma_S^2 - \zeta(\varsigma + \hat{L}\hat{\xi}))}{\gamma_{Pf}^2 - \gamma_S^2} + \frac{\gamma_{EM}^2 G^{fr} - s^2\rho}{\gamma_{Pf}^2 - \gamma_{EM}^2} F_{Pf} \\ &+ \frac{Z_{Pf}(\zeta(\varsigma + \hat{L}\hat{\xi}) - \gamma_{EM}^2)}{\gamma_{Pf}^2 - \gamma_{EM}^2} \end{aligned} \tag{B.46}$$

$$\breve{G}^{v1,f_1^f} = C_{S1}^{v1,ff} ik_1 ik_1 \breve{G}_S + C_{S2}^{v1,ff} \breve{G}_S + C_{EM1}^{v1,ff} ik_1 ik_1 \breve{G}_{EM} + C_{EM2}^{v1,ff} \breve{G}_{EM}$$
$$C_{Ps}^{v1,ff} ik_1 ik_1 \breve{G}_{Ps} + C_{Pf}^{v1,ff} ik_1 ik_1 \breve{G}_{Pf} \quad \text{(B.47)}$$

$$\breve{G}^{v1,f_3^f} = C_{S1}^{v1,ff} ik_1 ik_3 \breve{G}_S + C_{EM1}^{v1,ff} ik_1 ik_3 \breve{G}_{EM} + C_{Ps}^{v1,ff} ik_1 ik_3 \breve{G}_{Ps} + C_{Pf}^{v1,ff} ik_1 ik_3 \breve{G}_{Pf} \quad \text{(B.48)}$$

B.5 Particle velocity response to volume injection

$$F_{S,Ps} = \frac{s\rho^f \hat{k}}{\eta} \frac{C\left(-s^2\rho^f M\gamma_{Ps}^2 + s^2 C\rho^E(1+\frac{\hat{\xi}\hat{L}}{\varsigma})\gamma_{Ps}^2\right) + \left(\frac{s\eta}{\zeta\hat{k}\varsigma} - M\right)\left(-s^2\rho M\gamma_{Ps}^2 - (C^2 - HM)\gamma_{Ps}^2\gamma_S^2 + s^2\rho^f C\gamma_{Ps}^2\right)}{G^{fr}\left(\gamma_S^2 - \gamma_{EM}^2\right)\left(\gamma_{Ps}^2 - \gamma_{Pf}^2\right)\left(C^2 - HM\right)} \quad \text{(B.49)}$$

$$F_{EM,Ps} = \frac{s\rho^f \hat{k}}{\eta} \frac{C\left(-s^2\rho^f M\gamma_{Ps}^2 + s^2 C\rho^E(1+\frac{\hat{\xi}\hat{L}}{\varsigma})\gamma_{Ps}^2\right) + \left(\frac{s\eta}{\zeta\hat{k}\varsigma} - M\right)\left(-s^2\rho M\gamma_{Ps}^2 - (C^2 - HM)\gamma_{Ps}^2\gamma_{EM}^2 + s^2\rho^f C\gamma_{Ps}^2\right)}{G^{fr}\left(\gamma_S^2 - \gamma_{EM}^2\right)\left(\gamma_{Ps}^2 - \gamma_{Pf}^2\right)\left(C^2 - HM\right)} \quad \text{(B.50)}$$

$$F_{S,Pf} = \frac{s\rho^f \hat{k}}{\eta} \frac{C\left(-s^2\rho^f M\gamma_{Pf}^2 + s^2 C\rho^E(1+\frac{\hat{\xi}\hat{L}}{\varsigma})\gamma_{Pf}^2\right) + \left(\frac{s\eta}{\zeta\hat{k}\varsigma} - M\right)\left(-s^2\rho M\gamma_{Pf}^2 - (C^2 - HM)\gamma_{Pf}^2\gamma_S^2 + s^2\rho^f C\gamma_{Pf}^2\right)}{G^{fr}\left(\gamma_S^2 - \gamma_{EM}^2\right)\left(\gamma_{Ps}^2 - \gamma_{Pf}^2\right)\left(C^2 - HM\right)} \quad \text{(B.51)}$$

$$F_{EM,Pf} = \frac{s\rho^f \hat{k}}{\eta} \frac{C\left(-s^2\rho^f M\gamma_{Pf}^2 + s^2 C\rho^E(1+\frac{\hat{\xi}\hat{L}}{\varsigma})\gamma_{Pf}^2\right) + \left(\frac{s\eta}{\zeta\hat{k}\varsigma} - M\right)\left(-s^2\rho M\gamma_{Pf}^2 - (C^2 - HM)\gamma_{Pf}^2\gamma_{EM}^2 + s^2\rho^f C\gamma_{Pf}^2\right)}{G^{fr}\left(\gamma_S^2 - \gamma_{EM}^2\right)\left(\gamma_{Ps}^2 - \gamma_{Pf}^2\right)\left(C^2 - HM\right)} \quad \text{(B.52)}$$

$$Z_{S,Ps} =$$

$$- \left(\gamma_S^2 - \zeta(\varsigma + \hat{L}\hat{\xi})\right) \frac{(H - G^{fr}) \left(s^2 \rho^f M \gamma_{Ps}^2 - s^2 C \rho^E (1 + \frac{\hat{\xi}\hat{L}}{\varsigma}) \gamma_{Ps}^2\right) + \left(\frac{s^2 \rho^f}{\zeta\varsigma} - C\right) (s^2 \rho M \gamma_{Ps}^2 + (C^2 - HM) \gamma_{Ps}^2 \gamma_S^2 - s^2 \rho^f C \gamma_{Ps}^2)}{G^{fr} \left(\gamma_S^2 - \gamma_{EM}^2\right) \left(\gamma_{Ps}^2 - \gamma_{Pf}^2\right) (C^2 - HM)} \tag{B.53}$$

$$Z_{EM,Ps} =$$

$$- \left(\zeta(\varsigma + \hat{L}\hat{\xi}) - \gamma_{EM}^2\right) \frac{(H - G^{fr}) \left(s^2 \rho^f M \gamma_{Ps}^2 - s^2 C \rho^E (1 + \frac{\hat{\xi}\hat{L}}{\varsigma}) \gamma_{Ps}^2\right) + \left(\frac{s^2 \rho^f}{\zeta\varsigma} - C\right) (s^2 \rho M \gamma_{Ps}^2 + (C^2 - HM) \gamma_{Ps}^2 \gamma_{EM}^2 - s^2 \rho^f C \gamma_{Ps}^2)}{G^{fr} \left(\gamma_S^2 - \gamma_{EM}^2\right) \left(\gamma_{Ps}^2 - \gamma_{Pf}^2\right) (C^2 - HM)} \tag{B.54}$$

$$Z_{S,Pf} =$$

$$- \left(\gamma_S^2 - \zeta(\varsigma + \hat{L}\hat{\xi})\right) \frac{(H - G^{fr}) \left(s^2 \rho^f M \gamma_{Pf}^2 - s^2 C \rho^E (1 + \frac{\hat{\xi}\hat{L}}{\varsigma}) \gamma_{Pf}^2\right) + \left(\frac{s^2 \rho^f}{\zeta\varsigma} - C\right) (s^2 \rho M \gamma_{Pf}^2 + (C^2 - HM) \gamma_{Pf}^2 \gamma_S^2 - s^2 \rho^f C \gamma_{Pf}^2)}{G^{fr} \left(\gamma_S^2 - \gamma_{EM}^2\right) \left(\gamma_{Ps}^2 - \gamma_{Pf}^2\right) (C^2 - HM)} \tag{B.55}$$

$$Z_{EM,Pf} =$$

$$- \left(\zeta(\varsigma + \hat{L}\hat{\xi}) - \gamma_{EM}^2\right) \frac{(H - G^{fr}) \left(s^2 \rho^f M \gamma_{Pf}^2 - s^2 C \rho^E (1 + \frac{\hat{\xi}\hat{L}}{\varsigma}) \gamma_{Pf}^2\right) + \left(\frac{s^2 \rho^f}{\zeta\varsigma} - C\right) (s^2 \rho M \gamma_{Pf}^2 + (C^2 - HM) \gamma_{Pf}^2 \gamma_{EM}^2 - s^2 \rho^f C \gamma_{Pf}^2)}{G^{fr} \left(\gamma_S^2 - \gamma_{EM}^2\right) \left(\gamma_{Ps}^2 - \gamma_{Pf}^2\right) (C^2 - HM)} \tag{B.56}$$

$$\begin{aligned} C_S^{v1,q} = \frac{\zeta\varsigma - \gamma_S^2}{\gamma_{Ps}^2 - \gamma_S^2} F_{S,Ps} - \frac{\zeta\varsigma - \gamma_S^2}{\gamma_{Pf}^2 - \gamma_S^2} F_{S,Pf} + \frac{Z_{S,Ps}}{\gamma_{Ps}^2 - \gamma_S^2} - \frac{Z_{S,Pf}}{\gamma_{Pf}^2 - \gamma_S^2} \\ + \frac{s\rho^f \hat{k} M}{\eta G^{fr}} \frac{\zeta\varsigma - \gamma_S^2}{\gamma_S^2 - \gamma_{EM}^2} + \frac{\gamma_S^2 - \zeta(\varsigma + \hat{L}\hat{\xi})}{G^{fr}(\gamma_S^2 - \gamma_{EM}^2)} C \end{aligned} \tag{B.57}$$

$$\begin{aligned} C_{EM}^{v1,q} = \frac{\gamma_{EM}^2 - \zeta\varsigma}{\gamma_{Ps}^2 - \gamma_{EM}^2} F_{EM,Ps} - \frac{\gamma_{EM}^2 - \zeta\varsigma}{\gamma_{Pf}^2 - \gamma_{EM}^2} F_{EM,Pf} + \frac{Z_{EM,Ps}}{\gamma_{Ps}^2 - \gamma_{EM}^2} - \frac{Z_{EM,Pf}}{\gamma_{Pf}^2 - \gamma_{EM}^2} \\ + \frac{s\rho^f \hat{k} M}{\eta G^{fr}} \frac{\gamma_{EM}^2 - \zeta\varsigma}{\gamma_S^2 - \gamma_{EM}^2} - \frac{\zeta(\varsigma + \hat{L}\hat{\xi}) - \gamma_{EM}^2}{G^{fr}(\gamma_S^2 - \gamma_{EM}^2)} C \end{aligned} \tag{B.58}$$

$$\begin{aligned} C_{Ps}^{v1,q} = -\frac{\zeta\varsigma - \gamma_S^2}{\gamma_{Ps}^2 - \gamma_S^2} F_{S,Ps} - \frac{Z_{S,Ps}}{\gamma_{Ps}^2 - \gamma_S^2} + -\frac{\gamma_{EM}^2 - \zeta\varsigma}{\gamma_{Ps}^2 - \gamma_{EM}^2} F_{EM,Ps} - \frac{Z_{EM,Ps}}{\gamma_{Ps}^2 - \gamma_{EM}^2} \\ - \frac{s\rho^f \hat{k}}{\eta G^{fr}} \frac{\frac{s\eta}{\zeta\hat{k}\varsigma} - M}{\gamma_{Ps}^2 - \gamma_{Pf}^2} \gamma_{Ps}^2 + \frac{1}{G^{fr}} \frac{\frac{s^2\rho^f}{\zeta\varsigma} - C}{\gamma_{Ps}^2 - \gamma_{Pf}^2} \gamma_{Ps}^2 \end{aligned} \tag{B.59}$$

$$\begin{aligned} C_{Pf}^{v1,q} = \frac{\zeta\varsigma - \gamma_S^2}{\gamma_{Pf}^2 - \gamma_S^2} F_{S,Pf} + \frac{Z_{S,Pf}}{\gamma_{Pf}^2 - \gamma_S^2} + \frac{\gamma_{EM}^2 - \zeta\varsigma}{\gamma_{Pf}^2 - \gamma_{EM}^2} F_{EM,Pf} + \frac{Z_{EM,Pf}}{\gamma_{Pf}^2 - \gamma_{EM}^2} \\ + \frac{s\rho^f \hat{k}}{\eta G^{fr}} \frac{\frac{s\eta}{\zeta\hat{k}\varsigma} - M}{\gamma_{Ps}^2 - \gamma_{Pf}^2} \gamma_{Pf}^2 - \frac{1}{G^{fr}} \frac{\frac{s^2\rho^f}{\zeta\varsigma} - C}{\gamma_{Ps}^2 - \gamma_{Pf}^2} \gamma_{Pf}^2 \end{aligned} \tag{B.60}$$

$$\breve{G}^{v1,q} \quad = \quad C_S^{v1,q} i k_1 \breve{G}_S \;+\; C_{EM}^{v1,q} i k_1 \breve{G}_{EM} \;+\; C_{Ps}^{v1,q} i k_1 \breve{G}_{Ps} \;+\; C_{Pf}^{v1,q} i k_1 \breve{G}_{Pf} \tag{B.61}$$

B.6 Particle velocity response to shear strain

$$F_{Ps} = \frac{s\rho^f \hat{k}}{\eta} \frac{C(4MG^{fr}\gamma_{Ps}^2 - 4s^2G^{fr}\rho^E(1+\hat{L}\hat{\xi}/\varsigma)) + \left(\frac{s\eta}{\zeta\hat{k}\varsigma} - M\right)(4CG^{fr}\gamma_{Ps}^2 - 4s^2\rho^f G^{fr}}{G^{fr}\left(\gamma_S^2 - \gamma_{EM}^2\right)\left(\gamma_{Ps}^2 - \gamma_{Pf}^2\right)(C^2 - HM)} \tag{B.62}$$

$$F_{Pf} = \frac{s\rho^f \hat{k}}{\eta} \frac{C(4MG^{fr}\gamma_{Pf}^2 - 4s^2G^{fr}\rho^E(1+\hat{L}\hat{\xi}/\varsigma)) + \left(\frac{s\eta}{\zeta\hat{k}\varsigma} - M\right)(4CG^{fr}\gamma_{Pf}^2 - 4s^2\rho^f G^{fr}}{G^{fr}\left(\gamma_S^2 - \gamma_{EM}^2\right)\left(\gamma_{Ps}^2 - \gamma_{Pf}^2\right)(C^2 - HM)} \tag{B.63}$$

$$Z_{Ps} = \frac{\left(H - G^{fr}\right)(4MG^{fr}\gamma_{Ps}^2 - 4s^2G^{fr}\rho^E(1+\hat{L}\hat{\xi}/\varsigma)) + \left(\frac{s^2\rho^f}{\zeta\varsigma} - C\right)(4CG^{fr}\gamma_{Ps}^2 - 4s^2\rho^f G^{fr}}{G^{fr}\left(\gamma_S^2 - \gamma_{EM}^2\right)\left(\gamma_{Ps}^2 - \gamma_{Pf}^2\right)(C^2 - HM)} \tag{B.64}$$

$$Z_{Pf} = \frac{\left(H - G^{fr}\right)(4MG^{fr}\gamma_{Pf}^2 - 4s^2G^{fr}\rho^E(1+\hat{L}\hat{\xi}/\varsigma)) + \left(\frac{s^2\rho^f}{\zeta\varsigma} - C\right)(4CG^{fr}\gamma_{Pf}^2 - 4s^2\rho^f G^{fr}}{G^{fr}\left(\gamma_S^2 - \gamma_{EM}^2\right)\left(\gamma_{Ps}^2 - \gamma_{Pf}^2\right)(C^2 - HM)} \tag{B.65}$$

$$C_{S1}^{v1,h13} = -\frac{\zeta\varsigma - \gamma_S^2}{\gamma_{Ps}^2 - \gamma_S^2} F_{Ps} + \frac{\zeta\varsigma - \gamma_S^2}{\gamma_{Pf}^2 - \gamma_S^2} F_{Pf} - \frac{Z_{Ps}(\gamma_S^2 - \zeta(\varsigma + \hat{L}\hat{\xi}))}{\gamma_{Ps}^2 - \gamma_S^2} + \frac{Z_{Pf}(\gamma_S^2 - \zeta(\varsigma + \hat{L}\hat{\xi}))}{\gamma_{Pf}^2 - \gamma_S^2} \tag{B.66}$$

$$C_{EM1}^{v1,h13} = -\frac{\gamma_{EM}^2 - \zeta\varsigma}{\gamma_{Ps}^2 - \gamma_{EM}^2} F_{Ps} + \frac{\gamma_{EM}^2 - \zeta\varsigma}{\gamma_{Pf}^2 - \gamma_{EM}^2} F_{Pf} - \frac{Z_{Ps}(\zeta(\varsigma + \hat{L}\hat{\xi}) - \gamma_{EM}^2)}{\gamma_{Ps}^2 - \gamma_{EM}^2} + \frac{Z_{Pf}(\zeta(\varsigma + \hat{L}\hat{\xi}) - \gamma_{EM}^2)}{\gamma_{Pf}^2 - \gamma_{EM}^2} \tag{B.67}$$

$$C_{Ps}^{v1,h13} = +\frac{\zeta\varsigma - \gamma_S^2}{\gamma_{Ps}^2 - \gamma_S^2} F_{Ps} + \frac{Z_{Ps}(\gamma_S^2 - \zeta(\varsigma + \hat{L}\hat{\xi}))}{\gamma_{Ps}^2 - \gamma_S^2} + \frac{\gamma_{EM}^2 - \zeta\varsigma}{\gamma_{Ps}^2 - \gamma_{EM}^2} F_{Ps} + \frac{Z_{Ps}(\zeta(\varsigma + \hat{L}\hat{\xi}) - \gamma_{EM}^2)}{\gamma_{Ps}^2 - \gamma_{EM}^2} \tag{B.68}$$

$$C_{Pf}^{v1,h13} = -\frac{\zeta\varsigma - \gamma_S^2}{\gamma_{Pf}^2 - \gamma_S^2} F_{Pf} - \frac{Z_{Pf}(\gamma_S^2 - \zeta(\varsigma + \hat{L}\hat{\xi}))}{\gamma_{Pf}^2 - \gamma_S^2} - \frac{\gamma_{EM}^2 - \zeta\varsigma}{\gamma_{Pf}^2 - \gamma_{EM}^2} F_{Pf} - \frac{Z_{Pf}(\zeta(\varsigma + \hat{L}\hat{\xi}) - \gamma_{EM}^2)}{\gamma_{Pf}^2 - \gamma_{EM}^2} \tag{B.69}$$

$$C_{EM2}^{v1,h13} = \frac{\zeta(\varsigma + \hat{L}\hat{\xi}) - \gamma_{EM}^2}{\gamma_S^2 - \gamma_{EM}^2} \tag{B.70}$$

$$C_{S2}^{v1,h13} = \frac{\gamma_S^2 - \zeta(\varsigma + \hat{L}\hat{\xi})}{\gamma_S^2 - \gamma_{EM}^2} \tag{B.71}$$

$$\breve{G}^{v_1,h_{13}} = C_{S1}^{v1,h13} ik_1 ik_1 ik_3 \breve{G}_S + C_{S2}^{v1,h13} ik_3 \breve{G}_S + C_{EM1}^{v1,h13} ik_1 ik_1 ik_3 \breve{G}_{EM} + C_{EM2}^{v1,h13} ik_3 \breve{G}_{EM} + C_{Ps}^{v1,h13} ik_1 ik_1 ik_3 \breve{G}_{Ps} + C_{Pf}^{v1,h13} ik_1 ik_1 ik_3 \breve{G}_{Pf} \tag{B.72}$$

B.7 Particle velocity response to tensile strain

$$A_1 = \frac{s\rho^f \hat{k}}{\eta G^{fr}} \frac{1}{(\gamma_S^2 - \gamma_{EM}^2)(\gamma_{Ps}^2 - \gamma_{Pf}^2)(C^2 - HM)}$$

$$A_2 = \frac{1}{G^{fr}} \frac{1}{(\gamma_S^2 - \gamma_{EM}^2)(\gamma_{Ps}^2 - \gamma_{Pf}^2)(C^2 - HM)}$$

$$F_{S,Ps} = (-Cs^2\rho^f\gamma_{Ps}^2 + C^2\gamma_{Ps}^2\gamma_S^2 + s^2\rho^E(1+\frac{\hat{\xi}\hat{L}}{\varsigma})K_G\gamma_{Ps}^2 - MK_G\gamma_S^2\gamma_{Ps}^2)/(\gamma_{Ps}^2 - \gamma_S^2) \tag{B.73}$$

$$Z_{S,Ps} = (-Cs^2\rho\gamma_{Ps}^2 + CH\gamma_{Ps}^2\gamma_S^2 + s^2\rho^f K_G\gamma_{Ps}^2 - CK_G\gamma_S^2\gamma_{Ps}^2)/(\gamma_{Ps}^2 - \gamma_S^2) \tag{B.74}$$

$$F_{EM,Ps} = (-Cs^2\rho^f\gamma_{Ps}^2 + C^2\gamma_{Ps}^2\gamma_{EM}^2 + s^2\rho^E(1+\frac{\hat{\xi}\hat{L}}{\varsigma})K_G\gamma_{Ps}^2 - MK_G\gamma_{EM}^2\gamma_{Ps}^2)/(\gamma_{Ps}^2 - \gamma_{EM}^2) \tag{B.75}$$

$$Z_{EM,Ps} = (-Cs^2\rho\gamma_{Ps}^2 + CH\gamma_{Ps}^2\gamma_{EM}^2 + s^2\rho^f K_G\gamma_{Ps}^2 - CK_G\gamma_{EM}^2\gamma_{Ps}^2)/(\gamma_{Ps}^2 - \gamma_{EM}^2) \tag{B.76}$$

$$F_{S,Pf} = (-Cs^2\rho^f\gamma_{Pf}^2 + C^2\gamma_{Pf}^2\gamma_S^2 + s^2\rho^E(1+\frac{\hat{\xi}\hat{L}}{\varsigma})K_G\gamma_{Ps}^2 - MK_G\gamma_S^2\gamma_{Pf}^2)/(\gamma_{Pf}^2 - \gamma_S^2) \tag{B.77}$$

$$Z_{S,Pf} = (-Cs^2\rho\gamma_{Pf}^2 + CH\gamma_{Pf}^2\gamma_S^2 + s^2\rho^f K_G\gamma_{Ps}^2 - CK_G\gamma_S^2\gamma_{Pf}^2)/(\gamma_{Pf}^2 - \gamma_S^2) \tag{B.78}$$

$$F_{EM,Pf} = (-Cs^2\rho^f\gamma_{Pf}^2 + C^2\gamma_{Pf}^2\gamma_{EM}^2 + s^2\rho^E(1+\frac{\hat{\xi}\hat{L}}{\varsigma})K_G\gamma_{Ps}^2 - MK_G\gamma_{EM}^2\gamma_{Pf}^2)/(\gamma_{Pf}^2 - \gamma_{EM}^2) \tag{B.79}$$

$$Z_{EM,Pf} = (-Cs^2\rho\gamma_{Pf}^2 + CH\gamma_{Pf}^2\gamma_{EM}^2 + s^2\rho^f K_G\gamma_{Ps}^2 - CK_G\gamma_{EM}^2\gamma_{Pf}^2)/(\gamma_{Pf}^2 - \gamma_{EM}^2) \tag{B.80}$$

$$Y_{Ps} = A_1(\gamma_S^2 - \gamma_{EM}^2)[-C^3\gamma_{Ps}^2 + CMK_G\gamma_{Ps}^2 + \left(\frac{s\eta}{\zeta\hat{k}\varsigma} - M\right)(-CH\gamma_{Ps}^2 + CK_G\gamma_{Ps}^2)] \tag{B.81}$$

$$Y_{Pf} = A_1(\gamma_S^2 - \gamma_{EM}^2)[-C^3\gamma_{Pf}^2 + CMK_G\gamma_{Pf}^2 + \left(\frac{s\eta}{\zeta\hat{k}\varsigma} - M\right)(-CH\gamma_{Pf}^2 + CK_G\gamma_{Pf}^2)] \tag{B.82}$$

$$Z_{Ps} = A_2(\gamma_{EM}^2 - \gamma_S^2)[(-C^2\gamma_{Ps}^2 + MK_G\gamma_{Ps}^2)(H-G) + \left(\frac{s^2\rho^f}{\zeta\varsigma} - C\right)(-CH\gamma_{Ps}^2 + CK_G\gamma_{Ps}^2)] \tag{B.83}$$

$$Z_{Pf} = A_2(\gamma_{EM}^2 - \gamma_S^2)[(-C^2\gamma_{Pf}^2 + MK_G\gamma_{Pf}^2)(H-G) + \left(\frac{s^2\rho^f}{\zeta\varsigma} - C\right)(-CH\gamma_{Pf}^2 + CK_G\gamma_{Pf}^2)] \tag{B.84}$$

Operator on $ik_1\breve{G}_{Ps}$,

$$\begin{aligned} C_{Ps}^{v1,h11;33} = &-\left(A_1(\gamma_{EM}^2 - \zeta\varsigma)C + A_2(\zeta(\varsigma + \hat{L}\hat{\xi}) - \gamma_{EM}^2)(H - G^{fr})\right) F_{EM,Ps} \\ &- \left(A_1(\zeta\varsigma - \gamma_S^2)C + A_2(\gamma_S^2 - \zeta(\varsigma + \hat{L}\hat{\xi}))(H - G^{fr})\right) F_{S,Ps} \\ &- \left(A_2(\frac{s^2\rho^f}{\zeta\varsigma} - C)(\gamma_S^2 - \zeta(\varsigma + \hat{L}\hat{\xi}) + A_1(\zeta\varsigma - \gamma_S^2)\left(\frac{s\eta}{\zeta\hat{k}\varsigma} - M\right)\right) Z_{S,Ps} \\ &- \left(A_2(\frac{s^2\rho^f}{\zeta\varsigma} - C)(\zeta(\varsigma + \hat{L}\hat{\xi}) - \gamma_{EM}^2) + A_1(\gamma_{EM}^2 - \zeta\varsigma)\left(\frac{s\eta}{\zeta\hat{k}\varsigma} - M\right)\right) Z_{EM,Ps} \\ &+ Y_{Ps} + Z_{Ps} \end{aligned}$$

Operator on $ik_1\breve{G}_{Pf}$,

$$\begin{aligned} C_{Pf}^{v1,h11;33} = &+\left(A_1(\gamma_{EM}^2 - \zeta\varsigma)C + A_2(\zeta(\varsigma + \hat{L}\hat{\xi}) - \gamma_{EM}^2)(H - G^{fr})\right) F_{EM,Pf} \\ &+ \left(A_1(\zeta\varsigma - \gamma_S^2)C + A_2(\gamma_S^2 - \zeta(\varsigma + \hat{L}\hat{\xi}))(H - G^{fr})\right) F_{S,Pf} \\ &+ \left(A_2(\frac{s^2\rho^f}{\zeta\varsigma} - C)(\gamma_S^2 - \zeta(\varsigma + \hat{L}\hat{\xi})) + A_1(\zeta\varsigma - \gamma_S^2)\left(\frac{s\eta}{\zeta\hat{k}\varsigma} - M\right)\right) Z_{S,Pf} \\ &+ \left(A_2(\frac{s^2\rho^f}{\zeta\varsigma} - C)(\zeta(\varsigma + \hat{L}\hat{\xi}) - \gamma_{EM}^2) + A_1(\gamma_{EM}^2 - \zeta\varsigma)\left(\frac{s\eta}{\zeta\hat{k}\varsigma} - M\right)\right) Z_{EM,Pf} \\ &- Y_{Pf} - Z_{Pf} \end{aligned}$$

Operator on $ik_1\breve{G}_S$,

$$\begin{aligned} C_{SV}^{v1,h11;33} = &+\left(A_1(\zeta\varsigma - \gamma_S^2)C + A_2(\gamma_S^2 - \zeta(\varsigma + \hat{L}\hat{\xi}))(H - G^{fr})\right) F_{S,Ps} \\ &+ \left(A_2(\frac{s^2\rho^f}{\zeta\varsigma} - C)(\gamma_S^2 - \zeta(\varsigma + \hat{L}\hat{\xi}) + A_1(\zeta\varsigma - \gamma_S^2)\left(\frac{s\eta}{\zeta\hat{k}\varsigma} - M\right)\right) Z_{S,Ps} \\ &- \left(A_1(\zeta\varsigma - \gamma_S^2)C + A_2(\gamma_S^2 - \zeta(\varsigma + \hat{L}\hat{\xi})(H - G^{fr})\right) F_{S,Pf} \\ &- \left(A_2(\frac{s^2\rho^f}{\zeta\varsigma} - C)(\gamma_S^2 - \zeta(\varsigma + \hat{L}\hat{\xi})) + A_1(\zeta\varsigma - \gamma_S^2)\left(\frac{s\eta}{\zeta\hat{k}\varsigma} - M\right)\right) Z_{S,Pf} \\ &+ \frac{1}{G^{fr}}\frac{\gamma_S^2 - \zeta(\varsigma + \hat{L}\hat{\xi})}{\gamma_S^2 - \gamma_{EM}^2}[H; H - 2G^{fr}]ik_1 + \frac{s\rho^f\hat{k}}{\eta G^{fr}}\frac{\zeta\varsigma - \gamma_S^2}{\gamma_S^2 - \gamma_{EM}^2}Cik_1 \end{aligned}$$

Operator on $ik_1\breve{G}_{EM}$,

$$\begin{aligned}C_{EM}^{v1,h11;33} = &+\left(A_1(\gamma_{EM}^2-\zeta\varsigma)C + A_2(\zeta(\varsigma+\hat{L}\hat{\xi})-\gamma_{EM}^2)(H-G^{fr})\right)F_{EM,Ps}\\
&+\left(A_2(\frac{s^2\rho^f}{\zeta\varsigma}-C)(\zeta(\varsigma+\hat{L}\hat{\xi})-\gamma_{EM}^2)+A_1(\gamma_{EM}^2-\zeta\varsigma)\left(\frac{s\eta}{\zeta\hat{k}\varsigma}-M\right)\right)Z_{EM,Ps}\\
&-\left(A_1(\gamma_{EM}^2-\zeta\varsigma)C + A_2(\zeta(\varsigma+\hat{L}\hat{\xi})-\gamma_{EM}^2)(H-G^{fr})\right)F_{EM,Pf}\\
&-\left(A_2(\frac{s^2\rho^f}{\zeta\varsigma}-C)(\zeta(\varsigma+\hat{L}\hat{\xi})-\gamma_{EM}^2)+A_1(\gamma_{EM}^2-\zeta\varsigma)\left(\frac{s\eta}{\zeta\hat{k}\varsigma}-M\right)\right)Z_{EM,Pf}\\
&+\frac{1}{G^{fr}}\frac{\zeta(\varsigma+\hat{L}\hat{\xi})-\gamma_{EM}^2}{\gamma_S^2-\gamma_{EM}^2}[H;H-2G^{fr}]ik_1+\frac{s\rho^f\hat{k}}{\eta G^{fr}}\frac{\gamma_{EM}^2-\zeta\varsigma}{\gamma_S^2-\gamma_{EM}^2}Cik_1\end{aligned}$$

The triple operators on h_{11} are defined separately,

$$F_{Ps,k1^2} = (MG^{fr}\frac{4}{3}\gamma_{Ps}^2 - s^2\rho^E(1+\frac{\hat{\xi}\hat{L}}{\varsigma})G^{fr}\frac{4}{3}) \tag{B.85}$$

$$F_{Ps,k3^2} = (s^2\rho^E(1+\frac{\hat{\xi}\hat{L}}{\varsigma})G^{fr}\frac{2}{3}+k_1^2 - MG^{fr}\frac{2}{3}\gamma_{Ps}^2) \tag{B.86}$$

$$F_{Pf,k1^2} = (MG^{fr}\frac{4}{3}\gamma_{Pf}^2 - s^2\rho^E(1+\frac{\hat{\xi}\hat{L}}{\varsigma})G^{fr}\frac{4}{3}) \tag{B.87}$$

$$F_{Pf,k3^2} = (s^2\rho^E(1+\frac{\hat{\xi}\hat{L}}{\varsigma})G^{fr}\frac{2}{3}+k_1^2 - MG^{fr}\frac{2}{3}\gamma_{Pf}^2) \tag{B.88}$$

$$Z_{Ps,k1^2} = (CG^{fr}\frac{4}{3}\gamma_{Ps}^2 - s^2\rho^f G^{fr}\frac{4}{3}) \tag{B.89}$$

$$Z_{Ps,k3^2} = (s^2\rho^f G^{fr}\frac{2}{3} - CG^{fr}\frac{2}{3}\gamma_{Ps}^2) \tag{B.90}$$

$$Z_{Pf,k1^2} = (CG^{fr}\frac{4}{3}\gamma_{Pf}^2 - s^2\rho^f G^{fr}\frac{4}{3}) \tag{B.91}$$

$$Z_{Pf,k3^2} = (s^2\rho^f G^{fr}\frac{2}{3} - CG^{fr}\frac{2}{3}\gamma_{Pf}^2) \tag{B.92}$$

Shear operator on $ik_1^3\breve{G}_{Ps}$,

$$\begin{aligned}C_{*Ps_k1}^{v1} = &-\left(A_1(\gamma_{EM}^2-\zeta\varsigma)C + A_2(\zeta(\varsigma+\hat{L}\hat{\xi})-\gamma_{EM}^2)(H-G^{fr})\right)F_{Ps,k1^2}/(\gamma_{Ps}^2-\gamma_{EM}^2)\\
&-\left(A_1(\zeta\varsigma-\gamma_S^2)C + A_2(\gamma_S^2-\zeta(\varsigma+\hat{L}\hat{\xi}))(H-G^{fr})\right)F_{Ps,k1^2}/(\gamma_{Ps}^2-\gamma_S^2)\\
&+\left(A_2(\frac{s^2\rho^f}{\zeta\varsigma}-C)(\gamma_S^2-\zeta(\varsigma+\hat{L}\hat{\xi}))-A_1(\zeta\varsigma-\gamma_S^2)\left(\frac{s\eta}{\zeta\hat{k}\varsigma}-M\right)\right)Z_{Ps,k1^2}/(\gamma_{Ps}^2-\gamma_S^2)\\
&-\left(A_2(\frac{s^2\rho^f}{\zeta\varsigma}-C)(\zeta(\varsigma+\hat{L}\hat{\xi})-\gamma_{EM}^2)+A_1(\gamma_{EM}^2-\zeta\varsigma)\left(\frac{s\eta}{\zeta\hat{k}\varsigma}-M\right)\right)Z_{Ps,k1^2}/(\gamma_{Ps}^2-\gamma_{EM}^2)\end{aligned} \tag{B.93}$$

Shear operator on $ik_1ik_3^2\breve{G}_{Ps}$,

$$\begin{aligned}
C^{v1}_{*Ps_k3} = &-\left(A_1(\gamma_{EM}^2-\zeta\varsigma)C + A_2(\zeta(\varsigma+\hat{L}\hat{\xi})-\gamma_{EM}^2)(H-G^{fr})\right) F_{Ps,k3^2}/(\gamma_{Ps}^2-\gamma_{EM}^2)\\
&-\left(A_1(\zeta\varsigma-\gamma_S^2)C + A_2(\gamma_S^2-\zeta(\varsigma+\hat{L}\hat{\xi}))(H-G^{fr})\right) F_{Ps,k3^2}/(\gamma_{Ps}^2-\gamma_S^2)\\
&+\left(A_2(\frac{s^2\rho^f}{\zeta\varsigma}-C)(\gamma_S^2-\zeta(\varsigma+\hat{L}\hat{\xi}))-A_1(\zeta\varsigma-\gamma_S^2)\left(\frac{s\eta}{\zeta\hat{k}\varsigma}-M\right)\right) Z_{Ps,k3^2}/(\gamma_{Ps}^2-\gamma_S^2)\\
&-\left(A_2(\frac{s^2\rho^f}{\zeta\varsigma}-C)(\zeta(\varsigma+\hat{L}\hat{\xi})-\gamma_{EM}^2)+A_1(\gamma_{EM}^2-\zeta\varsigma)\left(\frac{s\eta}{\zeta\hat{k}\varsigma}-M\right)\right) Z_{Ps,k3^2}/(\gamma_{Ps}^2-\gamma_{EM}^2)
\end{aligned}\tag{B.94}$$

Shear operator on $ik_1^3\breve{G}_{Pf}$,

$$\begin{aligned}
C^{v1}_{*Pf_k1} = &+\left(A_1(\gamma_{EM}^2-\zeta\varsigma)C + A_2(\zeta(\varsigma+\hat{L}\hat{\xi})-\gamma_{EM}^2)(H-G^{fr})\right) F_{Pf,k1^2}/(\gamma_{Pf}^2-\gamma_{EM}^2)\\
&+\left(A_1(\zeta\varsigma-\gamma_S^2)C + A_2(\gamma_S^2-\zeta(\varsigma+\hat{L}\hat{\xi}))(H-G^{fr})\right) F_{Pf,k1^2}/(\gamma_{Pf}^2-\gamma_S^2)\\
&-\left(A_2(\frac{s^2\rho^f}{\zeta\varsigma}-C)(\gamma_S^2-\zeta(\varsigma+\hat{L}\hat{\xi}))-A_1(\zeta\varsigma-\gamma_S^2)\left(\frac{s\eta}{\zeta\hat{k}\varsigma}-M\right)\right) Z_{Pf,k1^2}/(\gamma_{Pf}^2-\gamma_S^2)\\
&+\left(A_2(\frac{s^2\rho^f}{\zeta\varsigma}-C)(\zeta(\varsigma+\hat{L}\hat{\xi})-\gamma_{EM}^2)+A_1(\gamma_{EM}^2-\zeta\varsigma)\left(\frac{s\eta}{\zeta\hat{k}\varsigma}-M\right)\right) F_{Pf,k1^2}/(\gamma_{Pf}^2-\gamma_{EM}^2)
\end{aligned}\tag{B.95}$$

Shear operator on $ik_3^2ik_1\breve{G}_{Pf}$,

$$\begin{aligned}
C^{v1}_{*Pf_k3} = &+\left(A_1(\gamma_{EM}^2-\zeta\varsigma)C + A_2(\zeta(\varsigma+\hat{L}\hat{\xi})-\gamma_{EM}^2)(H-G^{fr})\right) F_{Pf,k3^2}/(\gamma_{Pf}^2-\gamma_{EM}^2)\\
&+\left(A_1(\zeta\varsigma-\gamma_S^2)C + A_2(\gamma_S^2-\zeta(\varsigma+\hat{L}\hat{\xi}))(H-G^{fr})\right) F_{Pf,k3^2}/(\gamma_{Pf}^2-\gamma_S^2)\\
&-\left(A_2(\frac{s^2\rho^f}{\zeta\varsigma}-C)(\gamma_S^2-\zeta(\varsigma+\hat{L}\hat{\xi}))-A_1(\zeta\varsigma-\gamma_S^2)\left(\frac{s\eta}{\zeta\hat{k}\varsigma}-M\right)\right) Z_{Pf,k3^2}/(\gamma_{Pf}^2-\gamma_S^2)\\
&+\left(A_2(\frac{s^2\rho^f}{\zeta\varsigma}-C)(\zeta(\varsigma+\hat{L}\hat{\xi})-\gamma_{EM}^2)+A_1(\gamma_{EM}^2-\zeta\varsigma)\left(\frac{s\eta}{\zeta\hat{k}\varsigma}-M\right)\right) F_{Pf,k3^2}/(\gamma_{Pf}^2-\gamma_{EM}^2)
\end{aligned}\tag{B.96}$$

Operator on $ik_1^3\breve{G}_S$,

$$\begin{aligned}
C^{v1}_{*SV_k1} = &-\left(A_1(\zeta\varsigma-\gamma_S^2)C + A_2(\gamma_S^2-\zeta(\varsigma+\hat{L}\hat{\xi}))(H-G^{fr})\right) F_{Ps,k1^2}/(\gamma_{Ps}^2-\gamma_S^2)\\
&+\left(-A_2(\frac{s^2\rho^f}{\zeta\varsigma}-C)(\gamma_S^2-\zeta(\varsigma+\hat{L}\hat{\xi}))-A_2(\zeta\varsigma-\gamma_S^2)\left(\frac{s\eta}{\zeta\hat{k}\varsigma}-M\right)\right) Z_{Ps,k1^2}/(\gamma_{Ps}^2-\gamma_S^2)\\
&+\left(A_1(\zeta\varsigma-\gamma_S^2)C + A_2(\gamma_S^2-\zeta(\varsigma+\hat{L}\hat{\xi})(H-G^{fr})\right) F_{Pf,k1^2}/(\gamma_{Pf}^2-\gamma_S^2)\\
&-\left(-A_2(\frac{s^2\rho^f}{\zeta\varsigma}-C)(\gamma_S^2-\zeta(\varsigma+\hat{L}\hat{\xi}))-A_1(\zeta\varsigma-\gamma_S^2)\left(\frac{s\eta}{\zeta\hat{k}\varsigma}-M\right)\right) Z_{Pf,k1^2}/(\gamma_{Pf}^2-\gamma_S^2)
\end{aligned}\tag{B.97}$$

Operator on $ik_3^2 ik_1 \breve{G}_S$,

$$\begin{aligned}
C^{v1}_{*SV_k3} = &-\left(A_1(\zeta\varsigma-\gamma_S^2)C + A_2(\gamma_S^2-\zeta(\varsigma+\hat{L}\hat{\xi}))(H-G^{fr})\right)F_{Ps,k3^2}/(\gamma_{Ps}^2-\gamma_S^2)\\
&+\left(-A_2(\frac{s^2\rho^f}{\zeta\varsigma}-C)(\gamma_S^2-\zeta(\varsigma+\hat{L}\hat{\xi}))-A_2(\zeta\varsigma-\gamma_S^2)\left(\frac{s\eta}{\zeta\hat{k}\varsigma}-M\right)\right)Z_{Ps,k3^2}/(\gamma_{Ps}^2-\gamma_S^2)\\
&+\left(A_1(\zeta\varsigma-\gamma_S^2)C + A_2(\gamma_S^2-\zeta(\varsigma+\hat{L}\hat{\xi})(H-G^{fr})\right)F_{Pf,k3^2}/(\gamma_{Pf}^2-\gamma_S^2)\\
&-\left(-A_2(\frac{s^2\rho^f}{\zeta\varsigma}-C)(\gamma_S^2-\zeta(\varsigma+\hat{L}\hat{\xi}))-A_1(\zeta\varsigma-\gamma_S^2)\left(\frac{s\eta}{\zeta\hat{k}\varsigma}-M\right)\right)Z_{Pf,k3^2}/(\gamma_{Pf}^2-\gamma_S^2)
\end{aligned} \tag{B.98}$$

Operator on $ik_1^3 \breve{G}_{EM}$,

$$\begin{aligned}
C^{v1}_{*EM_k1} = &+\left(A_1(\gamma_{EM}^2-\zeta\varsigma)C + A_2(\zeta(\varsigma+\hat{L}\hat{\xi})-\gamma_{EM}^2)(H-G^{fr})\right)F_{Ps,k1^2}/(\gamma_{Ps}^2-\gamma_{EM}^2)\\
&+\left(A_2(\frac{s^2\rho^f}{\zeta\varsigma}-C)(\zeta(\varsigma+\hat{L}\hat{\xi})-\gamma_{EM}^2)+A_1(\gamma_{EM}^2-\zeta\varsigma)\left(\frac{s\eta}{\zeta\hat{k}\varsigma}-M\right)\right)Z_{Ps,k1^2}/(\gamma_{Ps}^2-\gamma_{EM}^2)\\
&-\left(A_1(\gamma_{EM}^2-\zeta\varsigma)C + A_2(\zeta(\varsigma+\hat{L}\hat{\xi})-\gamma_{EM}^2)(H-G^{fr})\right)F_{Pf,k1^2}/(\gamma_{Pf}^2-\gamma_{EM}^2)\\
&-\left(A_2(\frac{s^2\rho^f}{\zeta\varsigma}-C)(\zeta(\varsigma+\hat{L}\hat{\xi})-\gamma_{EM}^2)+A_1(\gamma_{EM}^2-\zeta\varsigma)\left(\frac{s\eta}{\zeta\hat{k}\varsigma}-M\right)\right)Z_{Pf,k1^2}/(\gamma_{Pf}^2-\gamma_{EM}^2)
\end{aligned} \tag{B.99}$$

Operator on $ik_3^2 ik_1 \breve{G}_{EM}$,

$$\begin{aligned}
C^{v1}_{*EM_k3} = &+\left(A_1(\gamma_{EM}^2-\zeta\varsigma)C + A_2(\zeta(\varsigma+\hat{L}\hat{\xi})-\gamma_{EM}^2)(H-G^{fr})\right)F_{Ps,k3^2}/(\gamma_{Ps}^2-\gamma_{EM}^2)\\
&+\left(A_2(\frac{s^2\rho^f}{\zeta\varsigma}-C)(\zeta(\varsigma+\hat{L}\hat{\xi})-\gamma_{EM}^2)+A_1(\gamma_{EM}^2-\zeta\varsigma)\left(\frac{s\eta}{\zeta\hat{k}\varsigma}-M\right)\right)Z_{Ps,k3^2}/(\gamma_{Ps}^2-\gamma_{EM}^2)\\
&-\left(A_1(\gamma_{EM}^2-\zeta\varsigma)C + A_2(\zeta(\varsigma+\hat{L}\hat{\xi})-\gamma_{EM}^2)(H-G^{fr})\right)F_{Pf,k3^2}/(\gamma_{Pf}^2-\gamma_{EM}^2)\\
&-\left(A_2(\frac{s^2\rho^f}{\zeta\varsigma}-C)(\zeta(\varsigma+\hat{L}\hat{\xi})-\gamma_{EM}^2)+A_1(\gamma_{EM}^2-\zeta\varsigma)\left(\frac{s\eta}{\zeta\hat{k}\varsigma}-M\right)\right)Z_{Pf,k3^2}/(\gamma_{Pf}^2-\gamma_{EM}^2)
\end{aligned} \tag{B.100}$$

$$\begin{aligned}
\breve{G}^{v1,h11} = &C^{v1,h11}_{Ps} ik_1 \breve{G}_{Ps} + C^{v1,h11}_{Pf} ik_1 \breve{G}_{Pf} + C^{v1,h11}_{SV} ik_1 \breve{G}_S + C^{v1,h11}_{EM} ik_1 \breve{G}_{EM}\\
&+ C^{v1}_{*Ps_k1} ik_1 ik_1 ik_1 \breve{G}_{Ps} + C^{v1}_{*Ps_k3} ik_3 ik_3 ik_1 \breve{G}_{Ps}\\
&+ C^{v1}_{*Pf_k1} ik_1 ik_1 ik_1 \breve{G}_{Pf} + C^{v1}_{*Pf_k3} ik_3 ik_3 ik_1 \breve{G}_{Pf}\\
&+ C^{v1}_{*SV_k1} ik_1 ik_1 ik_1 \breve{G}_{SV} + C^{v1}_{*SV_k3} ik_3 ik_3 ik_1 \breve{G}_{SV}\\
&+ C^{v1}_{*EM_k1} ik_1 ik_1 ik_1 \breve{G}_{EM} + C^{v1}_{*EM_k3} ik_3 ik_3 ik_1 \breve{G}_{EM}
\end{aligned} \tag{B.101}$$

For the operators on the shear terms in the h_{33} source greens function, the double k terms simply have to be switched, the rest stays the same.

$$
\begin{aligned}
\breve{G}^{v1,h33} = C^{v1,h11}_{Ps} ik_1 \breve{G}_{Ps} + C^{v1,h11}_{Pf} ik_1 \breve{G}_{Pf} + C^{v1,h11}_{SV} ik_1 \breve{G}_{S} + C^{v1,h11}_{EM} ik_1 \breve{G}_{EM} \\
+ C^{v1}_{*Ps_k 3} ik_1 ik_1 ik_1 \breve{G}_{Ps} + C^{v1}_{*Ps_k 1} ik_3 ik_3 ik_1 \breve{G}_{Ps} \\
+ C^{v1}_{*Pf_k 3} ik_1 ik_1 ik_1 \breve{G}_{Pf} + C^{v1}_{*Pf_k 1} ik_3 ik_3 ik_1 \breve{G}_{Pf} \\
+ C^{v1}_{*SV_k 3} ik_1 ik_1 ik_1 \breve{G}_{SV} + C^{v1}_{*SV_k 1} ik_3 ik_3 ik_1 \breve{G}_{SV} \\
+ C^{v1}_{*EM_k 3} ik_1 ik_1 ik_1 \breve{G}_{EM} + C^{v1}_{*EM_k 1} ik_3 ik_3 ik_1 \breve{G}_{EM}
\end{aligned} \tag{B.102}
$$

B.8 Particle velocity response to the electric dipole

This Green's function gave erroneous modelling results, because it turned out an unexpected dominant SV-wave arrival. It requires a recalculation, starting from wave equation B.6.

$$
\begin{aligned}
F_{\gamma_{EM}\gamma_{Ps}} = & \left[\hat{k} s \rho^f C(\gamma_{EM}^2 - \zeta\varsigma) + (H - G^{fr})(\zeta(\varsigma + \hat{L}\hat{\xi}) - \gamma_{EM}^2)\eta\right] \\
& \left[\frac{\hat{L}}{\varsigma\hat{k}} s^3 \rho^f \eta - \frac{s^2 C \rho^E \hat{L} \gamma_{Ps}^2}{\varsigma} + (\hat{\xi}^{-1} - 1) C M \gamma_{Ps}^2 \gamma_{EM}^2\right] \\
& + \hat{\xi}^{-1}\left[\hat{k} s \rho^f (\gamma_{EM}^2 - \zeta\varsigma)\left(\frac{s\eta}{\zeta\hat{k}\varsigma} - M\right) + (\frac{s^2\rho^f}{\zeta\varsigma} - C)\left(\zeta(\varsigma + \hat{L}\hat{\xi}) - \gamma_{EM}^2\right)\eta\right] \\
& \left[(\frac{(\rho^f)^2}{\rho\rho^E} - 1)\frac{s^3\rho\eta}{\hat{k}} + s^2\gamma_{Ps}^2(\rho M + \rho^E H - 2\rho^f C) + (C^2 - HM)\gamma_{Ps}^2\gamma_{EM}^2\right]
\end{aligned} \tag{B.103}
$$

$$
\begin{aligned}
F_{\gamma_{EM}\gamma_{Pf}} = & \left[\hat{k} s \rho^f C(\gamma_{EM}^2 - \zeta\varsigma) + (H - G^{fr})(\zeta(\varsigma + \hat{L}\hat{\xi}) - \gamma_{EM}^2)\eta\right] \\
& \left[\frac{\hat{L}}{\varsigma\hat{k}} s^3 \rho^f \eta - \frac{s^2 C \rho^E \hat{L} \gamma_{Pf}^2}{\varsigma} + (\hat{\xi}^{-1} - 1) C M \gamma_{Pf}^2 \gamma_{EM}^2\right] \\
& + \hat{\xi}^{-1}\left[\hat{k} s \rho^f (\gamma_{EM}^2 - \zeta\varsigma)\left(\frac{s\eta}{\zeta\hat{k}\varsigma} - M\right) + (\frac{s^2\rho^f}{\zeta\varsigma} - C)\left(\zeta(\varsigma + \hat{L}\hat{\xi}) - \gamma_{EM}^2\right)\eta\right] \\
& \left[(\frac{(\rho^f)^2}{\rho\rho^E} - 1)\frac{s^3\rho\eta}{\hat{k}} + s^2\gamma_{Pf}^2(\rho M + \rho^E H - 2\rho^f C) + (C^2 - HM)\gamma_{Pf}^2\gamma_{EM}^2\right]
\end{aligned} \tag{B.104}
$$

$$F_{EM,Ps} = \frac{F_{\gamma_{EM}\gamma_{Ps}}}{\eta G^{fr}(\gamma_S^2-\gamma_{EM}^2)(C^2-HM)(\gamma_{Ps}^2-\gamma_{Pf}^2)(\gamma_{Ps}^2-\gamma_{EM}^2)} \tag{B.105}$$

$$F_{EM,Pf} = \frac{F_{\gamma_{EM}\gamma_{Pf}}}{\eta G^{fr}(\gamma_S^2-\gamma_{EM}^2)(C^2-HM)(\gamma_{Ps}^2-\gamma_{Pf}^2)(\gamma_{Pf}^2-\gamma_{EM}^2)} \tag{B.106}$$

$$F_{EM} = \frac{s\rho^f\hat{k}M}{\eta G^{fr}\hat{\xi}}\frac{\zeta\varsigma-\gamma_{EM}^2}{\gamma_S^2-\gamma_{EM}^2} + \frac{C}{G^{fr}\hat{\xi}}\frac{\gamma_{EM}^2-\zeta(\varsigma+\hat{L}\hat{\xi})}{\gamma_S^2-\gamma_{EM}^2} \tag{B.107}$$

$$\begin{aligned}
F_{\gamma_S\gamma_{Ps}} = &\left[\hat{k}s\rho^f C(\zeta\varsigma-\gamma_S^2)+(H-G^{fr})(\gamma_S^2-\zeta(\varsigma+\hat{L}\hat{\xi}))\eta\right]\\
&\left[\frac{\hat{L}}{\varsigma\hat{k}}s^3\rho^f\eta-\frac{s^2C\rho^E\hat{L}\gamma_{Ps}^2}{\varsigma}+(\hat{\xi}^{-1}-1)CM\gamma_{Ps}^2\gamma_S^2\right]\\
&+\hat{\xi}^{-1}\left[\hat{k}s\rho^f(\zeta\varsigma-\gamma_S^2)\left(\frac{s\eta}{\zeta\hat{k}\varsigma}-M\right)+(\frac{s^2\rho^f}{\zeta\varsigma}-C)\left(\gamma_S^2-\zeta(\varsigma+\hat{L}\hat{\xi})\right)\eta\right]\\
&\left[(\frac{(\rho^f)^2}{\rho\rho^E}-1)\frac{s^3\rho\eta}{\hat{k}}+s^2\gamma_{Ps}^2(\rho M+\rho^E H-2\rho^f C)+(C^2-HM)\gamma_{Ps}^2\gamma_S^2\right]
\end{aligned} \tag{B.108}$$

$$\begin{aligned}
F_{\gamma_S\gamma_{Pf}} = &\left[\hat{k}s\rho^f C(\zeta\varsigma-\gamma_S^2)+(H-G^{fr})(\gamma_S^2-\zeta(\varsigma+\hat{L}\hat{\xi}))\eta\right]\\
&\left[\frac{\hat{L}}{\varsigma\hat{k}}s^3\rho^f\eta-\frac{s^2C\rho^E\hat{L}\gamma_{Pf}^2}{\varsigma}+(\hat{\xi}^{-1}-1)CM\gamma_{Pf}^2\gamma_S^2\right]\\
&+\hat{\xi}^{-1}\left[\hat{k}s\rho^f(\zeta\varsigma-\gamma_S^2)\left(\frac{s\eta}{\zeta\hat{k}\varsigma}-M\right)+(\frac{s^2\rho^f}{\zeta\varsigma}-C)\left(\gamma_S^2-\zeta(\varsigma+\hat{L}\hat{\xi})\right)\eta\right]\\
&\left[(\frac{(\rho^f)^2}{\rho\rho^E}-1)\frac{s^3\rho\eta}{\hat{k}}+s^2\gamma_{Pf}^2(\rho M+\rho^E H-2\rho^f C)+(C^2-HM)\gamma_{Pf}^2\gamma_S^2\right]
\end{aligned} \tag{B.109}$$

$$F_{S,Ps} = \frac{F_{\gamma_S\gamma_{Ps}}}{\eta G^{fr}(\gamma_S^2-\gamma_{EM}^2)(C^2-HM)(\gamma_{Ps}^2-\gamma_{Pf}^2)(\gamma_{Ps}^2-\gamma_S^2)} \tag{B.110}$$

$$F_{S,Pf} = \frac{F_{\gamma_S\gamma_{Pf}}}{\eta G^{fr}(\gamma_S^2-\gamma_{EM}^2)(C^2-HM)(\gamma_{Ps}^2-\gamma_{Pf}^2)(\gamma_{Pf}^2-\gamma_S^2)} \tag{B.111}$$

$$F_S = \frac{s\rho^f\hat{k}M}{\eta G^{fr}\hat{\xi}}\frac{\gamma_S^2-\zeta\varsigma}{\gamma_S^2-\gamma_{EM}^2} + \frac{C}{G^{fr}\hat{\xi}}\frac{\zeta(\varsigma+\hat{L}\hat{\xi})-\gamma_S^2}{\gamma_S^2-\gamma_{EM}^2} \tag{B.112}$$

$$A = \frac{s\rho^f\hat{k}\left[(\hat{\xi}^{-1}-1)C^2M+\hat{\xi}^{-1}\left(\frac{s\eta}{\zeta\hat{k}\varsigma}-M\right)(C^2-HM)\right]}{\eta G^{fr}(C^2-HM)(\gamma_{Ps}^2-\gamma_{Pf}^2)} \tag{B.113}$$

$$B = \frac{\left[(1-\hat{\xi}^{-1})(H-G^{fr})CM-\hat{\xi}^{-1}\left(\frac{s^2\rho^f}{\zeta\varsigma}-C\right)(C^2-HM)\right]}{G^{fr}(C^2-HM)(\gamma_{Ps}^2-\gamma_{Pf}^2)} \tag{B.114}$$

$$C_{S1}^{v1,J_1^e} = (F_{S,Ps} - F_{S,Pf} + F_S) \tag{B.115}$$

$$C_{S2}^{v1,J_1^e} = -\frac{\zeta \hat{L} s^2 \rho^f}{G^{fr}} \frac{1}{\gamma_S^2 - \gamma_{EM}^2} \tag{B.116}$$

$$C_{EM1}^{v1,J_1^e} = +(F_{EM,Ps} - F_{EM,Pf} + F_{EM}) \tag{B.117}$$

$$C_{EM2}^{v1,J_1^e} = \frac{\zeta \hat{L} s^2 \rho^f}{G^{fr}} \frac{1}{\gamma_S^2 - \gamma_{EM}^2} \tag{B.118}$$

$$C_{Pf}^{v1,J_1^e} = (F_{EM,Pf} + F_{S,Pf} - \gamma_{Pf}^2 (A+B)) \tag{B.119}$$

$$C_{Ps}^{v1,J^e} = (\gamma_{Ps}^2 (A+B) - F_{EM,Ps} - F_{S,Ps}) \tag{B.120}$$

$$\breve{G}^{v_1,J_1^e} = C_{Ps}^{v1,J^e} ik_1 ik_1 \breve{G}_{Ps} + C_{Pf}^{v1,J^e} ik_1 ik_1 \breve{G}_{Pf} + C_{S1}^{v1,J^e} ik_1 ik_1 \breve{G}_S + C_{EM1}^{v1,J^e} ik_1 ik_1 \breve{G}_{EM} + C_{S2}^{v1,J^e} \breve{G}_S + C_{EM2}^{v1,J^e} \breve{G}_{EM} \tag{B.121}$$

$$\breve{G}^{v_1,J_3^e} = C_{Ps}^{v1,J^e} ik_1 ik_3 \breve{G}_{Ps} + C_{Pf}^{v1,J^e} ik_1 ik_3 \breve{G}_{Pf} + C_{S1}^{v1,J^e} ik_1 ik_3 \breve{G}_S + C_{EM1}^{v1,J^e} ik_1 ik_3 \breve{G}_{EM} \tag{B.122}$$

B.9 Electric field response to the bulk force

$$F_{Ps} = \zeta \hat{L} \frac{sM\gamma_{Ps}^2 C + \left(\frac{s\eta}{\zeta \hat{k} \varsigma} - M\right)(sC\gamma_{Ps}^2 - s^3 \rho^f) - Cs^3 \rho^E \left(1 + \frac{\hat{\xi}\hat{L}}{\varsigma}\right)}{sG^{fr}\left(\gamma_S^2 - \gamma_{EM}^2\right)\left(\gamma_{Ps}^2 - \gamma_{Pf}^2\right)(C^2 - HM)} \tag{B.123}$$

$$F_{Pf} = \zeta \hat{L} \frac{sM\gamma_{Pf}^2 C + \left(\frac{s\eta}{\zeta \hat{k} \varsigma} - M\right)(sC\gamma_{Pf}^2 - s^3 \rho^f) - Cs^3 \rho^E \left(1 + \frac{\hat{\xi}\hat{L}}{\varsigma}\right)}{sG^{fr}\left(\gamma_S^2 - \gamma_{EM}^2\right)\left(\gamma_{Ps}^2 - \gamma_{Pf}^2\right)(C^2 - HM)} \tag{B.124}$$

$$Z_{Ps} = \zeta \hat{L} s \rho^f \frac{(H - G^{fr})\left(sM\gamma_{Ps}^2 - s^3 \rho^E (1 + \frac{\hat{\xi}\hat{L}}{\varsigma})\right) + \left(sC\gamma_{Ps}^2 - s^3 \rho^f\right)\left(\frac{s^2 \rho^f}{\zeta \varsigma} - C\right)}{G^{fr}\left(\gamma_S^2 - \gamma_{EM}^2\right)\left(\gamma_{Ps}^2 - \gamma_{Pf}^2\right)(C^2 - HM)} \tag{B.125}$$

$$Z_{Pf} = \zeta \hat{L} s \rho^f \frac{(H - G^{fr})\left(sM\gamma_{Pf}^2 - s^3 \rho^E (1 + \frac{\hat{\xi}\hat{L}}{\varsigma})\right) + \left(sC\gamma_{Pf}^2 - s^3 \rho^f\right)\left(\frac{s^2 \rho^f}{\zeta \varsigma} - C\right)}{G^{fr}\left(\gamma_S^2 - \gamma_{EM}^2\right)\left(\gamma_{Ps}^2 - \gamma_{Pf}^2\right)(C^2 - HM)} \tag{B.126}$$

$$C_{S1}^{E1,f1} = C_S^{E1,f3} = \left[F_{Pf} \frac{s^2\rho - \gamma_S^2 G^{fr}}{\gamma_{Pf}^2 - \gamma_S^2} - F_{Ps} \frac{s^2\rho - \gamma_S^2 G^{fr}}{\gamma_{Ps}^2 - \gamma_S^2} + \frac{Z_{Ps}}{\gamma_{Ps}^2 - \gamma_S^2} - \frac{Z_{Pf}}{\gamma_{Pf}^2 - \gamma_S^2} \right] \tag{B.127}$$

$$C_{S2}^{E1,f1} = -\frac{\zeta \hat{L} s^2 \rho^f}{G^{fr}(\gamma_S^2 - \gamma_{EM}^2)} \tag{B.128}$$

$$C_{EM1}^{E1,f1} = C_{EM}^{E1,f3} = + \left[F_{Pf} \frac{\gamma_{EM}^2 G^{fr} - s^2\rho}{\gamma_{Pf}^2 - \gamma_{EM}^2} - F_{Ps} \frac{\gamma_{EM}^2 G^{fr} - s^2\rho}{\gamma_{Ps}^2 - \gamma_{EM}^2} - \frac{Z_{Ps}}{\gamma_{Ps}^2 - \gamma_{EM}^2} + \frac{Z_{Pf}}{\gamma_{Pf}^2 - \gamma_{EM}^2} \right] \tag{B.129}$$

$$C_{EM2}^{E1,f1} = +\frac{\zeta \hat{L} s^2 \rho^f}{G^{fr}(\gamma_S^2 - \gamma_{EM}^2)} \tag{B.130}$$

$$C_{Ps}^{E1,f1} = C_{Ps}^{E1,f3} = + \left[F_{Ps} \frac{s^2\rho - \gamma_S^2 G^{fr}}{\gamma_{Ps}^2 - \gamma_S^2} - \frac{Z_{Ps}}{\gamma_{Ps}^2 - \gamma_S^2} + F_{Ps} \frac{\gamma_{EM}^2 G^{fr} - s^2\rho}{\gamma_{Ps}^2 - \gamma_{EM}^2} + \frac{Z_{Ps}}{\gamma_{Ps}^2 - \gamma_{EM}^2} \right] \tag{B.131}$$

$$C_{Pf}^{E1,f1} = C_{Pf}^{E1,f3} = \left[-F_{Pf} \frac{s^2\rho - \gamma_S^2 G^{fr}}{\gamma_{Pf}^2 - \gamma_S^2} + \frac{Z_{Pf}}{\gamma_{Pf}^2 - \gamma_S^2} - F_{Pf} \frac{\gamma_{EM}^2 G^{fr} - s^2\rho}{\gamma_{Pf}^2 - \gamma_{EM}^2} - \frac{Z_{Pf}}{\gamma_{Pf}^2 - \gamma_{EM}^2} \right] \tag{B.132}$$

$$\begin{aligned} \breve{G}^{E_1,f_1} = {} & C_{S1}^{E1,f1} ik_1 ik_1 \breve{G}_S + C_{S2}^{E1,f1} \breve{G}_S + C_{EM1}^{E1,f1} ik_1 ik_1 \breve{G}_{EM} + C_{EM2}^{E1,f1} \breve{G}_{EM} \\ & + C_{Ps}^{E1,f1} ik_1 ik_1 \breve{G}_{Ps} + C_{Ps}^{E1,f1} ik_1 ik_1 \breve{G}_{Pf} \end{aligned} \tag{B.133}$$

$$\breve{G}^{E_1,f_3} = C_S^{E1,f3} ik_1 ik_3 \breve{G}_S + C_{EM}^{E1,f3} ik_1 ik_3 \breve{G}_{EM} + C_{Ps}^{E1,f3} ik_1 ik_3 \breve{G}_{Ps} + C_{Pf}^{E1,f3} ik_1 ik_3 \breve{G}_{Pf} \tag{B.134}$$

B.10 Electric field response to the fluid force

$$F_{Ps} = \zeta\hat{L}\frac{C(sC\gamma_{Ps}^2 - s^3\rho^f) + \left(\frac{s\eta}{\zeta\hat{k}\varsigma} - M\right)(sH\gamma_{Ps}^2 - s^3\rho)}{sG^{fr}\left(\gamma_S^2 - \gamma_{EM}^2\right)\left(\gamma_{Ps}^2 - \gamma_{Pf}^2\right)(C^2 - HM)} \tag{B.135}$$

$$F_{Pf} = \zeta\hat{L}\frac{C(sC\gamma_{Pf}^2 - s^3\rho^f) + \left(\frac{s\eta}{\zeta\hat{k}\varsigma} - M\right)(sH\gamma_{Pf}^2 - s^3\rho)}{sG^{fr}\left(\gamma_S^2 - \gamma_{EM}^2\right)\left(\gamma_{Ps}^2 - \gamma_{Pf}^2\right)(C^2 - HM)} \tag{B.136}$$

$$Z_{Ps} = \zeta\hat{L}s\rho^f\frac{(H - G^{fr})\left(sC\gamma_{Ps}^2 - s^3\rho^f\right) + \left(\frac{s^2\rho^f}{\zeta\varsigma} - C\right)\left(sH\gamma_{Ps}^2 - s^3\rho\right)}{G^{fr}\left(\gamma_S^2 - \gamma_{EM}^2\right)\left(\gamma_{Ps}^2 - \gamma_{Pf}^2\right)(C^2 - HM)} \tag{B.137}$$

$$Z_{Pf} = \zeta\hat{L}s\rho^f\frac{(H - G^{fr})\left(sC\gamma_{Pf}^2 - s^3\rho^f\right) + \left(\frac{s^2\rho^f}{\zeta\varsigma} - C\right)\left(sH\gamma_{Pf}^2 - s^3\rho\right)}{G^{fr}\left(\gamma_S^2 - \gamma_{EM}^2\right)\left(\gamma_{Ps}^2 - \gamma_{Pf}^2\right)(C^2 - HM)} \tag{B.138}$$

$$C_{S1}^{E1,f^f} = \frac{s^2\rho - \gamma_S^2 G^{fr}}{\gamma_{Ps}^2 - \gamma_S^2}F_{Ps} - \frac{s^2\rho - \gamma_S^2 G^{fr}}{\gamma_{Pf}^2 - \gamma_S^2}F_{Pf} - \frac{Z_{Ps}}{\gamma_{Ps}^2 - \gamma_S^2} + \frac{Z_{Pf}}{\gamma_{Pf}^2 - \gamma_S^2} \tag{B.139}$$

$$C_{S2}^{E1,f^f} = \zeta\hat{L}\frac{s^2\rho - \gamma_S^2 G^{fr}}{G^{fr}(\gamma_S^2 - \gamma_{EM}^2)} \tag{B.140}$$

$$C_{EM1}^{E1,f^f} = \frac{\gamma_{EM}^2 G^{fr} - s^2\rho}{\gamma_{Ps}^2 - \gamma_{EM}^2}F_{Ps} - \frac{\gamma_{EM}^2 G^{fr} - s^2\rho}{\gamma_{Pf}^2 - \gamma_{EM}^2}F_{Pf} + \frac{Z_{Ps}}{\gamma_{Ps}^2 - \gamma_{EM}^2} - \frac{Z_{Pf}}{\gamma_{Pf}^2 - \gamma_{EM}^2} \tag{B.141}$$

$$C_{EM2}^{E1,f^f} = \zeta\hat{L}\frac{\gamma_{EM}^2 G^{fr} - s^2\rho}{G^{fr}(\gamma_S^2 - \gamma_{EM}^2)} \tag{B.142}$$

$$C_{Ps}^{E1,f^f} = -\frac{s^2\rho - \gamma_S^2 G^{fr}}{\gamma_{Ps}^2 - \gamma_S^2}F_{Ps} + \frac{Z_{Ps}}{\gamma_{Ps}^2 - \gamma_S^2} - \frac{\gamma_{EM}^2 G^{fr} - s^2\rho}{\gamma_{Ps}^2 - \gamma_{EM}^2}F_{Ps} - \frac{Z_{Ps}}{\gamma_{Ps}^2 - \gamma_{EM}^2} \tag{B.143}$$

$$C_{Pf}^{E1,f^f} = \frac{s^2\rho - \gamma_S^2 G^{fr}}{\gamma_{Pf}^2 - \gamma_S^2}F_{Pf} - \frac{Z_{Pf}}{\gamma_{Pf}^2 - \gamma_S^2} + \frac{\gamma_{EM}^2 G^{fr} - s^2\rho}{\gamma_{Pf}^2 - \gamma_{EM}^2}F_{Pf} + \frac{Z_{Pf}}{\gamma_{Pf}^2 - \gamma_{EM}^2} \tag{B.144}$$

$$\begin{aligned}\breve{G}^{E1,f_1^f} = {} & C_{S1}^{E1,f^f} ik_1 ik_1 \breve{G}_S + C_{S2}^{E1,f^f}\breve{G}_S + C_{EM1}^{E1,f^f} ik_1 ik_1 \breve{G}_{EM} + C_{EM2}^{E1,f^f}\breve{G}_{EM} \\ & + C_{Ps}^{E1,f^f} ik_1 ik_1 \breve{G}_{Ps} + C_{Pf}^{E1,f^f} ik_1 ik_1 \breve{G}_{Pf}\end{aligned} \tag{B.145}$$

$$\breve{G}^{E1,f_3^f} = C_{S1}^{E1,ff} ik_1 ik_3 \breve{G}_S + C_{EM1}^{E1,ff} ik_1 ik_3 \breve{G}_{EM} + C_{Ps}^{E1,ff} ik_1 ik_3 \breve{G}_{Ps} + C_{Pf}^{E1,ff} ik_1 ik_3 \breve{G}_{Pf} \tag{B.146}$$

B.11 Electric field response to volume injection rate

$$F_{S,Ps} = \zeta\hat{L}\frac{C\left(-s^2\rho^f M\gamma_{Ps}^2 + s^2 C\rho^E(1+\frac{\hat{\xi}\hat{L}}{\varsigma})\gamma_{Ps}^2\right) + \left(\frac{s\eta}{\zeta\hat{k}\varsigma} - M\right)\left(-s^2\rho M\gamma_{Ps}^2 - (C^2-HM)\gamma_{Ps}^2\gamma_S^2 + s^2\rho^f C\gamma_{Ps}^2\right)}{sG^{fr}\left(\gamma_S^2-\gamma_{EM}^2\right)\left(\gamma_{Ps}^2-\gamma_{Pf}^2\right)\left(C^2-HM\right)}$$

$$F_{EM,Ps} = \zeta\hat{L}\frac{C\left(-s^2\rho^f M\gamma_{Ps}^2 + s^2 C\rho^E(1+\frac{\hat{\xi}\hat{L}}{\varsigma})\gamma_{Ps}^2\right) + \left(\frac{s\eta}{\zeta\hat{k}\varsigma} - M\right)\left(-s^2\rho M\gamma_{Ps}^2 - (C^2-HM)\gamma_{Ps}^2\gamma_{EM}^2 + s^2\rho^f C\gamma_{Ps}^2\right)}{sG^{fr}\left(\gamma_S^2-\gamma_{EM}^2\right)\left(\gamma_{Ps}^2-\gamma_{Pf}^2\right)\left(C^2-HM\right)} \tag{B.147}$$

$$F_{S,Pf} = \zeta\hat{L}\frac{C\left(-s^2\rho^f M\gamma_{Pf}^2 + s^2 C\rho^E(1+\frac{\hat{\xi}\hat{L}}{\varsigma})\gamma_{Pf}^2\right) + \left(\frac{s\eta}{\zeta\hat{k}\varsigma} - M\right)\left(-s^2\rho M\gamma_{Pf}^2 - (C^2-HM)\gamma_{Pf}^2\gamma_S^2 + s^2\rho^f C\gamma_{Pf}^2\right)}{sG^{fr}\left(\gamma_S^2-\gamma_{EM}^2\right)\left(\gamma_{Ps}^2-\gamma_{Pf}^2\right)\left(C^2-HM\right)} \tag{B.148}$$

$$F_{EM,Pf} = \zeta\hat{L}\frac{C\left(-s^2\rho^f M\gamma_{Pf}^2 + s^2 C\rho^E(1+\frac{\hat{\xi}\hat{L}}{\varsigma})\gamma_{Pf}^2\right) + \left(\frac{s\eta}{\zeta\hat{k}\varsigma} - M\right)\left(-s^2\rho M\gamma_{Pf}^2 - (C^2-HM)\gamma_{Pf}^2\gamma_{EM}^2 + s^2\rho^f C\gamma_{Pf}^2\right)}{sG^{fr}\left(\gamma_S^2-\gamma_{EM}^2\right)\left(\gamma_{Ps}^2-\gamma_{Pf}^2\right)\left(C^2-HM\right)} \tag{B.149}$$

$$Z_{S,Ps} = \zeta\hat{L}s\rho^f\frac{(H-G^{fr})\left(s^2\rho^f M\gamma_{Ps}^2 - s^2 C\rho^E(1+\frac{\hat{\xi}\hat{L}}{\varsigma})\gamma_{Ps}^2\right) + \left(\frac{s^2\rho^f}{\zeta\varsigma} - C\right)\left(s^2\rho M\gamma_{Ps}^2 + (C^2-HM)\gamma_{Ps}^2\gamma_S^2 - s^2\rho^f C\gamma_{Ps}^2\right)}{G^{fr}\left(\gamma_S^2-\gamma_{EM}^2\right)\left(\gamma_{Ps}^2-\gamma_{Pf}^2\right)\left(C^2-HM\right)} \tag{B.150}$$

$$Z_{EM,Ps} = \zeta\hat{L}s\rho^f\frac{(H-G^{fr})\left(-s^2\rho^f M\gamma_{Ps}^2 + s^2 C\rho^E(1+\frac{\hat{\xi}\hat{L}}{\varsigma})\gamma_{Ps}^2\right) + \left(\frac{s^2\rho^f}{\zeta\varsigma} - C\right)\left(-s^2\rho M\gamma_{Ps}^2 - (C^2-HM)\gamma_{Ps}^2\gamma_{EM}^2 + s^2\rho^f C\gamma_{Ps}^2\right)}{G^{fr}\left(\gamma_S^2-\gamma_{EM}^2\right)\left(\gamma_{Ps}^2-\gamma_{Pf}^2\right)\left(C^2-HM\right)} \tag{B.151}$$

$$Z_{S,Pf} = \zeta\hat{L}s\rho^f\frac{(H-G^{fr})\left(s^2\rho^f M\gamma_{Pf}^2 - s^2 C\rho^E(1+\frac{\hat{\xi}\hat{L}}{\varsigma})\gamma_{Pf}^2\right) + \left(\frac{s^2\rho^f}{\zeta\varsigma} - C\right)\left(s^2\rho M\gamma_{Pf}^2 + (C^2-HM)\gamma_{Pf}^2\gamma_S^2 - s^2\rho^f C\gamma_{Pf}^2\right)}{G^{fr}\left(\gamma_S^2-\gamma_{EM}^2\right)\left(\gamma_{Ps}^2-\gamma_{Pf}^2\right)\left(C^2-HM\right)} \tag{B.152}$$

$$Z_{EM,Pf} = \zeta\hat{L}s\rho^f\frac{(H-G^{fr})\left(-s^2\rho^f M\gamma_{Pf}^2 + s^2 C\rho^E(1+\frac{\hat{\xi}\hat{L}}{\varsigma})\gamma_{Pf}^2\right) + \left(\frac{s^2\rho^f}{\zeta\varsigma} - C\right)\left(-s^2\rho M\gamma_{Pf}^2 - (C^2-HM)\gamma_{Pf}^2\gamma_{EM}^2 + s^2\rho^f C\gamma_{Pf}^2\right)}{G^{fr}\left(\gamma_S^2-\gamma_{EM}^2\right)\left(\gamma_{Ps}^2-\gamma_{Pf}^2\right)\left(C^2-HM\right)} \tag{B.153}$$

$$C_S^{E1,q} = \frac{s^2\rho - \gamma_S^2 G^{fr}}{\gamma_{Ps}^2 - \gamma_S^2} F_{S,Ps} - \frac{s^2\rho - \gamma_S^2 G^{fr}}{\gamma_{Pf}^2 - \gamma_S^2} F_{S,Pf} + \frac{Z_{S,Ps}}{\gamma_{Ps}^2 - \gamma_S^2} - \frac{Z_{S,Pf}}{\gamma_{Pf}^2 - \gamma_S^2} + \frac{\zeta \hat{L} M}{s G^{fr}} \frac{s^2\rho - \gamma_S^2 G^{fr}}{\gamma_S^2 - \gamma_{EM}^2} - \frac{\zeta \hat{L} s \rho^f C}{G^{fr}(\gamma_S^2 - \gamma_{EM}^2)} \quad \text{(B.154)}$$

$$C_{EM}^{E1,q} = \frac{\gamma_{EM}^2 G^{fr} - s^2\rho}{\gamma_{Ps}^2 - \gamma_{EM}^2} F_{EM,Ps} - \frac{\gamma_{EM}^2 G^{fr} - s^2\rho}{\gamma_{Pf}^2 - \gamma_{EM}^2} F_{EM,Pf} + \frac{Z_{EM,Ps}}{\gamma_{Ps}^2 - \gamma_{EM}^2} - \frac{Z_{EM,Pf}}{\gamma_{Pf}^2 - \gamma_{EM}^2} + \frac{\zeta \hat{L} M}{s G^{fr}} \frac{\gamma_{EM}^2 G^{fr} - s^2\rho}{\gamma_S^2 - \gamma_{EM}^2} - \frac{\zeta \hat{L} s \rho^f C}{G^{fr}(\gamma_S^2 - \gamma_{EM}^2)} \quad \text{(B.155)}$$

$$C_{Ps}^{E1,q} = -\frac{s^2\rho - \gamma_S^2 G^{fr}}{\gamma_{Ps}^2 - \gamma_S^2} F_{S,Ps} - \frac{Z_{S,Ps}}{\gamma_{Ps}^2 - \gamma_S^2} - \frac{\gamma_{EM}^2 G^{fr} - s^2\rho}{\gamma_{Ps}^2 - \gamma_{EM}^2} F_{EM,Ps} - \frac{Z_{EM,Ps}}{\gamma_{Ps}^2 - \gamma_{EM}^2} - \zeta \hat{L} \frac{\frac{s\eta}{\zeta \hat{k} \varsigma} - M}{s(\gamma_{Ps}^2 - \gamma_{Pf}^2)} \gamma_{Ps}^2 \quad \text{(B.156)}$$

$$C_{Pf}^{E1,q} = \frac{s^2\rho - \gamma_S^2 G^{fr}}{\gamma_{Pf}^2 - \gamma_S^2} F_{S,Pf} + \frac{Z_{S,Pf}}{\gamma_{Pf}^2 - \gamma_S^2} + \frac{\gamma_{EM}^2 G^{fr} - s^2\rho}{\gamma_{Pf}^2 - \gamma_{EM}^2} F_{EM,Pf} + \frac{Z_{EM,Pf}}{\gamma_{Pf}^2 - \gamma_{EM}^2} + \zeta \hat{L} \frac{\frac{s\eta}{\zeta \hat{k} \varsigma} - M}{s(\gamma_{Ps}^2 - \gamma_{Pf}^2)} \gamma_{Pf}^2 \quad \text{(B.157)}$$

$$\breve{G}^{E1,q} = C_S^{E1,q} i k_1 \breve{G}_S + C_{EM}^{E1,q} i k_1 \breve{G}_{EM} + C_{Ps}^{E1,q} i k_1 \breve{G}_{Ps} + C_{Pf}^{E1,q} i k_1 \breve{G}_{Pf} \quad \text{(B.158)}$$

B.12 Electric field response to a shear strain

$$F_{Ps} = \zeta \hat{L} \frac{C(4MG^{fr}\gamma_{Ps}^2 - 4s^2 G^{fr} \rho^E (\varsigma + \hat{L}\hat{\xi})) + \left(\frac{s\eta}{\zeta \hat{k} \varsigma} - M\right)(4CG^{fr}\gamma_{Ps}^2 - 4s^2 \rho^f G^{fr}}{s G^{fr} \left(\gamma_S^2 - \gamma_{EM}^2\right)\left(\gamma_{Ps}^2 - \gamma_{Pf}^2\right)(C^2 - HM)} \quad \text{(B.159)}$$

$$F_{Pf} = \zeta \hat{L} \frac{C(4MG^{fr}\gamma_{Pf}^2 - 4s^2 G^{fr} \rho^E (\varsigma + \hat{L}\hat{\xi})) + \left(\frac{s\eta}{\zeta \hat{k} \varsigma} - M\right)(4CG^{fr}\gamma_{Pf}^2 - 4s^2 \rho^f G^{fr}}{s G^{fr} \left(\gamma_S^2 - \gamma_{EM}^2\right)\left(\gamma_{Ps}^2 - \gamma_{Pf}^2\right)(C^2 - HM)} \quad \text{(B.160)}$$

$$Z_{Ps} = \zeta\hat{L}s\rho^f \frac{\left(H - G^{fr}\right)(4MG^{fr}\gamma_{Ps}^2 - 4s^2G^{fr}\rho^E(\varsigma + \hat{L}\hat{\xi})) + \left(\frac{s^2\rho^f}{\zeta\varsigma} - C\right)(4CG^{fr}\gamma_{Ps}^2 - 4s^2\rho^f G^{fr}}{G^{fr}\left(\gamma_S^2 - \gamma_{EM}^2\right)\left(\gamma_{Ps}^2 - \gamma_{Pf}^2\right)(C^2 - HM)} \tag{B.161}$$

$$Z_{Pf} = \zeta\hat{L}s\rho^f \frac{\left(H - G^{fr}\right)(4MG^{fr}\gamma_{Pf}^2 - 4s^2G^{fr}\rho^E(\varsigma + \hat{L}\hat{\xi})) + \left(\frac{s^2\rho^f}{\zeta\varsigma} - C\right)(4CG^{fr}\gamma_{Pf}^2 - 4s^2\rho^f G^{fr}}{G^{fr}\left(\gamma_S^2 - \gamma_{EM}^2\right)\left(\gamma_{Ps}^2 - \gamma_{Pf}^2\right)(C^2 - HM)} \tag{B.162}$$

$$C_{S1}^{E1,h13} = -\frac{s^2\rho - \gamma_S^2G^{fr}}{\gamma_{Ps}^2 - \gamma_S^2}F_{Ps} + \frac{s^2\rho - \gamma_S^2G^{fr}}{\gamma_{Pf}^2 - \gamma_S^2}F_{Pf} + \frac{Z_{Ps}}{\gamma_{Ps}^2 - \gamma_S^2} - \frac{Z_{Pf}}{\gamma_{Pf}^2 - \gamma_S^2} \tag{B.163}$$

$$\begin{aligned} C_{EM1}^{E1,h13} = {} & -\frac{\gamma_{EM}^2G^{fr} - s^2\rho}{\gamma_{Ps}^2 - \gamma_{EM}^2}F_{Ps} + \frac{\gamma_{EM}^2G^{fr} - s^2\rho}{\gamma_{Pf}^2 - \gamma_{EM}^2}F_{Pf} - \frac{Z_{Ps}}{\gamma_{Ps}^2 - \gamma_{EM}^2} \\ & + \frac{Z_{Pf}}{\gamma_{Pf}^2 - \gamma_{EM}^2} \end{aligned} \tag{B.164}$$

$$C_{Ps}^{E1,h13} = +\frac{s^2\rho - \gamma_S^2G^{fr}}{\gamma_{Ps}^2 - \gamma_S^2}F_{Ps} - \frac{Z_{Ps}}{\gamma_{Ps}^2 - \gamma_S^2} + \frac{\gamma_{EM}^2 - s^2\rho}{\gamma_{Ps}^2 - \gamma_{EM}^2}F_{Ps} + \frac{Z_{Ps}}{\gamma_{Ps}^2 - \gamma_{EM}^2} \tag{B.165}$$

$$C_{Pf}^{E1,h13} = -\frac{s^2\rho - \gamma_S^2G^{fr}}{\gamma_{Pf}^2 - \gamma_S^2}F_{Pf} + \frac{Z_{Pf}}{\gamma_{Pf}^2 - \gamma_S^2} - \frac{\gamma_{EM}^2 - s^2\rho}{\gamma_{Pf}^2 - \gamma_{EM}^2}F_{Pf} - \frac{Z_{Pf}}{\gamma_{Pf}^2 - \gamma_{EM}^2} \tag{B.166}$$

$$C_{S2}^{E1,h13} = -\frac{\zeta\hat{L}s\rho^f}{\gamma_S^2 - \gamma_{EM}^2} \tag{B.167}$$

$$C_{EM2}^{E1,h13} = \frac{\zeta\hat{L}s\rho^f}{\gamma_S^2 - \gamma_{EM}^2} \tag{B.168}$$

$$\begin{aligned} \breve{G}^{E_1,h_{13}} = {} & C_{S1}^{E1,h13}ik_1ik_1ik_3\breve{G}_S + C_{S2}^{E1,h13}ik_3\breve{G}_S + C_{EM1}^{E1,h13}ik_1ik_1ik_3\breve{G}_{EM} + C_{EM2}^{E1,h13}ik_3\breve{G}_{EM} \\ & + C_{Ps}^{E1,h13}ik_1ik_1ik_3\breve{G}_{Ps} + C_{Pf}^{E1,h13}ik_1ik_1ik_3\breve{G}_{Pf} \end{aligned} \tag{B.169}$$

B.13 Electric field response to a tensile strain source

$$A = \frac{\zeta \hat{L}}{G^{fr}} \frac{1}{(\gamma_S^2 - \gamma_{EM}^2)(\gamma_{Ps}^2 - \gamma_{Pf}^2)(C^2 - HM)}$$

$$F_{S,Ps} = A(-Cs^2\rho^f\gamma_{Ps}^2 + C^2\gamma_{Ps}^2\gamma_S^2 + s^2\rho^E(1 + \frac{\hat{\xi}\hat{L}}{\varsigma})K_G\gamma_{Ps}^2 - MK_G\gamma_S^2\gamma_{Ps}^2)/(\gamma_{Ps}^2 - \gamma_S^2) \tag{B.170}$$

$$Z_{S,Ps} = A(-Cs^2\rho\gamma_{Ps}^2 + CH\gamma_{Ps}^2\gamma_S^2 + s^2\rho^f K_G\gamma_{Ps}^2 - CK_G\gamma_S^2\gamma_{Ps}^2)/(\gamma_{Ps}^2 - \gamma_S^2) \tag{B.171}$$

$$F_{EM,Ps} = A(-Cs^2\rho^f\gamma_{Ps}^2 + C^2\gamma_{Ps}^2\gamma_{EM}^2 + s^2\rho^E(1 + \frac{\hat{\xi}\hat{L}}{\varsigma})K_G\gamma_{Ps}^2 - MK_G\gamma_{EM}^2\gamma_{Ps}^2)/(\gamma_{Ps}^2 - \gamma_{EM}^2) \tag{B.172}$$

$$Z_{EM,Ps} = A(-Cs^2\rho\gamma_{Ps}^2 + CH\gamma_{Ps}^2\gamma_{EM}^2 + s^2\rho^f K_G\gamma_{Ps}^2 - CK_G\gamma_{EM}^2\gamma_{Ps}^2)/(\gamma_{Ps}^2 - \gamma_{EM}^2) \tag{B.173}$$

$$F_{S,Pf} = A(-Cs^2\rho^f\gamma_{Pf}^2 + C^2\gamma_{Pf}^2\gamma_S^2 + s^2\rho^E(1 + \frac{\hat{\xi}\hat{L}}{\varsigma})K_G\gamma_S^2 - MK_G\gamma_S^2\gamma_{Pf}^2)/(\gamma_{Pf}^2 - \gamma_S^2) \tag{B.174}$$

$$Z_{S,Pf} = A(-Cs^2\rho\gamma_{Pf}^2 + CH\gamma_{Pf}^2\gamma_S^2 + s^2\rho^f K_G\gamma_S^2 - CK_G\gamma_S^2\gamma_{Pf}^2)/(\gamma_{Pf}^2 - \gamma_S^2) \tag{B.175}$$

$$F_{EM,Pf} = A(-Cs^2\rho^f\gamma_{Pf}^2 + C^2\gamma_{Pf}^2\gamma_{EM}^2 + s^2\rho^E(1 + \frac{\hat{\xi}\hat{L}}{\varsigma})K_G\gamma_{Pf}^2 - MK_G\gamma_{EM}^2\gamma_{Pf}^2)/(\gamma_{Pf}^2 - \gamma_{EM}^2) \tag{B.176}$$

$$Z_{EM,Pf} = A(-Cs^2\rho\gamma_{Pf}^2 + CH\gamma_{Pf}^2\gamma_{EM}^2 + s^2\rho^f K_G\gamma_{Pf}^2 - CK_G\gamma_{EM}^2\gamma_{Pf}^2)/(\gamma_{Pf}^2 - \gamma_{EM}^2) \tag{B.177}$$

$$Y_{Ps} = \frac{(\gamma_{EM}^2 - \gamma_S^2)G^{fr}}{s} A\left[-C^3\gamma_{Ps}^2 + CMK_G\gamma_{Ps}^2 + \left(\frac{s\eta}{\zeta\hat{k}\varsigma} - M\right)(-CH\gamma_{Ps}^2 + CK_G\gamma_{Ps}^2)\right] \tag{B.178}$$

$$Y_{Pf} = \frac{(\gamma_{EM}^2 - \gamma_S^2)G^{fr}}{s} A\left[-C^3\gamma_{Pf}^2 + CMK_G\gamma_{Pf}^2 + \left(\frac{s\eta}{\zeta\hat{k}\varsigma} - M\right)(-CH\gamma_{Pf}^2 + CK_G\gamma_{Pf}^2)\right] \tag{B.179}$$

Operator on $ik_1\breve{G}_{Ps}$,

$$C_{Ps}^{E1,h11;33} = -\left(\frac{\gamma_{EM}^2 G^{fr} - s^2\rho}{s}C + s\rho^f(H - G^{fr})\right)F_{EM,Ps}$$
$$-\left(\frac{s^2\rho - \gamma_S^2 G^{fr}}{s}C - s\rho^f(H - G^{fr})\right)F_{S,Ps}$$
$$+\left(\frac{s^3(\rho^f)^2}{\zeta\varsigma} - Cs\rho^f - \frac{s^2\rho - \gamma_S^2 G^{fr}}{s}\left(\frac{s\eta}{\zeta\hat{k}\varsigma} - M\right)\right)Z_{S,Ps}$$
$$-\left(\frac{s^3(\rho^f)^2}{\zeta\varsigma} - Cs\rho^f + \frac{\gamma_{EM}^2 G^{fr} - s^2\rho}{s}\left(\frac{s\eta}{\zeta\hat{k}\varsigma} - M\right)\right)Z_{EM,Ps} + Y_{Ps}$$

Operator on $\breve{G}_{Pf}$ (equal to the negative of the $\breve{G}_{Ps}$ operator, and all γ_{Ps}^2 replaced by γ_{Pf}^2),

$$C_{Pf}^{E1,h11;33} = +\left(\frac{\gamma_{EM}^2 G^{fr} - s^2\rho}{s}C + s\rho^f(H - G^{fr})\right)F_{EM,Pf}$$
$$+\left(\frac{s^2\rho - \gamma_S^2 G^{fr}}{s}C - s\rho^f(H - G^{fr})\right)F_{S,Pf}$$
$$-\left(\frac{s^3(\rho^f)^2}{\zeta\varsigma} - Cs\rho^f - \frac{s^2\rho - \gamma_S^2 G^{fr}}{s}\left(\frac{s\eta}{\zeta\hat{k}\varsigma} - M\right)\right)Z_{S,Pf}$$
$$+\left(\frac{s^3(\rho^f)^2}{\zeta\varsigma} - Cs\rho^f + \frac{\gamma_{EM}^2 G^{fr} - s^2\rho}{s}\left(\frac{s\eta}{\zeta\hat{k}\varsigma} - M\right)\right)Z_{EM,Pf} - Y_{Pf}$$

Operators on $\breve{G}_S$,

$$C_{S1}^{E1,h11;33} = +\left(\frac{s^2\rho - \gamma_S^2 G^{fr}}{s}C - s\rho^f(H - G^{fr})\right)F_{S,Ps}$$
$$-\left(\frac{s^3(\rho^f)^2}{\zeta\varsigma} - Cs\rho^f - \frac{s^2\rho - \gamma_S^2 G^{fr}}{s}\left(\frac{s\eta}{\zeta\hat{k}\varsigma} - M\right)\right)Z_{S,Ps}$$
$$-\left(\frac{s^2\rho - \gamma_S^2 G^{fr}}{s}C - s\rho^f(H - G^{fr})\right)F_{S,Pf}$$
$$+\left(\frac{s^3(\rho^f)^2}{\zeta\varsigma} - Cs\rho^f - \frac{s^2\rho - \gamma_S^2 G^{fr}}{s}\left(\frac{s\eta}{\zeta\hat{k}\varsigma} - M\right)\right)Z_{S,Pf}$$

$$C_{S2}^{E1,h11;33} = \frac{\zeta\hat{L}}{sG^{fr}(\gamma_S^2 - \gamma_{EM}^2)}\left(C(s^2\rho - \gamma_S^2 G^{fr}) - s^2\rho^f[H;H - 2G^{fr}]\right) \quad \text{(B.180)}$$

Operator on $ik_1\breve{G}_{EM}$,

$$\begin{aligned} C^{E1,h11;33}_{EM1} = &+ \left(\frac{\gamma^2_{EM} G^{fr} - s^2\rho}{s} C + s\rho^f (H - G^{fr}) \right) F_{EM,Ps} \\ &+ \left(\frac{s^3(\rho^f)^2}{\zeta\varsigma} - Cs\rho^f + \frac{\gamma^2_{EM} G^{fr} - s^2\rho}{s} \left(\frac{s\eta}{\zeta\hat{k}\varsigma} - M \right) \right) Z_{EM,Ps} \\ &- \left(\frac{\gamma^2_{EM} G^{fr} - s^2\rho}{s} C + s\rho^f (H - G^{fr}) \right) F_{EM,Pf} \\ &- \left(\frac{s^3(\rho^f)^2}{\zeta\varsigma} - Cs\rho^f + \frac{\gamma^2_{EM} G^{fr} - s^2\rho}{s} \left(\frac{s\eta}{\zeta\hat{k}\varsigma} - M \right) \right) Z_{EM,Pf} \end{aligned}$$

$$C^{E1,h11;33}_{EM2} \quad = \quad + \frac{\zeta\hat{L}}{sG^{fr}(\gamma^2_S - \gamma^2_{EM})} \left(C(\gamma^2_{EM} G^{fr} - s^2\rho) + s^2\rho^f [H; H - 2G^{fr}] \right) \tag{B.181}$$

Operators on triple spatial derivatives of all greens functions,

$$F_{Ps,k1} = A(MG^{fr}\frac{4}{3}\gamma_{Ps}^2 - s^2\rho^E(1 + \frac{\hat{\xi}\hat{L}}{\varsigma})G^{fr}\frac{4}{3}) \tag{B.182}$$

$$F_{Ps,k3} = A(s^2\rho^E(1 + \frac{\hat{\xi}\hat{L}}{\varsigma})G^{fr}\frac{2}{3} + k_1^2 - MG^{fr}\frac{2}{3}\gamma_{Ps}^2) \tag{B.183}$$

$$F_{Pf,k1} = A(MG^{fr}\frac{4}{3}\gamma_{Pf}^2 - s^2\rho^E(1 + \frac{\hat{\xi}\hat{L}}{\varsigma})G^{fr}\frac{4}{3}) \tag{B.184}$$

$$F_{Pf,k3} = A(s^2\rho^E(1 + \frac{\hat{\xi}\hat{L}}{\varsigma})G^{fr}\frac{2}{3} + k_1^2 - MG^{fr}\frac{2}{3}\gamma_{Pf}^2) \tag{B.185}$$

$$Z_{Ps,k1} = A(CG^{fr}\frac{4}{3}\gamma_{Ps}^2 - s^2\rho^f G^{fr}\frac{4}{3}) \tag{B.186}$$

$$Z_{Ps,k3} = A(s^2\rho^f G^{fr}\frac{2}{3} - CG^{fr}\frac{2}{3}\gamma_{Ps}^2) \tag{B.187}$$

$$Z_{Pf,k1} = A(CG^{fr}\frac{4}{3}\gamma_{Pf}^2 - s^2\rho^f G^{fr}\frac{4}{3}) \tag{B.188}$$

$$Z_{Pf,k3} = A(s^2\rho^f G^{fr}\frac{2}{3} - CG^{fr}\frac{2}{3}\gamma_{Pf}^2) \tag{B.189}$$

Operator on $ik_1^3\breve{G}_{Ps}$,

$$\begin{aligned}
C_{*Ps_k1}^{E1,h11} = &-\left(\frac{\gamma_{EM}^2 G^{fr} - s^2\rho}{s}C + s\rho^f(H - G^{fr})\right)\frac{F_{Ps,k1}}{\gamma_{Ps}^2 - \gamma_{EM}^2} \\
&- \left(\frac{s^2\rho - \gamma_S^2 G^{fr}}{s}C - s\rho^f(H - G^{fr})\right)\frac{F_{Ps,k1}}{\gamma_{Ps}^2 - \gamma_S^2} \\
&+ \left(\frac{s^3(\rho^f)^2}{\zeta\varsigma} - Cs\rho^f - \frac{s^2\rho - \gamma_S^2 G^{fr}}{s}\left(\frac{s\eta}{\zeta\hat{k}\varsigma} - M\right)\right)\frac{Z_{Ps,k1}}{\gamma_{Ps}^2 - \gamma_S^2} \\
&- \left(\frac{s^3(\rho^f)^2}{\zeta\varsigma} - Cs\rho^f + \frac{\gamma_{EM}^2 G^{fr} - s^2\rho}{s}\left(\frac{s\eta}{\zeta\hat{k}\varsigma} - M\right)\right)\frac{Z_{Ps,k1}}{\gamma_{Ps}^2 - \gamma_{EM}^2}
\end{aligned}$$

Operator on $ik_3^2 ik_1 \breve{G}_{Ps}$,

$$C_{*Ps_k3}^{E1,h11} = -\left(\frac{\gamma_{EM}^2 G^{fr} - s^2\rho}{s}C + s\rho^f(H - G^{fr})\right)\frac{F_{Ps,k3}}{\gamma_{Ps}^2 - \gamma_{EM}^2}$$

$$-\left(\frac{s^2\rho - \gamma_S^2 G^{fr}}{s}C - s\rho^f(H - G^{fr})\right)\frac{F_{Ps,k3}}{\gamma_{Ps}^2 - \gamma_S^2}$$

$$+\left(\frac{s^3(\rho^f)^2}{\zeta\varsigma} - Cs\rho^f - \frac{s^2\rho - \gamma_S^2 G^{fr}}{s}\left(\frac{s\eta}{\zeta\hat{k}\varsigma} - M\right)\right)\frac{Z_{Ps,k3}}{\gamma_{Ps}^2 - \gamma_S^2}$$

$$-\left(\frac{s^3(\rho^f)^2}{\zeta\varsigma} - Cs\rho^f + \frac{\gamma_{EM}^2 G^{fr} - s^2\rho}{s}\left(\frac{s\eta}{\zeta\hat{k}\varsigma} - M\right)\right)\frac{Z_{Ps,k3}}{\gamma_{Ps}^2 - \gamma_{EM}^2}$$

Operator on $ik_1^3 \breve{G}_{Pf}$,

$$C_{*Pf_k1}^{E1,h11} = +\left(\frac{\gamma_{EM}^2 G^{fr} - s^2\rho}{s}C + s\rho^f(H - G^{fr})\right)\frac{F_{Pf,k1}}{\gamma_{Pf}^2 - \gamma_{EM}^2}$$

$$+\left(\frac{s^2\rho - \gamma_S^2 G^{fr}}{s}C - s\rho^f(H - G^{fr})\right)\frac{F_{Pf,k1}}{\gamma_{Pf}^2 - \gamma_S^2}$$

$$-\left(\frac{s^3(\rho^f)^2}{\zeta\varsigma} - Cs\rho^f - \frac{s^2\rho - \gamma_S^2 G^{fr}}{s}\left(\frac{s\eta}{\zeta\hat{k}\varsigma} - M\right)\right)\frac{Z_{Pf,k1}}{\gamma_{Pf}^2 - \gamma_S^2}$$

$$+\left(\frac{s^3(\rho^f)^2}{\zeta\varsigma} - Cs\rho^f + \frac{\gamma_{EM}^2 G^{fr} - s^2\rho}{s}\left(\frac{s\eta}{\zeta\hat{k}\varsigma} - M\right)\right)\frac{Z_{Pf,k1}}{\gamma_{Pf}^2 - \gamma_{EM}^2}$$

Operator on $ik_3^2 ik_1 \breve{G}_{Pf}$,

$$C^{E1,h11}_{*Pf_k3} = + \left(\frac{\gamma_{EM}^2 G^{fr} - s^2\rho}{s} C + s\rho^f (H - G^{fr}) \right) \frac{F_{Pf,k3}}{\gamma_{Pf}^2 - \gamma_{EM}^2}$$

$$+ \left(\frac{s^2\rho - \gamma_S^2 G^{fr}}{s} C - s\rho^f (H - G^{fr}) \right) \frac{F_{Pf,k3}}{\gamma_{Pf}^2 - \gamma_S^2}$$

$$- \left(\frac{s^3(\rho^f)^2}{\zeta\varsigma} - Cs\rho^f - \frac{s^2\rho - \gamma_S^2 G^{fr}}{s} \left(\frac{s\eta}{\zeta\hat{k}\varsigma} - M \right) \right) \frac{Z_{Pf,k3}}{\gamma_{Pf}^2 - \gamma_S^2}$$

$$+ \left(\frac{s^3(\rho^f)^2}{\zeta\varsigma} - Cs\rho^f + \frac{\gamma_{EM}^2 G^{fr} - s^2\rho}{s} \left(\frac{s\eta}{\zeta\hat{k}\varsigma} - M \right) \right) \frac{Z_{Pf,k3}}{\gamma_{Pf}^2 - \gamma_{EM}^2}$$

Operator on $ik_1^3 \breve{G}_S$,

$$C^{E1,h11}_{*SV_k1} =$$

$$+ \left(\frac{s^2\rho - \gamma_S^2 G^{fr}}{s} C - s\rho^f (H - G^{fr}) \right) \frac{F_{Ps,k1}}{\gamma_{Ps}^2 - \gamma_S^2}$$

$$- \left(\frac{s^3(\rho^f)^2}{\zeta\varsigma} - Cs\rho^f - \frac{s^2\rho - \gamma_S^2 G^{fr}}{s} \left(\frac{s\eta}{\zeta\hat{k}\varsigma} - M \right) \right) \frac{Z_{Ps,k1}}{\gamma_{Ps}^2 - \gamma_S^2}$$

$$- \left(\frac{s^2\rho - \gamma_S^2 G^{fr}}{s} C - s\rho^f (H - G^{fr}) \right) \frac{F_{Pf,k1}}{\gamma_{Pf}^2 - \gamma_S^2}$$

$$+ \left(\frac{s^3(\rho^f)^2}{\zeta\varsigma} - Cs\rho^f - \frac{s^2\rho - \gamma_S^2 G^{fr}}{s} \left(\frac{s\eta}{\zeta\hat{k}\varsigma} - M \right) \right) \frac{Z_{Pf,k1}}{\gamma_{Pf}^2 - \gamma_S^2}$$

Operator on $ik_3^2 ik_1 \breve{G}_S$,

$$C^{E1,h11}_{*SV_k3} =$$

$$+\left(\frac{s^2\rho-\gamma_S^2 G^{fr}}{s}C - s\rho^f(H-G^{fr})\right)\frac{F_{Ps,k3}}{\gamma_{Ps}^2-\gamma_S^2}$$

$$-\left(\frac{s^3(\rho^f)^2}{\zeta\varsigma} - Cs\rho^f - \frac{s^2\rho-\gamma_S^2 G^{fr}}{s}\left(\frac{s\eta}{\zeta\hat{k}\varsigma}-M\right)\right)\frac{Z_{Ps,k3}}{\gamma_{Ps}^2-\gamma_S^2}$$

$$-\left(\frac{s^2\rho-\gamma_S^2 G^{fr}}{s}C - s\rho^f(H-G^{fr})\right)\frac{F_{Pf,k3}}{\gamma_{Pf}^2-\gamma_S^2}$$

$$+\left(\frac{s^3(\rho^f)^2}{\zeta\varsigma} - Cs\rho^f - \frac{s^2\rho-\gamma_S^2 G^{fr}}{s}\left(\frac{s\eta}{\zeta\hat{k}\varsigma}-M\right)\right)\frac{Z_{Pf,k3}}{\gamma_{Pf}^2-\gamma_S^2}$$

Operator on $ik_1^3 \breve{G}_{EM}$,

$$C^{E1,h11}_{*EM_k1} =$$

$$+\left(\frac{\gamma_{EM}^2 G^{fr}-s^2\rho}{s}C + s\rho^f(H-G^{fr})\right)\frac{F_{Ps,k1}}{\gamma_{Ps}^2-\gamma_{EM}^2}$$

$$+\left(\frac{s^3(\rho^f)^2}{\zeta\varsigma} - Cs\rho^f + \frac{\gamma_{EM}^2 G^{fr}-s^2\rho}{s}\left(\frac{s\eta}{\zeta\hat{k}\varsigma}-M\right)\right)\frac{Z_{Ps,k1}}{\gamma_{Ps}^2-\gamma_{EM}^2}$$

$$-\left(\frac{\gamma_{EM}^2 G^{fr}-s^2\rho}{s}C + s\rho^f(H-G^{fr})\right)\frac{F_{Pf,k1}}{\gamma_{Pf}^2-\gamma_{EM}^2}$$

$$-\left(\frac{s^3(\rho^f)^2}{\zeta\varsigma} - Cs\rho^f + \frac{\gamma_{EM}^2 G^{fr}-s^2\rho}{s}\left(\frac{s\eta}{\zeta\hat{k}\varsigma}-M\right)\right)\frac{Z_{Pf,k1}}{\gamma_{Pf}^2-\gamma_{EM}^2}$$

Operator on $ik_3^2 ik_1 \breve{G}_{EM}$,

$$C^{E1,h11}_{*EM_k3} =$$

$$+\left(\frac{\gamma_{EM}^2 G^{fr} - s^2\rho}{s} C + s\rho^f (H - G^{fr})\right) \frac{F_{Ps,k3}}{\gamma_{Ps}^2 - \gamma_{EM}^2}$$

$$+\left(\frac{s^3(\rho^f)^2}{\zeta\varsigma} - Cs\rho^f + \frac{\gamma_{EM}^2 G^{fr} - s^2\rho}{s}\left(\frac{s\eta}{\zeta\hat{k}\varsigma} - M\right)\right) \frac{Z_{Ps,k3}}{\gamma_{Ps}^2 - \gamma_{EM}^2}$$

$$-\left(\frac{\gamma_{EM}^2 G^{fr} - s^2\rho}{s} C + s\rho^f (H - G^{fr})\right) \frac{F_{Pf,k3}}{\gamma_{Pf}^2 - \gamma_{EM}^2}$$

$$-\left(\frac{s^3(\rho^f)^2}{\zeta\varsigma} - Cs\rho^f + \frac{\gamma_{EM}^2 G^{fr} - s^2\rho}{s}\left(\frac{s\eta}{\zeta\hat{k}\varsigma} - M\right)\right) \frac{Z_{Pf,k3}}{\gamma_{Pf}^2 - \gamma_{EM}^2}$$

$$\begin{aligned}
\breve{G}^{E1,h11} = {} & C^{E1,h11}_{Ps} ik_1 \breve{G}_{Ps} + C^{E1,h11}_{Pf} ik_1 \breve{G}_{Pf} + C^{E1,h11}_{SV} ik_1 \breve{G}_{S} + C^{E1,h11}_{EM} ik_1 \breve{G}_{EM} \\
& + C^{E1}_{*Ps_k1} ik_1 ik_1 ik_1 \breve{G}_{Ps} + C^{E1}_{*Ps_k3} ik_3 ik_3 ik_1 \breve{G}_{Ps} \\
& + C^{E1}_{*Pf_k1} ik_1 ik_1 ik_1 \breve{G}_{Pf} + C^{E1}_{*Pf_k3} ik_3 ik_3 ik_1 \breve{G}_{Pf} \\
& + C^{E1}_{*SV_k1} ik_1 ik_1 ik_1 \breve{G}_{SV} + C^{E1}_{*SV_k3} ik_3 ik_3 ik_1 \breve{G}_{SV} \\
& + C^{E1}_{*EM_k1} ik_1 ik_1 ik_1 \breve{G}_{EM} + C^{E1}_{*EM_k3} ik_3 ik_3 ik_1 \breve{G}_{EM}
\end{aligned}$$

For the operators on the shear terms in the h_{33} source greens function, the double k terms simply have to be switched, the rest stays the same.

$$\begin{aligned}
\breve{G}^{E1,h33} = {} & C^{E1,h11}_{Ps} ik_1 \breve{G}_{Ps} + C^{E1,h11}_{Pf} ik_1 \breve{G}_{Pf} + C^{E1,h11}_{SV} ik_1 \breve{G}_{S} + C^{E1,h11}_{EM} ik_1 \breve{G}_{EM} \\
& + C^{E1}_{*Ps_k3} ik_1 ik_1 ik_1 \breve{G}_{Ps} + C^{E1}_{*Ps_k1} ik_3 ik_3 ik_1 \breve{G}_{Ps} \\
& + C^{E1}_{*Pf_k3} ik_1 ik_1 ik_1 \breve{G}_{Pf} + C^{E1}_{*Pf_k1} ik_3 ik_3 ik_1 \breve{G}_{Pf} \\
& + C^{E1}_{*SV_k3} ik_1 ik_1 ik_1 \breve{G}_{SV} + C^{E1}_{*SV_k1} ik_3 ik_3 ik_1 \breve{G}_{SV} \\
& + C^{E1}_{*EM_k3} ik_1 ik_1 ik_1 \breve{G}_{EM} + C^{E1}_{*EM_k1} ik_3 ik_3 ik_1 \breve{G}_{EM}
\end{aligned}$$

B.14 Electric field response to an electric dipole

$$A = \frac{\zeta \hat{L}}{G^{fr}} \frac{1}{(\gamma_S^2 - \gamma_{EM}^2)(\gamma_{Ps}^2 - \gamma_{Pf}^2)(C^2 - HM)} \tag{B.190}$$

$$B_{S1} = \frac{s^2\rho - \gamma_S^2 G^{fr}}{s} \tag{B.191}$$

$$B_{S2} = B_{EM2} = s\rho^f \tag{B.192}$$

$$B_{EM1} = \frac{\gamma_{EM}^2 G^{fr} - s^2\rho}{s} \tag{B.193}$$

$$\begin{aligned}
F_{S,Ps} = (&-\frac{s^3\rho^f\eta}{\hat{\xi}\hat{k}} + \frac{s^2\rho^f M + s\eta C/\hat{k}}{\hat{\xi}}\gamma_{Ps}^2 - CM\gamma_{Ps}^2\gamma_S^2 + \frac{s^4\rho^E(1+\frac{\hat{\xi}\hat{L})}{\varsigma})\rho^f}{\xi} \\
&- \frac{s^2C\rho^E(1+\frac{\hat{\xi}\hat{L})}{\varsigma}) + s^2M\rho^f}{\xi}\gamma_{Ps}^2 + \frac{CM}{\xi}\gamma_{Ps}^2\gamma_S^2)A\,(CB_{S1} - (H-G)B_{S2}) \\
&+ (-\frac{s^3\rho\eta}{\hat{\xi}\hat{k}} + \frac{s^2\rho M + s\eta H/\hat{k}}{\hat{\xi}}\gamma_{Ps}^2 - \frac{MH}{\hat{\xi}}\gamma_{Ps}^2\gamma_S^2 \\
&+ \frac{(s^2\rho^f)^2}{\hat{\xi}} - \frac{2s^2\rho^f C}{\hat{\xi}}\gamma_{Ps}^2 + \frac{C^2}{\hat{\xi}}\gamma_{Ps}^2\gamma_S^2)A\left((\frac{s\eta}{\zeta\hat{k}\varsigma} - M)B_{S1} - (\frac{s^2\rho^f}{\zeta\varsigma} - C)B_{S2}\right)
\end{aligned}$$

$$\begin{aligned}
F_{S,Pf} = (&-\frac{s^3\rho^f\eta}{\hat{\xi}\hat{k}} + \frac{s^2\rho^f M + s\eta C/\hat{k}}{\xi}\gamma_{Pf}^2 - CM\gamma_{Pf}^2\gamma_S^2 + \frac{s^4\rho^E(1+\frac{\hat{\xi}\hat{L})}{\varsigma})\rho^f}{\xi} \\
&- \frac{s^2C\rho^E(1+\frac{\hat{\xi}\hat{L})}{\varsigma}) + s^2M\rho^f}{\xi}\gamma_{Pf}^2 + \frac{CM}{\xi}\gamma_{Pf}^2\gamma_S^2)A\,(CB_{S1} - (H-G)B_{S2}) \\
&+ (-\frac{s^3\rho\eta}{\hat{\xi}\hat{k}} + \frac{s^2\rho M + s\eta H/\hat{k}}{\hat{\xi}}\gamma_{Pf}^2 - \frac{MH}{\hat{\xi}}\gamma_{Pf}^2\gamma_S^2 \\
&+ \frac{(s^2\rho^f)^2}{\hat{\xi}} - \frac{2s^2\rho^f C}{\hat{\xi}}\gamma_{Pf}^2 + \frac{C^2}{\hat{\xi}}\gamma_{Pf}^2\gamma_S^2)A\left((\frac{s\eta}{\zeta\hat{k}\varsigma} - M)B_{S1} - (\frac{s^2\rho^f}{\zeta\varsigma} - C)B_{S2}\right)
\end{aligned}$$

$$F_{EM,Ps} = (-\frac{s^3\rho^f\eta}{\hat{\xi}\hat{k}} + \frac{s^2\rho^f M + s\eta C/\hat{k}}{\hat{\xi}}\gamma_{Ps}^2 - CM\gamma_{Ps}^2\gamma_{EM}^2 + \frac{s^4\rho^E(1+\frac{\hat{\xi}\hat{L})}{\varsigma})\rho^f}{\xi}$$

$$-\frac{s^2C\rho^E(1+\frac{\hat{\xi}\hat{L})}{\varsigma}) + s^2M\rho^f}{\xi}\gamma_{Ps}^2 + \frac{CM}{\xi}\gamma_{Ps}^2\gamma_S^2)A\,(CB_{EM1} + (H-G)B_{EM2})$$

$$+(-\frac{s^3\rho\eta}{\hat{\xi}\hat{k}} + \frac{s^2\rho M + s\eta H/\hat{k}}{\hat{\xi}}\gamma_{Ps}^2 - \frac{MH}{\hat{\xi}}\gamma_{Ps}^2\gamma_{EM}^2$$

$$+\frac{(s^2\rho^f)^2}{\hat{\xi}} - \frac{2s^2\rho^f C}{\hat{\xi}}\gamma_{Ps}^2 + \frac{C^2}{\hat{\xi}}\gamma_{Ps}^2\gamma_{EM}^2)A\left((\frac{s\eta}{\zeta\hat{k}\varsigma} - M)B_{EM1} + (\frac{s^2\rho^f}{\zeta\varsigma} - C)B_{EM2}\right)$$

$$F_{EM,Pf} = (-\frac{s^3\rho^f\eta}{\hat{\xi}\hat{k}} + \frac{s^2\rho^f M + s\eta C/\hat{k}}{\xi}\gamma_{Pf}^2 - CM\gamma_{Pf}^2\gamma_{EM}^2 + \frac{s^4\rho^E(1+\frac{\hat{\xi}\hat{L})}{\varsigma})\rho^f}{\xi}$$

$$-\frac{s^2C\rho^E(1+\frac{\hat{\xi}\hat{L})}{\varsigma}) + s^2M\rho^f}{\xi}\gamma_{Pf}^2 + \frac{CM}{\xi}\gamma_{Pf}^2\gamma_S^2)A\,(CB_{EM1} + (H-G)B_{EM2})$$

$$+(-\frac{s^3\rho\eta}{\hat{\xi}\hat{k}} + \frac{s^2\rho M + s\eta H/\hat{k}}{\hat{\xi}}\gamma_{Pf}^2 - \frac{MH}{\hat{\xi}}\gamma_{Pf}^2\gamma_{EM}^2$$

$$+\frac{(s^2\rho^f)^2}{\hat{\xi}} - \frac{2s^2\rho^f C}{\hat{\xi}}\gamma_{Pf}^2 + \frac{C^2}{\hat{\xi}}\gamma_{Pf}^2\gamma_{EM}^2)A\left((\frac{s\eta}{\zeta\hat{k}\varsigma} - M)B_{EM1} + (\frac{s^2\rho^f}{\zeta\varsigma} - C)B_{EM2}\right)$$

$$Y = \frac{\zeta\hat{L}}{sG^{fr}\xi}\frac{1}{\gamma_S^2 - \gamma_{EM}^2} \tag{B.194}$$

$$C_{S1}^{E1,Je} = \frac{F_{S,Ps}}{\gamma_{Ps}^2 - \gamma_S^2} + \frac{F_{S,Pf}}{\gamma_{Pf}^2 - \gamma_S^2} - Y(s^2\rho - \gamma_S^2 G^{fr} - s\rho^f \frac{C}{M})M \tag{B.195}$$

$$C_{S2}^{E1,J1e} = Y(s^2\rho - \gamma_S^2 G^{fr})\frac{s\eta}{\hat{k}} - Ys^3(\rho^f)^2 \tag{B.196}$$

$$C_{EM1}^{E1,Je} = \frac{F_{EM,Ps}}{\gamma_{Ps}^2 - \gamma_{EM}^2} + \frac{F_{EM,Pf}}{\gamma_{Pf}^2 - \gamma_{EM}^2} - Y(\gamma_{EM}^2 G^{fr} - s^2\rho + s\rho^f \frac{C}{M})M \tag{B.197}$$

$$C_{EM2}^{E1,J1e} = +Y(\gamma_{EM}^2 G^{fr} - s^2\rho)\frac{s\eta}{\hat{k}} + Ys^3(\rho^f)^2 \tag{B.198}$$

$$\begin{aligned} C_{Ps}^{E1,Je} = & -\frac{F_{S,Ps}}{\gamma_{Ps}^2 - \gamma_S^2} - \frac{F_{EM,Ps}}{\gamma_{Ps}^2 - \gamma_{EM}^2} + A\gamma_{Ps}^2 \frac{C^2 M\xi - C^2 M}{\xi} \frac{(\gamma_{EM}^2 - \gamma_S^2)G^{fr}}{s} \\ & + A\gamma_{Pf}^2 \frac{MH - C^2}{\xi}(\frac{s\eta}{\zeta\hat{k}\varsigma} - M)\frac{(\gamma_{EM}^2 - \gamma_S^2)G^{fr}}{s} \end{aligned} \tag{B.199}$$

$$\begin{aligned} C_{Pf}^{E1,Je} = & -\frac{F_{S,Pf}}{\gamma_{Pf}^2 - \gamma_S^2} - \frac{F_{EM,Pf}}{\gamma_{Pf}^2 - \gamma_{EM}^2} - A\gamma_{Pf}^2 \frac{C^2 M\xi - C^2 M}{\xi} \frac{(\gamma_{EM}^2 - \gamma_S^2)G^{fr}}{s} \\ & - A\gamma_{Pf}^2 \frac{MH - C^2}{\xi}(\frac{s\eta}{\zeta\hat{k}\varsigma} - M)\frac{(\gamma_{EM}^2 - \gamma_S^2)G^{fr}}{s} \end{aligned} \tag{B.200}$$

$$\begin{aligned} \breve{G}^{E_1,J_1^e} = & C_{S1}^{E1,Je} ik_1 ik_1 \breve{G}_{SV} + C_{S2}^{E1,J1e}\breve{G}_{SV} + C_{EM1}^{E1,Je} ik_1 ik_1 \breve{G}_{EM} \\ & + C_{EM2}^{E1,J1e}\breve{G}_{EM} + C_{Ps}^{E1,Je} ik_1 ik_1 \breve{G}_{Ps} + C_{Pf}^{E1,Je} ik_1 ik_1 \breve{G}_{Pf} \end{aligned} \tag{B.201}$$

$$\breve{G}^{E_1,J_3^e} = C_{S1}^{E1,Je} ik_1 ik_3 \breve{G}_{SV} + C_{EM1}^{E1,Je} ik_1 ik_3 \breve{G}_{EM} + C_{Ps}^{E1,Je} ik_1 ik_3 \breve{G}_{Ps} + C_{Pf}^{E1,Je} ik_1 ik_3 \breve{G}_{Pf} \tag{B.202}$$

Appendix C

Derivation of the interferometry relation

C.1 Derivation of the first order differential matrix equation for the 2D P-SV-TM mode

In this Appendix the first order equations will be written in the following general form of a matrix vector differential equation,

$$s\bar{A}_{ij}\hat{u}_j + \bar{B}_{ij}\hat{u}_j + C_{ik}D_{x,kj}\hat{u}_j = \hat{\bar{s}}_i \tag{C.1}$$

First of all, the grouped medium parameters are substituted back into the first order basic equations, described in Chapter 1. Now, unfortunately it is not possible to substitute the filtration velocity term in Maxwell's equations by the fluid phase equations of motion, which would eliminate the latter. This would be possible for SH-TE mode, but in this case there is another coupling to the P wave, via the filtration velocity. Therefore we would have to substitute for the filtration velocity also in the deformation equations, as well as the solid phase equations of motion, which would result in second order equations, which is not wanted for this purpose.

$$\varsigma = \hat{\sigma}^e + s\varepsilon - \hat{L}\hat{\xi} \tag{C.2}$$

$$\zeta = \hat{\sigma}^m + s\mu \tag{C.3}$$

$$\hat{\xi} = \eta\hat{L}/\hat{k} \tag{C.4}$$

The first order system of equations for the 2D P-SV-TM mode,

$$
\begin{aligned}
s\varepsilon\hat{E}_1 + \hat{\sigma}^e\hat{E}_1 - \frac{\eta\mathcal{L}_0}{\hat{k}}\mathcal{L}_0\hat{E}_1 + \frac{\eta\mathcal{L}_0}{\hat{k}}\hat{w}_1 + \partial_3\hat{H}_2 &= -\hat{J}_1^e, \\
s\varepsilon\hat{E}_3 + \hat{\sigma}^e\hat{E}_3 - \frac{\eta\mathcal{L}_0}{\hat{k}}\mathcal{L}_0\hat{E}_3 + \frac{\eta\mathcal{L}_0}{\hat{k}}\hat{w}_3 - \partial_1\hat{H}_2 &= -\hat{J}_3^e, \\
s\mu\hat{H}_2 + \hat{\sigma}^m\hat{H}_2 + \partial_3\hat{E}_1 - \partial_1\hat{E}_3 &= -\hat{J}_2^m, \\
s\rho\hat{v}_1 + s\rho^{(f)}\hat{w}_1 - \partial_1\tau_{11} - \partial_3\tau_{31} &= \hat{f}_1, \\
s\rho\hat{v}_3 + s\rho^{(f)}\hat{w}_3 - \partial_3\tau_{33} - \partial_1\tau_{31} &= \hat{f}_3, \\
-s\tau_{11} + S_{1111}\partial_1\hat{v}_1 + S_{1133}\partial_3\hat{v}_3 + C\left(\partial_1\hat{w}_1 + \partial_3\hat{w}_3\right) &= S_{1111}\hat{h}_{11} + S_{1133}\hat{h}_{33} + C\hat{q}, \\
-s\tau_{33} + S_{3333}\partial_3\hat{v}_3 + S_{3311}\partial_1\hat{v}_1 + C\left(\partial_1\hat{w}_1 + \partial_3\hat{w}_3\right) &= S_{3333}\hat{h}_{33} + S_{3311}\hat{h}_{11} + C\hat{q}, \\
-s\tau_{31} + S_{3131}\left(\partial_1\hat{v}_3 + \partial_3\hat{v}_1\right) &= 2S_{3131}\hat{h}_{31}, \\
s\rho^{(f)}\hat{v}_1 - \frac{\eta}{\hat{k}}\hat{E}_1 + \frac{\eta}{\hat{k}}\hat{w}_1 + \partial_1\hat{p} &= \hat{f}_1^{(f)}, \\
s\rho^{(f)}\hat{v}_3 - \frac{\eta}{\hat{k}}\hat{L}\hat{E}_3 + \frac{\eta}{\hat{k}}\hat{w}_3 + \partial_3\hat{p} &= \hat{f}_3^{(f)}, \\
s\hat{p} + C\left(\partial_1\hat{v}_1 + \partial_3\hat{v}_3\right) + M\left(\partial_1\hat{w}_1 + \partial_3\hat{w}_3\right) &= C\left(\hat{h}_{11} + \hat{h}_{33}\right) + M\hat{q},
\end{aligned}
$$

$$
\bar{u} = \begin{pmatrix} \hat{E}_1 \\ \hat{E}_3 \\ \hat{H}_2 \\ \hat{v}_1 \\ \hat{v}_3 \\ -\hat{\tau}_{11} \\ -\hat{\tau}_{33} \\ -\hat{\tau}_{31} \\ \hat{w}_1 \\ \hat{w}_3 \\ \hat{p} \end{pmatrix} \tag{C.6}
$$

$$
\bar{s} = \begin{pmatrix} -\hat{J}_1^e \\ -\hat{J}_3^e \\ -\hat{J}_2^m \\ \hat{f}_1 \\ \hat{f}_3 \\ (K_G + \frac{4}{3}G^{(fr)})\hat{h}_{11} + (K_G - \frac{2}{3}G^{(fr)})\hat{h}_{33} + C\hat{q} \\ (K_G + \frac{4}{3}G^{(fr)})\hat{h}_{11} + (K_G - \frac{2}{3}G^{(fr)})\hat{h}_{33} + C\hat{q} \\ 2G^{(fr)}\hat{h}_{31} \\ \hat{f}_1^{(f)} \\ \hat{f}_3^{(f)} \\ C\left(\hat{h}_{11} + \hat{h}_{33}\right) + M\hat{q} \end{pmatrix} \tag{C.7}
$$

$$\bar{A} = \begin{bmatrix} \varepsilon & 0 & 0 & 0 & 0 & 0 & 0 & 0 & 0 & 0 & 0 \\ 0 & \varepsilon & 0 & 0 & 0 & 0 & 0 & 0 & 0 & 0 & 0 \\ 0 & 0 & \mu & 0 & 0 & 0 & 0 & 0 & 0 & 0 & 0 \\ 0 & 0 & 0 & \rho & 0 & 0 & 0 & 0 & \rho^{(f)} & 0 & 0 \\ 0 & 0 & 0 & 0 & \rho & 0 & 0 & 0 & 0 & \rho^{(f)} & 0 \\ 0 & 0 & 0 & 0 & 0 & 1 & 0 & 0 & 0 & 0 & 0 \\ 0 & 0 & 0 & 0 & 0 & 0 & 1 & 0 & 0 & 0 & 0 \\ 0 & 0 & 0 & 0 & 0 & 0 & 0 & 1 & 0 & 0 & 0 \\ 0 & 0 & 0 & \rho^{(f)} & 0 & 0 & 0 & 0 & 0 & 0 & 0 \\ 0 & 0 & 0 & 0 & \rho^{(f)} & 0 & 0 & 0 & 0 & 0 & 0 \\ 0 & 0 & 0 & 0 & 0 & 0 & 0 & 0 & 0 & 0 & 1 \end{bmatrix} \tag{C.8}$$

$$\bar{B} = \begin{bmatrix} \hat{\sigma}^e - \frac{\eta\hat{L}^2}{\hat{k}} & 0 & 0 & 0 & 0 & 0 & 0 & 0 & \frac{\eta\hat{L}}{\hat{k}} & 0 & 0 \\ 0 & \hat{\sigma}^e - \frac{\eta\hat{L}^2}{\hat{k}} & 0 & 0 & 0 & 0 & 0 & 0 & 0 & \frac{\eta\hat{L}}{\hat{k}} & 0 \\ 0 & 0 & \hat{\sigma}^m & 0 & 0 & 0 & 0 & 0 & 0 & 0 & 0 \\ 0 & 0 & 0 & 0 & 0 & 0 & 0 & 0 & 0 & 0 & 0 \\ 0 & 0 & 0 & 0 & 0 & 0 & 0 & 0 & 0 & 0 & 0 \\ 0 & 0 & 0 & 0 & 0 & 0 & 0 & 0 & 0 & 0 & 0 \\ 0 & 0 & 0 & 0 & 0 & 0 & 0 & 0 & 0 & 0 & 0 \\ 0 & 0 & 0 & 0 & 0 & 0 & 0 & 0 & 0 & 0 & 0 \\ -\frac{\eta\hat{L}}{\hat{k}} & 0 & 0 & 0 & 0 & 0 & 0 & 0 & \frac{\eta}{\hat{k}} & 0 & 0 \\ 0 & -\frac{\eta\hat{L}}{\hat{k}} & 0 & 0 & 0 & 0 & 0 & 0 & 0 & \frac{\eta}{\hat{k}} & 0 \\ 0 & 0 & 0 & 0 & 0 & 0 & 0 & 0 & 0 & 0 & 0 \end{bmatrix} \tag{C.9}$$

$$\bar{B} = \begin{bmatrix} \bar{B}_{11} & \mathbf{O} & \bar{B}_{13} \\ \mathbf{O} & \mathbf{O} & \mathbf{O} \\ -\bar{B}_{13}^T & \mathbf{O} & \bar{B}_{33} \end{bmatrix} \tag{C.10a}$$

$$\bar{B}_{11} = \begin{bmatrix} \hat{\sigma}^e - \frac{\eta\hat{L}^2}{\hat{k}} & 0 & 0 \\ 0 & \hat{\sigma}^e - \frac{\eta\hat{L}^2}{\hat{k}} & 0 \\ 0 & 0 & \hat{\sigma}^m \end{bmatrix} \tag{C.10b}$$

$$\bar{B}_{13} = \begin{bmatrix} \frac{\eta\hat{L}}{\hat{k}} & 0 & 0 \\ 0 & \frac{\eta\hat{L}}{\hat{k}} & 0 \\ 0 & 0 & 0 \end{bmatrix} \tag{C.10c}$$

$$\bar{B}_{33} = \begin{bmatrix} \frac{\eta}{\hat{k}} & 0 & 0 \\ 0 & \frac{\eta}{\hat{k}} & 0 \\ 0 & 0 & 0 \end{bmatrix} \tag{C.10d}$$

The stiffness tensor parameters of the porous solid, S_{ijkl}, are substituted for and matrix C is written as follows,

$$
C = \begin{bmatrix}
1 & 0 & 0 & 0 & 0 & 0 & 0 & 0 & 0 & 0 & 0 \\
0 & 1 & 0 & 0 & 0 & 0 & 0 & 0 & 0 & 0 & 0 \\
0 & 0 & 1 & 0 & 0 & 0 & 0 & 0 & 0 & 0 & 0 \\
0 & 0 & 0 & 1 & 0 & 0 & 0 & 0 & 0 & 0 & 0 \\
0 & 0 & 0 & 0 & 1 & 0 & 0 & 0 & 0 & 0 & 0 \\
0 & 0 & 0 & 0 & 0 & K+4G/3 & K-2G/3 & 0 & 0 & 0 & C \\
0 & 0 & 0 & 0 & 0 & K-2G/3 & K+4G/3 & 0 & 0 & 0 & C \\
0 & 0 & 0 & 0 & 0 & 0 & 0 & G & 0 & 0 & 0 \\
0 & 0 & 0 & 0 & 0 & 0 & 0 & 0 & 1 & 0 & 0 \\
0 & 0 & 0 & 0 & 0 & 0 & 0 & 0 & 0 & 1 & 0 \\
0 & 0 & 0 & 0 & 0 & C & C & 0 & 0 & 0 & M
\end{bmatrix} \tag{C.11}
$$

$$
C^{-1} = \begin{bmatrix}
1 & 0 & 0 & 0 & 0 & 0 & 0 & 0 & 0 & 0 & 0 \\
0 & 1 & 0 & 0 & 0 & 0 & 0 & 0 & 0 & 0 & 0 \\
0 & 0 & 1 & 0 & 0 & 0 & 0 & 0 & 0 & 0 & 0 \\
0 & 0 & 0 & 1 & 0 & 0 & 0 & 0 & 0 & 0 & 0 \\
0 & 0 & 0 & 0 & 1 & 0 & 0 & 0 & 0 & 0 & 0 \\
0 & 0 & 0 & 0 & 0 & \frac{3C^2-M(3K+4G)}{4G(3C^2-M(G+3K))} & -\frac{M(2G-3K)+3C^2}{4G(3C^2-M(G+3K))} & 0 & 0 & 0 & \frac{3C}{6C^2-M(2G+6K)} \\
0 & 0 & 0 & 0 & 0 & -\frac{M(2G-3K)+3C^2}{4G(3C^2-M(G+3K))} & \frac{3C^2-M(3K+4G)}{4G(3C^2-M(G+3K))} & 0 & 0 & 0 & \frac{3C}{6C^2-M(2G+6K)} \\
0 & 0 & 0 & 0 & 0 & 0 & 0 & G^{-1} & 0 & 0 & 0 \\
0 & 0 & 0 & 0 & 0 & 0 & 0 & 0 & 1 & 0 & 0 \\
0 & 0 & 0 & 0 & 0 & 0 & 0 & 0 & 0 & 1 & 0 \\
0 & 0 & 0 & 0 & 0 & \frac{3C}{6C^2-M(2G+6K)} & \frac{3C}{6C^2-M(2G+6K)} & 0 & 0 & 0 & -\frac{3K+G}{3C^2-M(G+3K)}
\end{bmatrix} \tag{C.12}
$$

$$
D_x = \begin{bmatrix}
0 & 0 & \partial_3 & 0 & 0 & 0 & 0 & 0 & 0 & 0 & 0 \\
0 & 0 & -\partial_1 & 0 & 0 & 0 & 0 & 0 & 0 & 0 & 0 \\
\partial_3 & -\partial_1 & 0 & 0 & 0 & 0 & 0 & 0 & 0 & 0 & 0 \\
0 & 0 & 0 & 0 & 0 & \partial_1 & 0 & \partial_3 & 0 & 0 & 0 \\
0 & 0 & 0 & 0 & 0 & 0 & \partial_3 & \partial_1 & 0 & 0 & 0 \\
0 & 0 & 0 & \partial_1 & 0 & 0 & 0 & 0 & 0 & 0 & 0 \\
0 & 0 & 0 & 0 & \partial_3 & 0 & 0 & 0 & 0 & 0 & 0 \\
0 & 0 & 0 & \partial_3 & \partial_1 & 0 & 0 & 0 & 0 & 0 & 0 \\
0 & 0 & 0 & 0 & 0 & 0 & 0 & 0 & 0 & 0 & \partial_1 \\
0 & 0 & 0 & 0 & 0 & 0 & 0 & 0 & 0 & 0 & \partial_3 \\
0 & 0 & 0 & 0 & 0 & 0 & 0 & 0 & \partial_1 & \partial_3 & 0
\end{bmatrix} \tag{C.13}
$$

$$
C^{-1}\bar{B} = B = \bar{B} \tag{C.14}
$$

$$
C^{-1}\bar{A} = A \neq \bar{A} \tag{C.15}
$$

$C^{-1}\bar{A} = A =$

$$\begin{bmatrix} \varepsilon & 0 & 0 & 0 & 0 & 0 & 0 & 0 & 0 & 0 & 0 \\ 0 & \varepsilon & 0 & 0 & 0 & 0 & 0 & 0 & 0 & 0 & 0 \\ 0 & 0 & \mu & 0 & 0 & 0 & 0 & 0 & 0 & 0 & 0 \\ 0 & 0 & 0 & \rho & 0 & 0 & 0 & 0 & \rho^{(f)} & 0 & 0 \\ 0 & 0 & 0 & 0 & \rho & 0 & 0 & 0 & 0 & \rho^{(f)} & 0 \\ 0 & 0 & 0 & 0 & 0 & \frac{3C^2-M(3K+4G)}{4G(3C^2-M(G+3K))} & -\frac{M(2G-3K)+3C^2}{4G(3C^2-M(G+3K))} & 0 & 0 & 0 & \frac{3C}{6C^2-M(2G+6K)} \\ 0 & 0 & 0 & 0 & 0 & -\frac{M(2G-3K)+3C^2}{4G(3C^2-M(G+3K))} & \frac{3C^2-M(3K+4G)}{4G(3C^2-M(G+3K))} & 0 & 0 & 0 & \frac{3C}{6C^2-M(2G+6K)} \\ 0 & 0 & 0 & 0 & 0 & 0 & 0 & G^{-1} & 0 & 0 & 0 \\ 0 & 0 & 0 & \rho^{(f)} & 0 & 0 & 0 & 0 & 0 & 0 & 0 \\ 0 & 0 & 0 & 0 & \rho^{(f)} & 0 & 0 & 0 & 0 & 0 & 0 \\ 0 & 0 & 0 & 0 & 0 & \frac{3C}{6C^2-M(2G+6K)} & \frac{3C}{6C^2-M(2G+6K)} & 0 & 0 & 0 & -\frac{3K+G}{3C^2-M(G+3K)} \end{bmatrix} \tag{C.16}$$

$$C^{-1}\hat{\bar{s}} = \hat{s} \neq \hat{\bar{s}} \tag{C.17}$$

$$\hat{s} = \tag{C.18}$$

$$\begin{bmatrix} -\hat{J}_1^e \\ -\hat{J}_3^e \\ -\hat{J}_2^m \\ \hat{f}_1 \\ \hat{f}_3 \\ \frac{-6MG((K+\frac{4}{3}G)\hat{h}_{11}+(K-\frac{2}{3}G)\hat{h}_{33}+C\hat{q})}{4G(3C^2-M(G+3K))} + \frac{3C^2(\hat{h}_{11}+\hat{h}_{33}+\frac{M}{C}\hat{q})}{6C^2-M(2G+6K)} \\ \frac{-6MG((K+\frac{4}{3}G)\hat{h}_{11}+(K-\frac{2}{3}G)\hat{h}_{33}+C\hat{q})}{4G(3C^2-M(G+3K))} + \frac{3C^2(\hat{h}_{11}+\hat{h}_{33}+\frac{M}{C}\hat{q})}{6C^2-M(2G+6K)} \\ 2\hat{h}_{31} \\ \hat{f}_1^{(f)} \\ \hat{f}_3^{(f)} \\ \frac{6CG\hat{h}_{11}-8CG\hat{h}_{33}+(6C^2-6KM-2GM)\hat{q}}{6C^2-M(2G+6K)} \end{bmatrix} \tag{C.19}$$

Which is simplified by substituting $S = K - \frac{2}{3}G - \frac{C^2}{M}$ and $K_C = S + 2G$,

$$C^{-1}\hat{\bar{s}} = \hat{s} \neq \hat{\bar{s}} \tag{C.20}$$

$$\hat{s} = \tag{C.21}$$

$$\begin{bmatrix} -\hat{J}_1^e \\ -\hat{J}_3^e \\ -\hat{J}_2^m \\ \hat{f}_1 \\ \hat{f}_3 \\ \frac{K_C\hat{h}_{11}+S\hat{h}_{33}}{2(K_C-G)} \\ \frac{K_C\hat{h}_{11}+S\hat{h}_{33}}{2(K_C-G)} \\ 2\hat{h}_{31} \\ \hat{f}_1^{(f)} \\ \hat{f}_3^{(f)} \\ \frac{4G\hat{h}_{33}-3G\hat{h}_{11}}{\frac{3M}{2C}(K_C+S)} + \hat{q} \end{bmatrix} \tag{C.22}$$

The inverse of C is applied to the entire equation C.1, resulting in the following vectorial first order differential equation, which represents the entire 2D P-SV-TM system,

$$s\hat{A}_{ij}\hat{u}_j + \hat{B}_{ij}\hat{u}_j + D_{x,kj}\hat{u}_j = \hat{s}_i \tag{C.23}$$

C.2 Derivation of reciprocity theorem of the correlation type

Now that the first order basic equations describing the P-SV-TM mode of the seismoelectric system in 2D have been put in the system matrix form, we can easily manipulate it into a reciprocity theorem of the correlation type [15]. Two independent physical states u_A and u_B are defined in the same domain D, enclosed by boundary, ∂D. The '$*$' indicates conjugation, meaning that all fields in state A are time reversed. For each state the location of the source as well as the location where the generated field is measured can be defined independently, as well as their own unique system matrix **A** and loss term matrix **B**. However, we assume here that the two different fields affect the same domain, therefore **A** and **B** are equal for both states. Another relevant assumption is that the flow velocity of the medium is zero for both states. The interaction of the power spectrum of these two fields can be quantified by a so-called interaction quantity of the form: $D_{x,kj}\hat{u}^*_{A,k}\hat{u}_{B,j}$ (for more details on interaction quantities, refer to Hoop et al. 1988 [4]). This interaction quantity represents the variation of the cross-correlation or power spectrum of the two field states in space. In [15], Gauss' divergence theorem is applied to this interaction quantity by integrating it over the domain and transforming part of the volume integral into a boundary integral. The latter action is possible due to the spatial derivatives contained in $D_{x,kj}$. The resulting reciprocity theorem of the correlation type in 2D is as follows,

$$\int_D \hat{u}_A^\dagger \hat{s}_B + \hat{s}_A^\dagger \hat{u}_B = -\oint_{\partial D} \hat{u}_A^\dagger N_x \hat{u}_B dx + \int_D \hat{u}_A^\dagger (B + B^\dagger)\hat{u}_B d^2x \tag{C.24}$$

We adjust equation C.24 such that we can represent all 11 different wave fields as a Greens function generated by any of the 11 sources. To establish this, the source vector is replaced by a diagonal matrix containing spatial Dirac delta functions in the place of every source function $\hat{s}$. Consequently, the field vector $\hat{u}$ has to be replaced by an 11x11 - matrix, containing 121 Greens function representations of all possible field response-source combinations, which is as follows,

$$\hat{G} = \begin{bmatrix}
\hat{G}^{E_1,J_1^e} & \hat{G}^{E_1,J_3^e} & \hat{G}^{E_1,J_2^m} & \hat{G}^{E_1,f_1} & \hat{G}^{E_1,f_3} & \hat{G}^{E_1,CH1} & \hat{G}^{E_1,CH1} & \hat{G}^{E_1,2h_{31}} & \hat{G}^{E_1,f_1^f} & \hat{G}^{E_1,f_3^f} & \hat{G}^{E_1,Cq} \\
\hat{G}^{E_3,J_1^e} & \hat{G}^{E_3,J_3^e} & \hat{G}^{E_3,J_2^m} & \hat{G}^{E_3,f_1} & \hat{G}^{E_3,f_3} & \hat{G}^{E_3,CH1} & \hat{G}^{E_3,CH1} & \hat{G}^{E_3,2h_{31}} & \hat{G}^{E_3,f_1^f} & \hat{G}^{E_3,f_3^f} & \hat{G}^{E_3,Cq} \\
\hat{G}^{H_2,J_1^e} & \hat{G}^{H_2,J_3^e} & \hat{G}^{H_2,J_2^m} & \hat{G}^{H_2,f_1} & \hat{G}^{H_2,f_3} & \hat{G}^{H_2,CH1} & \hat{G}^{H_2,CH1} & \hat{G}^{H_2,2h_{31}} & \hat{G}^{H_2,f_1^f} & \hat{G}^{H_2,f_3^f} & \hat{G}^{H_2,Cq} \\
\hat{G}^{v_1,J_1^e} & \hat{G}^{v_1,J_3^e} & \hat{G}^{v_1,J_2^m} & \hat{G}^{v_1,f_1} & \hat{G}^{v_1,f_3} & \hat{G}^{v_1,CH1} & \hat{G}^{v_1,CH1} & \hat{G}^{v_1,2h_{31}} & \hat{G}^{v_1,f_1^f} & \hat{G}^{v_1,f_3^f} & \hat{G}^{v_1,f_3^f} \\
\hat{G}^{v_3,J_1^e} & \hat{G}^{v_3,J_3^e} & \hat{G}^{v_3,J_2^m} & \hat{G}^{v_3,f_1} & \hat{G}^{v_3,f_3} & \hat{G}^{v_3,CH1} & \hat{G}^{v_3,CH1} & \hat{G}^{v_3,2h_{31}} & \hat{G}^{v_3,f_1^f} & \hat{G}^{v_3,f_3^f} & \hat{G}^{v_3,Cq} \\
\hat{G}^{\tau_{11},J_1^e} & \hat{G}^{\tau_{11},J_3^e} & \hat{G}^{\tau_{11},J_2^m} & \hat{G}^{\tau_{11},f_1} & \hat{G}^{\tau_{11},f_3} & \hat{G}^{\tau_{11},CH1} & \hat{G}^{\tau_{11},CH1} & \hat{G}^{\tau_{11},2h_{31}} & \hat{G}^{\tau_{11},f_1^f} & \hat{G}^{\tau_{11},f_3^f} & \hat{G}^{\tau_{11},Cq} \\
\hat{G}^{\tau_{33},J_1^e} & \hat{G}^{\tau_{33},J_3^e} & \hat{G}^{\tau_{33},J_2^m} & \hat{G}^{\tau_{33},f_1} & \hat{G}^{\tau_{33},f_3} & \hat{G}^{\tau_{33},CH1} & \hat{G}^{\tau_{33},CH1} & \hat{G}^{\tau_{33},2h_{31}} & \hat{G}^{\tau_{33},f_1^f} & \hat{G}^{\tau_{33},f_3^f} & \hat{G}^{\tau_{33},Cq} \\
\hat{G}^{\tau_{31},J_1^e} & \hat{G}^{\tau_{31},J_3^e} & \hat{G}^{\tau_{31},J_2^m} & \hat{G}^{\tau_{31},f_1} & \hat{G}^{\tau_{31},f_3} & \hat{G}^{\tau_{31},CH1} & \hat{G}^{\tau_{31},CH1} & \hat{G}^{\tau_{31},2h_{31}} & \hat{G}^{\tau_{31},f_1^f} & \hat{G}^{\tau_{31},f_3^f} & \hat{G}^{\tau_{31},Cq} \\
\hat{G}^{w_1,J_1^e} & \hat{G}^{w_1,J_3^e} & \hat{G}^{w_1,J_2^m} & \hat{G}^{w_1,f_1} & \hat{G}^{w_1,f_3} & \hat{G}^{w_1,CH1} & \hat{G}^{w_1,CH1} & \hat{G}^{w_1,2h_{31}} & \hat{G}^{w_1,f_1^f} & \hat{G}^{w_1,f_3^f} & \hat{G}^{w_1,Cq} \\
\hat{G}^{w_3,J_1^e} & \hat{G}^{w_3,J_3^e} & \hat{G}^{w_3,J_2^m} & \hat{G}^{w_3,f_1} & \hat{G}^{w_3,f_3} & \hat{G}^{w_3,CH1} & \hat{G}^{w_3,CH1} & \hat{G}^{w_3,2h_{31}} & \hat{G}^{w_3,f_1^f} & \hat{G}^{w_3,f_3^f} & \hat{G}^{w_3,Cq} \\
\hat{G}^{p,J_1^e} & \hat{G}^{p,J_3^e} & \hat{G}^{p,J_2^m} & \hat{G}^{p,f_1} & \hat{G}^{p,f_3} & \hat{G}^{p,CH1} & \hat{G}^{p,CH1} & \hat{G}^{p,2h_{31}} & \hat{G}^{p,f_1^f} & \hat{G}^{p,f_3^f} & \hat{G}^{p,Cq}
\end{bmatrix} \tag{C.25}$$

Each unique element of this matrix function is a Greens function representation of a combination of a certain field and the source generating it. The substitution of this matrix into C.24 and some rewritings, turns the reciprocity theorem into the following matrix function,

$$\int_D \hat{G}^{\dagger}_{x_A,x_B} + \hat{G}_{x_B,x_A} = -\oint_{\partial D} \hat{G}_{x_B,x} N_x \hat{G}^{\dagger}_{x_A,x} dx + \int_D \hat{G}_{x_B,x} (B + B^{\dagger}) \hat{G}^{\dagger}_{x_A,x} d^2x \tag{C.26}$$

Matrix N_x contains the components of the normal vector of the boundary of the domain. It has to work on the field vector in parallel with the D_x matrix, therefore it is equal to D_x where ∂ is changed to n,

$$N_x = \begin{bmatrix}
0 & 0 & n_3 & 0 & 0 & 0 & 0 & 0 & 0 & 0 & 0 \\
0 & 0 & -n_1 & 0 & 0 & 0 & 0 & 0 & 0 & 0 & 0 \\
n_3 & -n_1 & 0 & 0 & 0 & 0 & 0 & 0 & 0 & 0 & 0 \\
0 & 0 & 0 & 0 & 0 & n_1 & 0 & n_3 & 0 & 0 & 0 \\
0 & 0 & 0 & 0 & 0 & 0 & n_3 & n_1 & 0 & 0 & 0 \\
0 & 0 & 0 & n_1 & 0 & 0 & 0 & 0 & 0 & 0 & 0 \\
0 & 0 & 0 & 0 & n_3 & 0 & 0 & 0 & 0 & 0 & 0 \\
0 & 0 & 0 & n_3 & n_1 & 0 & 0 & 0 & 0 & 0 & 0 \\
0 & 0 & 0 & 0 & 0 & 0 & 0 & 0 & 0 & 0 & n_1 \\
0 & 0 & 0 & 0 & 0 & 0 & 0 & 0 & 0 & 0 & n_3 \\
0 & 0 & 0 & 0 & 0 & 0 & 0 & 0 & n_1 & n_3 & 0
\end{bmatrix} \tag{C.27}$$

For the domain integral we the matrix summation $B + B^{\dagger}$ needs to be defined,

$$
B+B^{\dagger}=\begin{bmatrix}
2\Re(\hat{\sigma}^e-\frac{\eta\hat{L}^2}{\hat{k}}) & 0 & 0 & 0 & 0 & 0 & 0 & 0 & 2i\Im(\frac{\eta\hat{L}}{\hat{k}}) & 0 & 0\\
0 & 2\Re(\hat{\sigma}^e-\frac{\eta\hat{L}^2}{\hat{k}}) & 0 & 0 & 0 & 0 & 0 & 0 & 0 & 2i\Im(\frac{\eta\hat{L}}{\hat{k}}) & 0\\
0 & 0 & 2\Re(\hat{\sigma}^m) & 0 & 0 & 0 & 0 & 0 & 0 & 0 & 0\\
0 & 0 & 0 & 0 & 0 & 0 & 0 & 0 & 0 & 0 & 0\\
0 & 0 & 0 & 0 & 0 & 0 & 0 & 0 & 0 & 0 & 0\\
0 & 0 & 0 & 0 & 0 & 0 & 0 & 0 & 0 & 0 & 0\\
0 & 0 & 0 & 0 & 0 & 0 & 0 & 0 & 0 & 0 & 0\\
0 & 0 & 0 & 0 & 0 & 0 & 0 & 0 & 0 & 0 & 0\\
-2i\Im(\frac{\eta\hat{L}}{\hat{k}}) & 0 & 0 & 0 & 0 & 0 & 0 & 0 & 2\Re(\frac{\eta}{\hat{k}}) & 0 & 0\\
0 & -2i\Im(\frac{\eta\hat{L}}{\hat{k}}) & 0 & 0 & 0 & 0 & 0 & 0 & 0 & 2\Re(\frac{\eta}{\hat{k}}) & 0\\
0 & 0 & 0 & 0 & 0 & 0 & 0 & 0 & 0 & 0 & 0
\end{bmatrix} \tag{C.28}
$$

We select one element from this representation in order to find an expression which can be modelled. The selected element for this experiment is the Green's function which relates the x_1 component of the causal electric field response at x_b due to a x_1 directed impulse force on the bulk at x_a. Selecting this specific element from the causal Green's function (state B), yields the following interferometric relation,

$$
\begin{aligned}
&G^{E_1,f_1}(\bar{x}_B,\bar{x}_A,\omega)+G^{*v_1,J_1^e}(\bar{x}_A,\bar{x}_B,\omega)\\
&=-\oint_{\partial D}[n_3G^{*v_1,J_2^m}_{\bar{x}_A}G^{E_1,J_1^e}_{\bar{x}_B}-\ n_1G^{*v_1,J_2^m}_{\bar{x}_A}G^{E_1,J_3^e}_{\bar{x}_B}+\ n_3G^{*v_1,J_1^e}_{\bar{x}_A}G^{E_1,J_2^m}_{\bar{x}_B}-\ n_1G^{*v_1,J_3^e}_{\bar{x}_A}G^{E_1,J_2^m}_{\bar{x}_B}\\
&+n_1G^{*v_1,CH1}_{\bar{x}_A}G^{E_1,f_1}_{\bar{x}_B}+n_3G^{*v_1,2h_{31}}_{\bar{x}_A}G^{E_1,f_1}_{\bar{x}_B}+n_3G^{*v_1,CH1}_{\bar{x}_A}G^{E_1,f_3}_{\bar{x}_B}+n_1G^{*v_1,2h_{31}}_{\bar{x}_A}G^{E_1,f_3}_{\bar{x}_B}+n_1G^{*v_1,f_1}_{\bar{x}_A}G^{E_1,CH1}_{\bar{x}_B}\\
&+\ n_3G^{*v_1,f_3}_{\bar{x}_A}G^{E_1,CH1}_{\bar{x}_B}+\ n_3G^{*v_1,f_1}_{\bar{x}_A}G^{E_1,2h_{31}}_{\bar{x}_B}+\ n_1G^{*v_1,f_3}_{\bar{x}_A}G^{E_1,2h_{31}}_{\bar{x}_B}+\ n_1G^{*v_1,Cq}_{\bar{x}_A}G^{E_1,f_1^f}_{\bar{x}_B}\\
&+\ n_3G^{*v_1,Cq}_{\bar{x}_A}G^{E_1,f_3^f}_{\bar{x}_B}+\ n_1G^{*v_1,f_1^f}_{\bar{x}_A}G^{E_1,Cq}_{\bar{x}_B}+\ n_3G^{*v_1,f_3^f}_{\bar{x}_A}G^{E_1,Cq}_{\bar{x}_B}]\ \mathrm{d}\bar{x}\\
&+\int_D[2\Re(\hat{\sigma}^e-\frac{\eta\hat{L}^2}{\hat{k}})G^{*v_1,J_1^e}_{\bar{x}_A}G^{E_1,J_1^e}_{\bar{x}_B}+2i\Im(\frac{\eta\hat{L}}{\hat{k}})G^{*v_1,f_1^f}_{\bar{x}_A}G^{E_1,J_1^e}_{\bar{x}_B}\\
&+2\Re(\hat{\sigma}^e-\frac{\eta\hat{L}^2}{\hat{k}})G^{*v_1,J_3^e}_{\bar{x}_A}G^{E_1,J_3^e}_{\bar{x}_B}+2i\Im(\frac{\eta\hat{L}}{\hat{k}})G^{*v_1,f_3^f}_{\bar{x}_A}G^{E_1,J_3^e}_{\bar{x}_B}+2\Re(\sigma^m)G^{v_1,J_2^m}_{\bar{x}_A}G^{E_1,J_2^m}_{\bar{x}_B}\\
&-2i\Im(\frac{\eta\hat{L}}{\hat{k}})G^{v_1,J_1^e}_{\bar{x}_A}G^{E_1,f_1^f}_{\bar{x}_B}+2\Re(\frac{\eta}{\hat{k}})G^{v_1,f_1^f}_{\bar{x}_A}G^{E_1,f_1^f}_{\bar{x}_B}\\
&-2i\Im(\frac{\eta\hat{L}}{\hat{k}})G^{v_1,J_3^e}_{\bar{x}_A}G^{E_1,f_3^f}_{\bar{x}_B}+2\Re(\frac{\eta}{\hat{k}})G^{v_1,f_3^f}_{\bar{x}_A}G^{E_1,f_3^f}_{\bar{x}_B}]\ \mathrm{d}\bar{x}^2
\end{aligned} \tag{C.29}
$$

Appendix D

Medium parameters

For further details on these medium parameters, the reader is referred to Pride [7].

Table D.1: Overview of the relevant medium parameters for the homogeneous medium. Note that for the slow P- and TM- wave speeds the lower and upper frequency limit is given.

Property	Unit	Value Medium	Dimension
Porosity	ϕ	0.3	[$-$]
Pore fluid density	ρ_f	$1.0 \cdot 10^3$	[kg m^{-3}]
Solid density	ρ_s	$2.7 \cdot 10^3$	[kg m^{-3}]
Shear modulus framework of grains	G^{fr}	$9.0 \cdot 10^9$	[Pa]
Pore fluid viscosity	η	$1.0 \cdot 10^{-3}$	[kg m^{-1} s^{-1}]
Static permeability	k_0	$1.3 \cdot 10^{-12}$	[m^2]
Static electrokinetic coupling	$\mathcal{L}_0$	$1.048 \cdot 10^{-8}$	[m^2 s^{-1} V^{-1}]
Tortuosity	α_∞	3.0	[-]
Relative perm. of the (pore) fluid	ϵ_{rf}	80	[-]
Relative perm. of the solid	ϵ_{rs}	4	[-]
Bulk electric conductivity	σ^e	$9.3 \cdot 10^{-7}$	[S m^{-1}]
Magnetic permeability	μ	$1.256 \cdot 10^{-6}$	[NA^{-2}]
Fast P-wave speed	v_{Pf}	$3.122 \cdot 10^3$	[m s^{-1}]
Slow P-wave speed	v_{Ps}	$1.636 - 8.149 \cdot 10^1$	[m s^{-1}]
SV-wave speed	v_{SV}	$2.027 \cdot 10^3$	[m s^{-1}]
EM-wave speed	v_{EM}	$7.257 \cdot 10^5 - 4.104 \cdot 10^7$	[m s^{-1}]

Bibliography

[1] Milton Abramowitz and Irene A. Stegun. *Handbook of mathematical functions.* 1972.

[2] M A Biot. Theory of propagation of elastic waves in a fluid-saturated porous solid. I. Low-frequency range. *The Journal of the Acoustical Society of America*, 28(2):168–178, 1956.

[3] Jon F. Claerbout. Synthesis of a layered medium from its acoustic transmission response. *Geophysics*, 33(2):264–269, 1967.

[4] A. T. De Hoop and A. J. Stam. Time-domain reciprocity theorems for elastodynamic wave fields in solids with relaxation and their application to inverse problems. *Wave Motion*, 10:479–489, 1988.

[5] Sjoerd a. L. de Ridder, Evert Slob, and Kees Wapenaar. Interferometric seismoelectric Green's function representations. *Geophysical Journal International*, 178(3):1289–1304, September 2009.

[6] David J. Griffiths. *Introduction to electrodynamics.* 2008.

[7] S. Pride. Governing equations for the coupled electromagnetics and acoustics of porous media. *Physical Review B*, 50(21):15678–15696, 1994.

[8] Steven R. Pride and Matthijs W. Haartsen. Electroseismic wave properties. *The Journal of the Acoustical Society of America*, 100(3):1301, 1996.

[9] F. C. Schoemaker, N. Grobbe, M. D. Schakel, S. a. L. de Ridder, E. C. Slob, and D. M. J. Smeulders. Experimental validation of the electrokinetic theory and development of seismoelectric interferometry by cross-correlation. *International Journal of Geophysics*, 2012:1–23, 2012.

[10] G. T. Schuster, J. Yu, J. Sheng, and J. Rickett. Interferometric/daylight seismic imaging. *Geophysical Journal International*, 157(2):838–852, May 2004.

[11] Seth Stein and Michael Wysession. *An introduction to global seismology, earthquakes and Earth structure.* 2003.

[12] Kees Wapenaar. Retrieving the elastodynamic Green's function of an arbitrary inhomogeneous medium by cross correlation. *Physical Review Letters*, 93(25):1–4, December 2004.

[13] Kees Wapenaar. Reciprocity theorems for seismoelectric waves. *J. Seism. Expl.*, 12:103–112, 2005.

[14] Kees Wapenaar, Deyan Draganov, Roel Snieder, Xander Campman, and Arie Verdel. Tutorial on seismic interferometry: Part 1 — Basic principles and applications. *Geophysics*, 75(5):195–209, 2010.

[15] Kees Wapenaar and Jacob Fokkema. Reciprocity theorems for diffusion , flow and waves. *A.S.M.E. Journal of Applied Mechanics*, 71:145–150, 2004.

[16] Kees Wapenaar and Evert Slob. Unified Green ' s function retrieval by cross correlation. *Physical Review Letters*, 234301(December):1–4, 2006.

[17] Kees Wapenaar, Joost van der Neut, Elmer Ruigrok, Deyan Draganov, Jürg Hunziker, Evert Slob, Jan Thorbecke, and Roel Snieder. Seismic interferometry by crosscorrelation and by multidimensional deconvolution: a systematic comparison. *Geophysical Journal International*, 185(3):1335–1364, June 2011.

[18] Öz Yilmaz. *Seismic data analysis. Volume II*, volume 10. 2001.